THE ALTERNATIVE APPROACHES FOR TAILINGS DISPOSAL OF THAILAND'S POTASH MINES

Miss Thao Nguyen Anh Ngo

A Thesis Submitted in Partial Fulfillment of the Requirements
for the Degree of Master of Engineering Program in Georesources and Petroleum Engineering
Department of Mining and Petroleum Engineering
Faculty of Engineering
Chulalongkorn University
Academic Year 2016

ทางเลือกการกำจัดหางแร่สำหรับเหมืองแร่โปแทชในประเทศไทย

นางสาวเทา เหงียน อานท์ โง

วิทยานิพนธ์นี้เป็นส่วนหนึ่งของการศึกษาตามหลักสูตรปริญญาวิศวกรรมศาสตรมหาบัณฑิต
สาขาวิชาวิศวกรรมทรัพยากรธรณีและปิโตรเลียม ภาควิชาวิศวกรรมเหมืองแร่และปิโตรเลียม
คณะวิศวกรรมศาสตร์ จุฬาลงกรณ์มหาวิทยาลัย
ปีการศึกษา 2559

Thesis Title	THE ALTERNATIVE APPROACHES FOR TAILINGS DISPOSAL OF THAILAND'S POTASH MINES
By	Miss Thao Nguyen Anh Ngo
Field of Study	Georesources and Petroleum Engineering
Thesis Advisor	Assistant Professor Sunthorn Pumjan, Ph.D.

Accepted by the Faculty of Engineering, Chulalongkorn University in Partial Fulfillment of the Requirements for the Master's Degree

.....Dean of the Faculty of Engineering

(Associate Professor Supot Teachavorasinskun, D.Eng.)

THESIS COMMITTEE

.....Chairman

(Associate Professor Dawan Wiwattanadate, Ph.D.)

.....Thesis Advisor

(Assistant Professor Sunthorn Pumjan, Ph.D.)

.....Examiner

(Assistant Professor Kreangkrai Maneeintr, Ph.D.)

.....External Examiner

(Associate Professor Pinyo Meechumna, Ph.D.)

เทา เหงียน อานท์ โง : ทางเลือกการกำจัดหางแร่สำหรับเหมืองแร่โปแทชในประเทศไทย (THE ALTERNATIVE APPROACHES FOR TAILINGS DISPOSAL OF THAILAND'S POTASH MINES) อ.ที่ปรึกษาวิทยานิพนธ์หลัก: สุนทร พุ่มจันทร์, 108 หน้า.

การศึกษานี้นำเสนอสองวิธีทางเลือกในการกำจัดหางแร่ที่เป็นของแข็งและของเหลวจากเหมืองแร่โพแทช ซึ่งเป็นหนึ่งในความท้าทายด้านสิ่งแวดล้อมในอุตสาหกรรมแร่โพแทช

ทางเลือกแรกคือวิธีการทำให้หางแร่แข็งตัวในรูปของแท่งคอนกรีต โดยการผสมกันระหว่าง หางแร่ ซีเมนต์ กับวัสดุมวลรวมละเอียดและหยาบ การออกแบบนี้พยายามหาอัตราส่วนการผสมที่ดีที่สุดสำหรับวัสดุผสมแท่งคอนกรีต ที่สัมพันธ์กับกำลังรับแรงกดแบบแกนเดียว (Unconfined Compressive Strength) โดยมุ่งใช้ส่วนผสมหางแร่ให้มากที่สุด และขณะเดียวกันสามารถรักษากำลังรับแรงกดขั้นต่ำได้ แท่งคอนกรีตที่แข็งตัวจะถูกใช้เป็นวัสดุถมกลับในห้องเหมืองแร่ของเหมืองแร่โพแทชใต้ดิน เพื่อลดผลกระทบต่อสิ่งแวดล้อมและทำให้การขุดเจาะเหมืองมีเสถียรภาพ ลดอัตราการทรุดตัวของเหมืองใต้ดิน

วิธีที่สองคือการอัดฉีดน้ำเกลือเข้มข้นสู่ชั้นหินชุดโคกกรวด แบบจำลองพื้นฐานถูกสร้างขึ้นประกอบด้วยบ่ออัดฉีดน้ำเกลือ 1 บ่อ ด้วยการอัดฉีดแบบอัตราคงที่ที่ 165 ลบ.ม. / วัน แบบจำลองแนวคิดที่เหมาะสมในการดำเนินการกำจัดน้ำเกลือเข้มข้น ได้ถูกออกแบบให้มีจำนวนบ่ออัดฉีดน้ำเกลือ 8 หลุม โดยกำหนดอัตราการอัดฉีดและเวลาแปรตามปริมาตรน้ำเกลือที่ปล่อยออกมาจากโรงแต่งแร่

ผลจากการทดลองแสดงให้เห็นว่า ค่า UCS ของแท่งคอนกรีตมีผลจากปัจจัยดังต่อไปนี้ ปริมาณซีเมนต์, อัตราส่วนน้ำต่อปูนซิเมนต์, และระยะเวลาการบ่ม ส่วนผสม ID 20/5/5 / 70T ซึ่งผสมจากปูนซีเมนต์ 20%, เม็ดทรายละเอียดละเอียด 5%, เม็ดหยาบ 5%, และหางแร่ 70% เป็นส่วนผสมที่เหมาะสมที่สุด ที่สามารถผสมหางแร่ได้สูงสุดถึง 70% และมีกำลังรับแรงอัดที่ 6.17 เมกกะปาสคาล สูงกว่าข้อกำหนดขั้นต่ำที่กำหนดไว้ที่ 5 เมกกะปาสคาล ในภาพรวม ประมาณ 54.5 ล้านตันของหางแร่ถูกนำไปใช้ทำแท่งคอนกรีต แท่งคอนกรีตจะถูกนำไปถมกลับลงในแผงผลิตแร่ในเหมืองใต้ดินตลอดอายุของเหมือง ในขณะเดียวกันการถมกลับเพิ่มความแข็งแรงของเสาค้ำยันขึ้นประมาณ 1.49 เท่า และสามารถลดอัตราการทรุดตัวของเหมืองใต้ดิน

จากผลของการสร้างแบบจำลองการอัดฉีดน้ำเกลือ แบบจำลองภายใต้สถานการณ์ปกติ ที่อัตราการอัดฉีดสูงสุด 165 ลบ.ม. / วัน จะเพิ่มแรงดันก้นหลุมเป็น 842 กิโลปาสคาล ซึ่งแรงดันก้นหลุมดังกล่าวไม่เกินแรงดันที่ทำให้เกิดการแตกหักของชั้นหินตลอดช่วงระยะเวลาอัดฉีด 21 ปี น้ำเกลือเคลื่อนที่ลงในแนวดิ่งจากจุดอัดฉีดไปยังชั้นหินทรายด้านล่าง และการกระจายตัวของน้ำเกลือเข้มข้นครอบคลุมพื้นที่ 0.142 ตารางกิโลเมตร (รัศมีการกระจายตัว = 212.5 เมตร) แบบจำลองสำหรับแนวคิดในการดำเนินงานประกอบด้วย 8 หลุมอัดฉีด ซึ่งออกแบบมาเพื่อรองรับปริมาตรน้ำเกลือทั้งหมดที่ต้องการกำจัดจากโรงแต่งแร่ ในภาพรวมปริมาณน้ำเกลือที่อัดฉีดได้รวม 2.8 ล้านลูกบาศก์เมตร ตลอดช่วงระยะเวลาอัดฉีด 21 ปี

แนวทางการกำจัดของเสียเหมืองแร่โพแทชทั้งสองรายการ สามารถกำจัดทั้งหางแร่ของแข็งและน้ำเกลือเข้มข้นของเหมืองแร่โพแทช แนวทางนี้สามาถลดปริมาตรของเสียเหมืองแร่เกือบทั้งหมด ซึ่งก่อให้เกิดประโยชน์ต่อการพัฒนาด้านเทคนิคและลดผลกระทบต่อสิ่งแวดล้อมในอุตสาหกรรมโพแทชในประเทศไทย

ภาควิชา วิศวกรรมเหมืองแร่และปิโตรเลียม ลายมือชื่อนิสิต .....

สาขาวิชา วิศวกรรมทรัพยากรธรณีและปิโตรเลียม ลายมือชื่อ อ.ที่ปรึกษาหลัก .....

ปีการศึกษา 2559

5871211921 : MAJOR GEORESOURCES AND PETROLEUM ENGINEERING
KEYWORDS:

THAO NGUYEN ANH NGO: THE ALTERNATIVE APPROACHES FOR TAILINGS DISPOSAL OF THAILAND'S POTASH MINES. ADVISOR: ASST. PROF. SUNTHORN PUMJAN, Ph.D., 108 pp.

This study involves the two alternative approaches to dispose of solid and liquid brine wastes which is one of the biggest environmental challenge in potash industry.

The first alternative approach is solidification method that can solidify the solid tailing into the concrete block by mixing with binder as cement, and additional fine and coarse aggregates. The design provides the optimizing mixing ratio for concrete block mixture materials in relation to the uniaxial compressive strength (UCS). The expected result is the optimal mixture that maximize the solid tailing concentration and archives the minimum UCS strength requirement of backfilling materials in Thailand Potash mine. The solidified concrete blocks are then used as backfill materials into the mine-out room of the underground potash mine to minimize significantly the environmental impact and stabilize excavations and minimize convergences and subsidence of the underground mine.

The second alternative approach is deep well injection of liquid brine waste into the Khok Kruat Formation. The base case simulation was modeled with one injection well at rate of 165 m^3/day. To annually dispose brine waste, the operational optimum conceptual model was designed of eight injection wells at different injection rates and time following the brine volume discharged.

The results from the experimental work show that the UCS values of the concrete blocks are affected by the following factors; cement content, water to cement ratio, and curing time. The mixture ID 20/5/5/70T which made from 20% cement, 5% fine aggregate, 5% coarse aggregate and 70% solid tailing, is the optimum mixture that satisfy the maximum solid waste concentration of 70%. It generates the compressive strength of 6.17 MPa, which is greater than the requirement of 5 MPa. Approximately 54.5 million tons of solid tailing can be disposed into the mine-out panels for the entire mine life. The pillar strength increases about 1.49 times, and thus minimize the subsidence of the underground mine.

According to the results of waste brine injection, the base case simulation model at maximum injection rate of 165 m^3/day increases the bottom-hole pressure to 842 KPa, and not exceeding the formation fracture pressure during the 21-years injection period. The brine salinity moves downward from the injection point to the bottom of the sand layer, and the plume migration of covers the area of 0.142 km^2 (radius of plume migration = 212.5 m) at the bottom layer. The operational conceptual model of eight wells was designed to accommodate the disposed brine volume from the plant. The cumulative injected brine volume of 2.8 million cubic meters is recorded through 21-years injection program.

The two conjunctive potash mine waste disposal programs take care of both solid and liquid potash mine wastes. These approaches will achieve the close to zero waste potash mining operation, and consequentially provide the benefits of technical aspects and reduce the environmental impacts in Potash industry in Thailand.

Department:	Mining and Petroleum Engineering	Student's Signature	.....
Field of Study:	Georesources and Petroleum Engineering	Advisor's Signature	.....
Academic Year:	2016		

ACKNOWLEDGEMENTS

First of all, I would like to express my deepest gratitude to my thesis supervisor, Assistant Professor. Dr. Sunthorn Pumjan for having given me the opportunity to undertake this work and learn lots of interesting new things both in the study program and daily life. For the freedom that he gave me to realize the new ideas, and for his patient guidance and useful recommendations during my research. I am especially grateful for presenting his kindness all the time, sharing his experiences whenever I need and his enthusiastic encouragement in all of the things I have done since the first met.

Furthermore, I would like to thank the rest of my thesis committee: Assoc. Prof. Dr. Dawan Wiwattanadate, Assoc. Prof. Dr. Pinyo Meechumna and Asst. Prof. Dr. Kreangkrai Maneeintr for the time and efforts they put into reading, examining the thesis, and for their valuable comments.

I would like to express my very great appreciation to AUN-Seed-Net Scholarship for their supporting and funding this research. I would like to thank to International School of Engineering and Department of Mining and Petroleum Engineering for their essential supports.

I would also like to extend my thanks to Asia Pacific Potash Corporation Limited, APPC Company for their assistance with the collection of thesis data.

This research was carried out at the Mining Laboratory, Chulalongkorn University. It would like to thank to Concrete Laboratory, Department of Civil Engineering for offering me the equipment and helping in testing of concrete compression test.

I would also like to thank Asst. Prof. Dr. Kreangkrai Maneeintr and his students for their guidance and help me in running the simulation program.

I owe words of appreciation to Asst. Prof. Dr. Aksara Putthividhya from Water Resources Engineering Department for her first help and continuous support throughout my years in Thailand. Her thoughtful efforts have given me the opportunity to study in Chulalongkorn University.

I am grateful to all my friends in Viet Nam and Thailand, whom always willing to help and give their best suggestions. A special thank from the bottom of my heart to Mr. Thuc Nguyen Nhu who always besides, encourages and inspires me.

Finally, I would like to express my very profound gratitude to my parents, my siblings and my aunt's family for providing moral support and continuous encouragement throughout my years of study and through the processes of researching and writing this thesis. This accomplishment would not have been possible without them.

CONTENTS

Page

Page

Page

LIST OF TABLES

LIST OF FIGURES

LIST OF ABBREVIATIONS

APPC	Asia Pacific Potash Corporation Co. Ltd
bbl	barrel (bbl/d, bpd: barrel per day)
BHP	Bottom Hole Pressure
c_f	rock compressibility
CH_4 or C_1	Methane
CMG	Computer Modelling Group
CO_2	Carbon dioxide
EoS	Equation-of-State
ft	foot
ft^3	cubic feet
GEM	EOS-Compositional Reservoir Simulator
gpm	gallon per minute
lb/ft^3	pound per cubic feet
mD	millidarcy
stb	stock tank barrels
K	hydraulic conductivity
k	reservoir permeability
k_{rg}	gas relative permeability
k_{rw}	water relative permeability
P_f	formation pressure
PSD	Particle Size Distribution
psi	pounds per square inch
S_w	water saturation
Q	flow rate
UCS	Uniaxial Compressive Strength
XRF	X-Ray Fluorescence

Greek Letter

μ	viscosity of the fluid
ρ	density of the fluid
Φ	porosity
σ	stress

CHAPTER 1

INTRODUCTION

1.1. Introduction

Potash is a generic term for various potassium (K) salts. Over 90% of potash is used as fertilizer and is one of the three primary agricultural nutrients (N-P-K). Potassium increases crop quality and protects plants against diseases and insects. With the world's growing population, demand for potash continues to rise following higher demand for agricultural produced. Some by-products from potassium also use in the production of industrial and pharmaceutical goods. The importance of fertilizer consumption to the potash industry is evidenced by the fact that more than 95 per cent of all potash used in the United States is utilized as plant food [1]. Canada is the world's major potash exporter with the export value of 40%, while Asian countries are the world's main importers, with Thailand ranked 5th in Asia as a net importer.

The development of potash mining in Thailand could reduce import and thus reduce production costs for the agricultural and manufacturing industries. Thailand has abundant potash resources, with many exploitable deposits. Potash deposits are usually found in the Northeastern provinces such as Chaiyaphum, Udon Thani, Khon Kaen, Sakon Nakhon, and Nakhon Ratchasima. Moreover, these deposits are of high quality. For instance, the Sylvite potash commonly found in Udon Thani is one of the best types for manufacturing potassium fertilizers. In addition, potash deposits in Thailand can be found only 150-300 meters under the ground surface, making the mining cost much lower than many places in the world where potash mines are more than 1,000 meters underground. The details of potash deposits in Thailand are summarized in Table 1.1.

Table 1.1: Major potash deposits in Thailand [2]

Deposits	Location	Type	Thickness (meters)	Depth (meters)	Average grade (%K_2O)	Resource (million tonnes)
Bamnet Narong	Chaiyaphum	C	20.0–27.3	150–400	15.8	431
Dan Khun Thot	Nakhon Ratchasima	S, C	-	-	13.1	103
Udon South	Udon Thani	S, C	2.3	350	22.9	294
Udon North	Udon Thani	S, C	12		17.1	665
Wanon Niwat	Sakon Nakhon	S, C	4.3	438.8–488.1	19.8–40.4	-
Khon Kaen	Khon Kaen	S, C	1.4–8.6	132.6–139.2	9.3–24.0	-
Na Cheuk	Maha Sarakham	S, C	-	50	-	7

**Remark: S = Sylvite, C = Carnallite.*

Three potash projects are currently under development stages in Thailand; Bamnet Narong, Dan Khun Thot, and Udon Thani projects as followings.

- Bamnet Narong Project (APOT - Asean Potash Chaiyaphum Public Co. Ltd) in Chaiyaphum Province, with the average grade of 18% content of KCl. The deposit is a Carnallite ore ($KCl.MgCl_2.6H_2O$), which has average thickness of more than 15 m. at the depth of 100-250 m. from the ground. Room and pillars mining method was applied for the Bamnet Narong Potash Project. In term of processing potash ore, the project has selected the hot crystallization as the process for ore processing.

- Dan Khun Thot Project (Thai Kali Co. Ltd) in Nakhon Ratchasima Province, with the average grade of 21% content of KCl. The project started exploring for potash in the Dan Khun Thot District where Carnallite and Sylvite resource deposits were identified with economic ore grade. Thai Kali's mining company started construction of the mine in 2015 and plans to have an initial production in the year 2017.

- Udon Thani Project (APPC - Asia Pacific Potash Corporation Co. Ltd) in Udon Thani Province, with the average grade of 29-40% content of KCl. Room and pillar underground method was applied to excavate the Sylvinite ore type at

the depth of 300 – 380 m. The thickness of the deposit is varied from 1 to 10 m. (average 3.8 m.). Flotation and the hot leaching and crystallization are applied for ore processing. The waste generated from processing plant are solid tailing and disposal brine.

In general, the standard techniques for waste disposal employed by potash projects are backfill, tailing pile and evaporation pond. These techniques will be introduced in this study with the site selection of APPC Project in section 1.4.

This study proposes two alternative approaches as solidification and deep well injection. Solidification is the method that the solid tailing is solidified by binding materials, and then is used as a backfill materials into the mine-out room. Deep well injection involves injection of liquid brine waste into the deep formation for permanent storage and long-term monitoring.

1.2. Background

Potash, the compound with potassium (K) as main ingredient, is one of the three basic plant nutrients along with nitrogen (N) and phosphorus (P). Therefore, potash is very important for agriculture. The use of potash-based fertilizer increases by the time to meet the demand of food and animal feed in the world. There is 250 billion metric tons of potash resources in the world, and it can be found mostly in Canada, Russia, Belarus and Germany [3] as shown in Figure 1.1. Potash is produced worldwide at amounts of 35 million tons per year. As the world's largest potash producer, Canada provides 30% of global potash output as shown in Figure 1.2a. Figure 1.2b shows that Asia is the largest import market for potash. Asia's potash imports account for 38% of the world's total potash exports. Thailand is the 5th largest importer within Asia. The high demand for potash in Asia is rooted in a significant percentage of the workforce employed in the agricultural sector as well as the region's strong population growth.

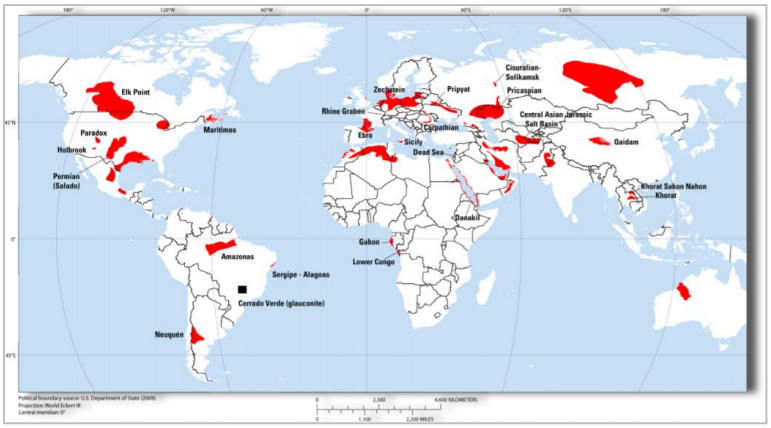

Figure 1.1: World map of significant potash-bearing marine evaporite basins (shown by red polygons) [4].

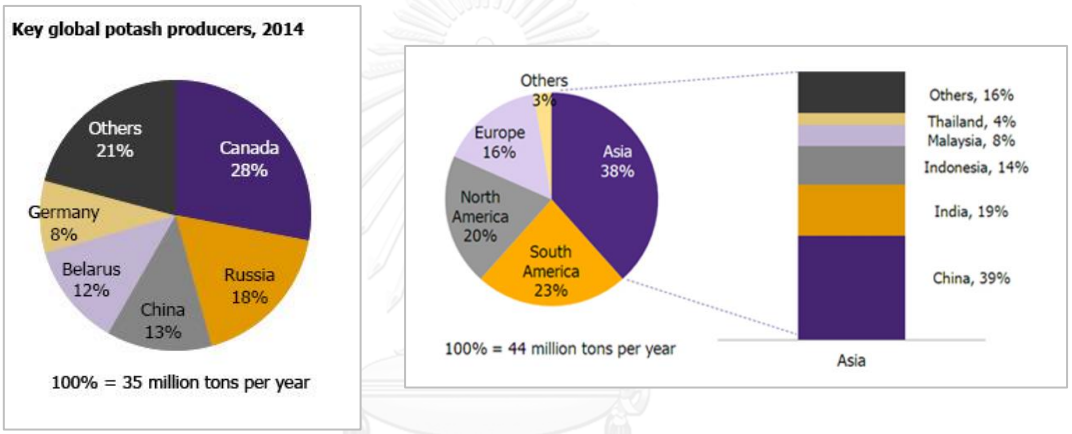

(a) (b)

Figure 1.2: (a) Global potash producers in 2014 and (b) Global potash importers in 2013 [5].

The potash deposits come originally from evaporate deposits and are often buried deep below the earth's surface as shown in Figure 1.3. The natural potash deposit created from the seawater was captured in a basin for millions of years. After the seawater was evaporated, the minerals in the seawater started sedimentation, which most components are sodium chloride (NaCl), potassium chloride (KCl) and magnesium chloride ($MgCl_2$). After that there was a change in the earth crust and the plates have moved to fill these basins and created potash and rock salt deposit within the basin [6].

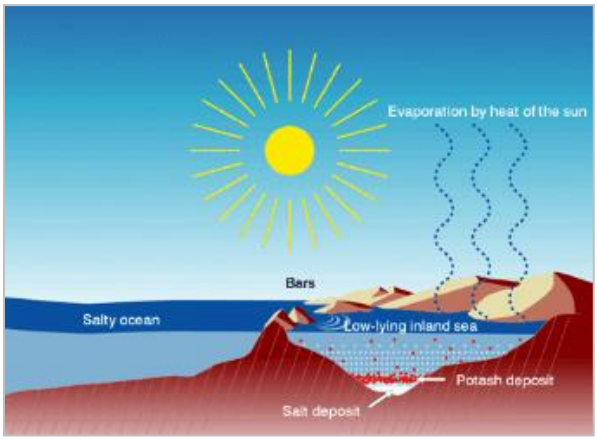

Figure 1.3: The formation of potash deposit [7].

Potash composition is often affected by secondary changes in the primary mineral deposits. The most common minerals in potash ore are listed in Table 1.2. The Sylvite (KCl) and Carnalite ($KCl.MgCl_2.6H_2O$) as dominant potassium minerals, and Halite (NaCl) is a by-product. Gypsum or Anhydrite commonly occurs at the edges of salt deposits and in the overlying strata.

Table 1.2: Minerals and chemical compositions in potash deposits [8]

Mineral name	Chemical composition
Halite	NaCl
Sylvite	KCl
Carnallite	$KCl.MgCl_2.6H_2O$
Kainite	$KMg(SO_4)Cl.3H_2O$
Anhydrite	$CaSO_4$
Gypsum	$CaSO_4.2H_2O$
Polyhalite	$K_2SO_4.\ MgSO_4.2CaSO_4.2H_2O$
Kieserite	$MgSO_4.H_2O$
Kainite	$KCl.MgSO_4.11H_2O$

Potash salt deposits always consist of a combination of several minerals as presented in Figure 1.4. Potash is usually extracted by room and pillar and sometimes longwall mining. Sometimes the solution mining method and evaporation method from brines are also applied.

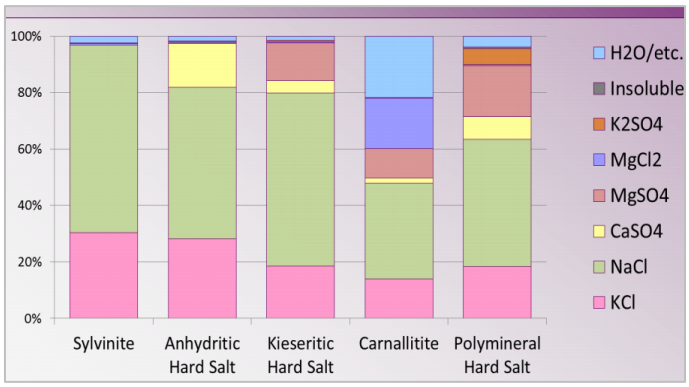

Figure 1.4: Types of potash and chemical composition [9].

The evaporate deposits in the Northeast of Thailand were discovered by the Department of Mineral Resources (DMR) in the 1950's during a groundwater drilling program. The high-grade potash resources were found in Khorat Plateau.

1.3. Potash Deposit in Thailand

Thick beds of rock salt have been found in the Sakon Nakhon and Khorat basins in the Northeastern Thailand. The Northeastern region occupies of about one-third of Thailand. The morphology of this area is known as the Khorat Plateau. The Plateau covers an area about 150,000 square km. The Phu Phan Range separates the Northeast into two basins as shown in Figure 1.5. They are the Khorat Basin (36,000 sq.km) located in the South and the Sakhon Nakhon Basin (21,000 sq.km) at the Northern part of the region. The two basins cover a total area about 60,000 square km [10].

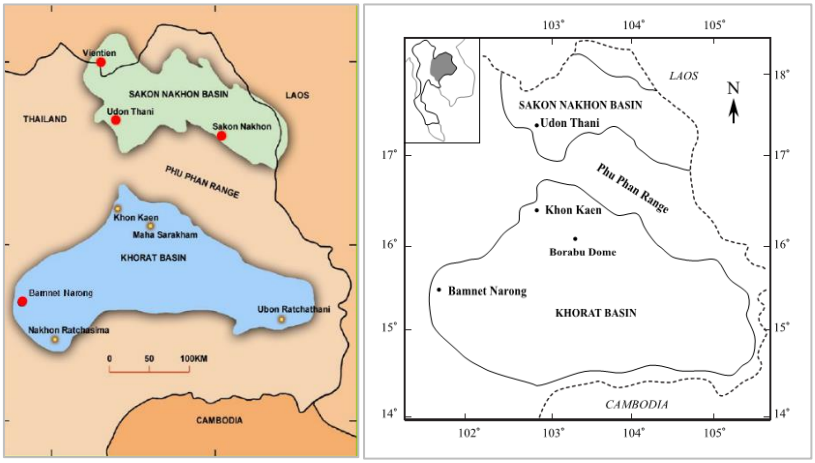

Figure 1.5: Khorat and Sakon Nakhon basins in the Northeast of Thailand [10].

Potash deposits occurred in the Cretaceous Maha Sarakam Formation (Ms). The formation is composed of claystone, shale, siltstone, sandstone, anhydrite, gypsum, potash, and rock salt. The siltstone and shale are in the upper part and anhydrite and salt are in the lower part of formation. The formation was deposited in late Cretaceous. It is underneath the Phu Thok Formation (Pt) and is underlain by sandstone and siltstone of Khok Kruat Formation (Kk) as shown in Figure 1.6.

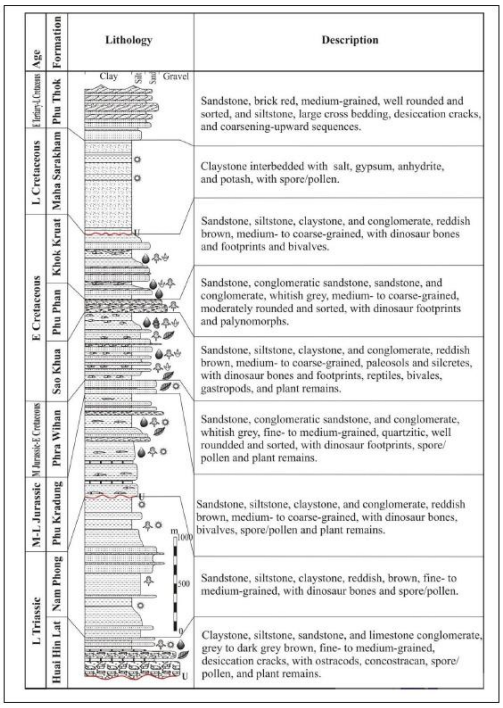

Figure 1.6: Stratigraphic column of the Khorat group [11].

General strata of Maha Sarakham Formation are shown in Figure 1.7. Suwanic and Mohamed studied the stratigraphy of the Maha Sarakham Formation, which can be summarized as follows [11]:

(1) *Basal Anhydrite Member* is found at the base of the Maha Sarakham Formation throughout both the Khorat and the Sakhon Nakhon basins. It conformably overlies the Khok Kruat sandstone of the Khorat Group. It is white to gray in color and has an average thickness of 1m. Its slope is 0-5 degrees.

(2) *Lower Salt Member* is the most widespread of the salt units in the Maha Sarakham Formation. Halite with associated anhydrite is the dominant

mineral. The potash layer can only be found in the upper part of this Member. It consists of high potassium mineral as Sylvite, Tachyhydrite and Carnallite.

(3) *Lower Clastics Member* comprises reddish brown claystone, invariably containing randomly oriented fractures filled with halite spar. The color of the claystone may be greenish-gray in the vicinity of the contacts with the underlying and overlying salt units.

(4) *Middle Salt Member* comprises well-bedded Halite with similar repetitive bed forms to those found in the upper part of the Lower salt.

(5) *Middle Clastics Member* consists of massive red to purple claystone and silty mudstone.

(6) *Upper Salt Member,* the halite found in this member is colorless to milky white, and brown to orange. The mineral grain sizes vary from moderate to fine.

(7) *Upper Clastics Member* is the upper most sedimentary rock layer overlying the Maha Sarakham Formation. It consists of pale reddish-brown silty claystone with minor sandy intervals.

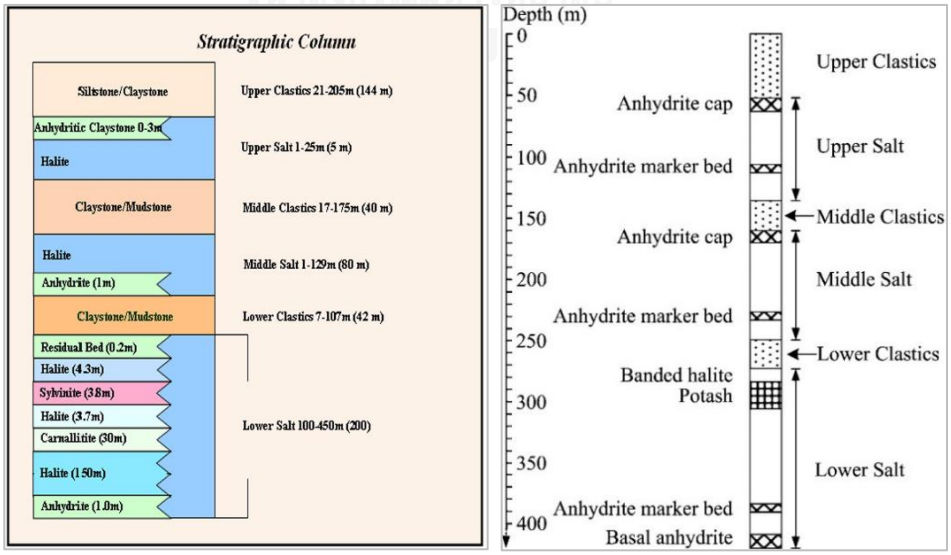

Figure 1.7: General stratigraphy of Maha Sarakham Formation [10].

1.4. Udon South Potash Project (Udon Thani Province, Thailand)

1.4.1. Project description

The Udon South Potash Deposit in Udon Thani Province is one of large potash deposits in Thailand. The potash industries have been proposed to produce the fertilizer grade potash (potassium chloride, KCl) since the 1990s by Asia Pacific Potash Corporation Company Limited (APPC). In 1984, Asia Pacific Potash Corporation Limited (APPC) signed the Udon Thani Potash Concession Agreement with the Government of the Kingdom of Thailand with the objective of exploring, developing and marketing a commercial deposit of Sylvinite type potash rock. The two deposits referred to as Udon South and Udon North are proven to contain what are considered to be amongst the highest-grade potash deposits in the world.

The ***Udon South Potash Project*** locates approximately 15 kilometers Southeast of Udon Thani. Udon South Potash Deposit is a high grade Sylvinite ore, which is a mixture of potassium chloride (Sylvite, KCl) and sodium chloride (Halite, NaCl). The total geological resource is 267.79 million tons of Sylvinite, and the mineable reserve is about 100.5 million tons. The raw ore used for KCl production has an average K_2O content of 23.77%, this equates to a KCl content of 37.63% in the raw ore. The mine life period is 21 years with planned production of 2.1 million ton of KCl per year [12]. The chemical compositions of Sylvinite potash ore in Udon South Deposit as shown in Table 1.3.

Table 1.3: Chemical compositions of Sylvinite potash ore in Udon South Deposit [10]

Composition	Percentage (%)
Potassium chloride, KCl	37.63
Sodium chloride, NaCl	57.40
$MgCl_2$	0.94
$CaSO_4$	0.57
Insolubles	2.40
H_2O	1.07
Total	100.0

General strata of Udon South Potash Deposit are shown in Figure 1.8. Table 1.4 shows the stratigraphic of the deposit in each layer member and its depth.

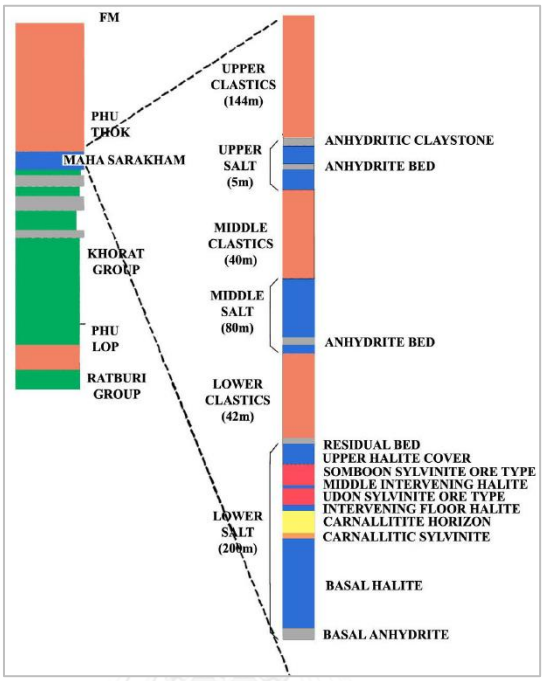

Figure 1.8: Stratigraphy of Maha Sarakham Formation in Udon South Deposit [10].

Table 1.4: Stratigraphic units of Udon South Deposit [12]

Formation	Layer	Depth (m)
Maha Sarakham (Ms)	Upper Clastics Member, UCM	142.5
	Upper Salts Member, USM	146.9
	Middle Clastics Member, MCM	183.9
	Middle Salts Member, MSM	268.9
	Lower Clastics Member, LCM	309
	Upper Halite Cover Unit, UHCU	315.82
	Sylvinite Unit, SU	
	Intervening Floor Halite Unit, IFHU	
	Carnalite Horizon Unit, CHU	
	Basal Halite Unit, BHU	404.02
	Basal Anhydrite Unit, BAU	406.02
Khok Kruat (Kk)	Conglomerate, Sandstone	420

Udon South Potash mine is the room and pillar mining. It starts with a decline to connect to the development tunnels, and to the mining panels to excavate the Sylvinite ore type at the depth of 300 - 380 m. as shown in Figure 1.9.

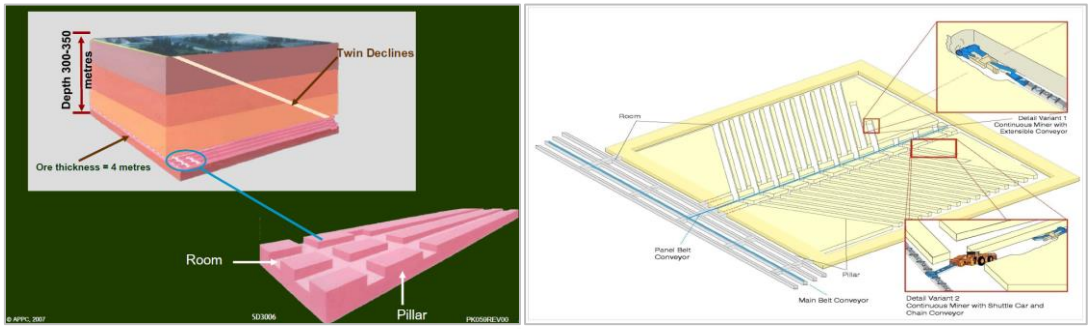

Figure 1.9: The room and pillar mining method at Udon South Potash Deposit [10].

The density of the Sylvinite mineral deposit is 2.07 ton/cubic meter. The thickness of the deposit is varied from 1 to 10 m. (average 3.8 m.). The depth of potash layer is varied from 160 to 420 meters [10]. The potash ore that extracted from the mine will be transported to the ore processing plant for separating potash ore from salt and clay mixture. The Sylvite ore processing in Udon South Potash Deposit is presented as follows.

1.4.2. Sylvite Potash ore processing

In Udon South Potash Deposit, the flotation and the hot leaching and crystallization are applied. The flotation is the most suitable for Sylvite. It yields low cost of production and consume less energy. Although the crystallization uses high energy and water consumption, but it increases the produced potash ore and reduces the ore loss in the brine in the ore dressing process [12]. Alternatively, a process route comprising hot leaching of ore, brine evaporation followed by KCl crystallization would also be possible in order to minimize the amounts of disposal brine. The evaporation of brine enables a further possible production of an additional NaCl product with a purity of at least 99% NaCl. The $MgCl_2$ control crystallization is used to release and control the amount of magnesium content in the process. $MgCl_2$ is removed with the disposal brine after Mg control crystallization [12].

The potash processing activities generate waste products including solid tailings and brines. The mass and volume balance amongst extracted ore, products and wastes as followed.

1.4.3. Potash wastes from ore processing

The material balance from production of KCl in Udon South Potash Deposit are showed in Figure 1.10. The ore dressing plant design capacity is 6,003,000 tons a year. The plant produces concentrate at average of 2.1 million tons per year. The solid tailing is generated approximately 3.8 million tons per year. It will produce a by-product, sodium chloride salt of 103,000 tons/year. The processing plant also generates the disposal brine with an average amount of 167,068 ton per year (130,522 m^3/year) [10].

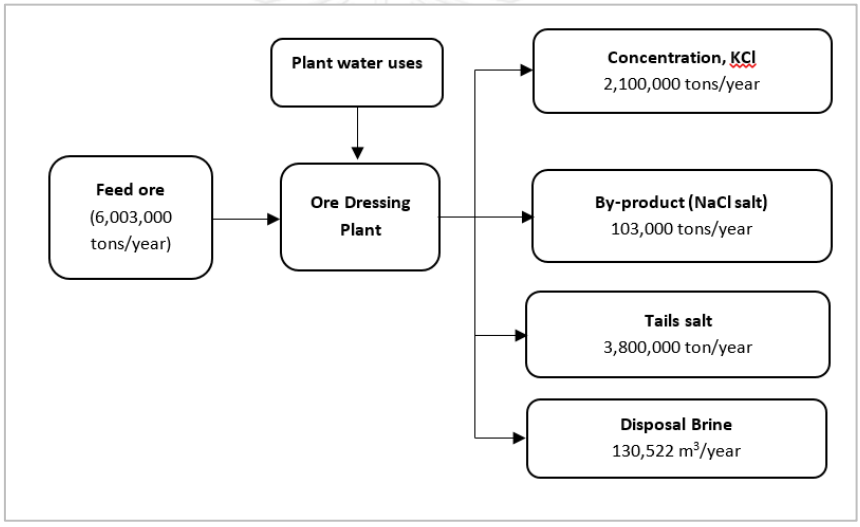

Figure 1.10: The material balance at potash production in APPC project [12].

The solid tailing accumulated on surface area and the release of brine to the local environment is the prime environmental problem facing the potash mining industry. To reduce the environmental impacts, it requires strategies to dispose these wastes. There are many waste disposal options available in potash industry such as:

- Intentional placement of wastes on or in land (tailings pile, evaporation pond);
- Surface discharge to the ocean or river;
- Deep well injection into the underground formations, and

- Backfill into the underground workings and emplacement as hydraulic backfill to support the worked-out underground and minimize the land subsidence.

In Udon South Potash mine, the slurry backfill, tailing pile and evaporation pond are applied for brine and tailing management as shown in Figure 1.11. In slurry backfill, the brine is added to the solid tailings and the resulting slurry is pumped for backfill. The diagram of a slurry backfill plant is showed in Figure 1.12. The slurry will be transported as a suspension from the surface to mine cavities by a closed pipeline system. This slurry backfill technology is a very efficient backfill method, because of its combination of tailings and brine disposal.

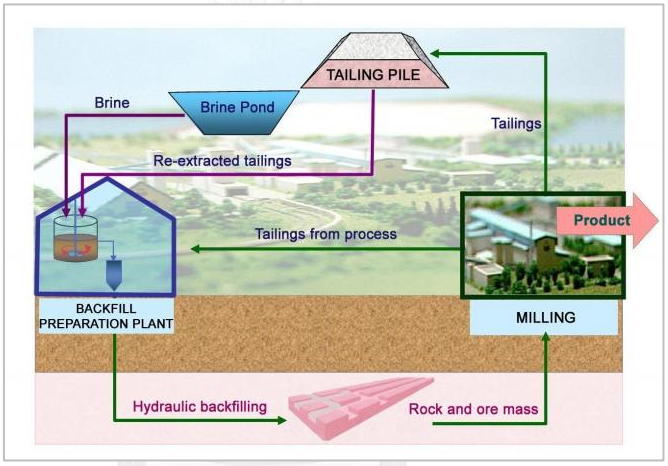

Figure 1.11: Brine and tailing management in Udon South Potash mine [10].

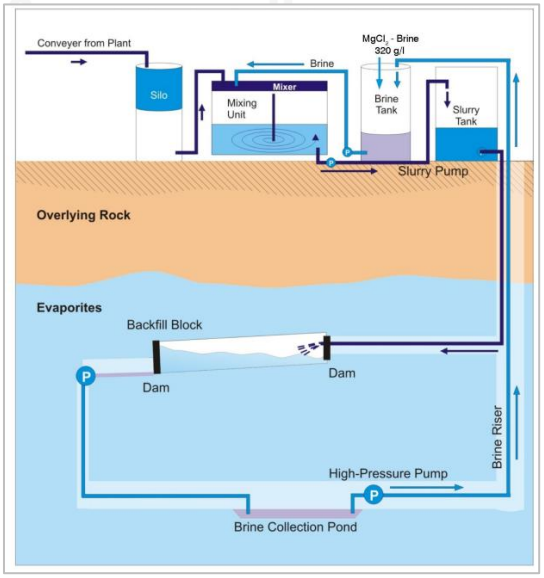

Figure 1.12: Diagram of a slurry backfill plant [12].

Therefore, the alternative approaches for the solid tailing and liquid brine waste disposal will be investigated in this study.

1.5. Objectives of the study

The disposal program of mine wastes including brine and solid tailing produced by the Udon South Potash Deposit in Thailand are the topic of this thesis. The overall objective is to introduce the solidification and deep well injection waste treatment programs in taking care of the solid tailing and liquid brine waste, respectively. To achieve the above objective, this research work will perform:

(1) Provides the procedures and experimental framework for solidification of solid tailing. The experimental results will determine the maximum solid tailing that can be solidified into the concrete block.

(2) Provides the procedures and input parameters for GEM Simulation as deep well injection method for liquid brine waste disposal program. The results from the model will be the maximum amount of brine that can be injected into the deep groundwater formation utilizing the volume of eliminated brine from processing plant.

1.6. Thesis organization

This thesis consists of five chapters. Each chapter provides the following.

Chapter 1 provides background, study area, objectives, and summary of the outline of the research.

Chapter 2 presents a literature reviews on applied disposal methods and previous researches related to research purpose of this study. The chapter explains theories and concepts related to the solidification method and deep well injection.

Chapter 3 shows the methodology of experimental work of solidification method for solid tailing (describing material preparation and procedures), and the GEM

Simulation Model for brine injection (describing reservoir model description, grid discretization, and fluid properties).

Chapter 4 exhibits results and discussions that obtained from the experiment and simulation.

Chapter 5 provides the conclusions on the effectiveness of two alternatives approaches on disposal of potash wastes in Udon South Potash Deposit in terms of the amount of wastes and environmental impacts. From the results of this research, the recommendations will be made.

CHAPTER 2

THEORIES AND LITERATURE REVIEWS

This research work investigates the two potash mine waste disposal programs; solidification of solid tailing and deep well injection of liquid brine waste. The previous studied related to these methods will be discussed in turn.

2.1. Solidification method

Solidification is the method that the waste is solidified by binding materials. The diagram of solidification method is showed in Figure 2.1. The inert materials commonly used are processing solid tailings, sand or gravel, waste rock. Binding agents, such as Portland cement, slag, lime or fly ash, are applied to improve the mechanical properties of the solidified block. The advantages of cementitious solidification include the wide availability of cementitious reagents, which are inexpensive and easy to operate. Among them, Portland cement is the most commonly used [13]. In some case, chemical additives are employed to decrease of permeability and encapsulate the hazardous constituents of the wastes. The solidification can accomplish: 1) decreases surface area of a waste's mass through which transfer/contaminant leakage can occur, and 2) prevents the transport by eliminating or significantly hindering the mobility of contaminants in wastes.

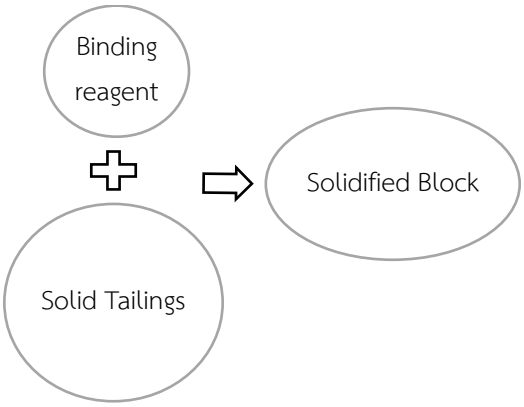

Figure 2.1: Diagram of solidification technique.

By this solidification method, disposal and usage of solid waste materials from potash processing process can minimize significantly the environmental impact and the cost for backfill materials. Besides, solidified tailing concrete block as mine backfill can stabilize excavations and minimize convergences and subsidence of the underground mine.

2.2. Deep well injection method

2.2.1. Introduction

Deep well injection is the method that the fluid is injected into deep underground formation, which is the porous rock such as sandstone or limestone as shown in Figure 2.2. Injected fluids may include water, wastewater, brine (salt water), or water mixed with chemicals.

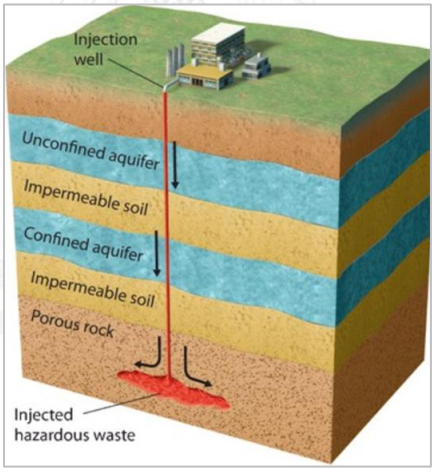

Figure 2.2: Injection well [14].

Injection wells may vary in depth from a few hundred feet to several thousand feet depending on the class of well used, geological considerations, the depth to groundwater aquifers at the selected site. The average injection well is about 2,000 ft. deep (about 1 mile). Deep well injection is presently applied worldwide for disposal of industrial, municipal and liquid hazardous wastes, storing CO_2, enhancing oil production and solution mining. Deep well injection is a proven liquid wastes disposal technology. Deep well injection of liquid wastes into underground formations initiated

in the 1930s by the US petroleum industry, which had an increasing need to dispose of saline water co-produced with oil and gas [15]. Under the Federal UIC regulations, there are currently six different well classifications as shown in Table 2.1 [16].

Table 2.1: Classification of injection wells

Class	Description
I	Industrial and municipal waste disposal wells
II	Oil and gas related injection wells
III	Solution mining wells
IV	Shallow hazardous and radioactive waste injection wells
V	Wells used to inject fluids not classified in other 4 well classes
VI	Geologic sequestration wells, Carbon dioxide (CO_2)

As can be seen in Table 2.1, Class V well is used to inject non-hazardous fluids underground. Class V wells include any wells that are not already classified as Classes I-IV or Class VI wells. Therefore, to dispose the brine into the underground formation, the well is called the brine disposal well, and it is categorized as Class V underground injection well.

In brine injection, a 3D fluid flow GEM Simulator can be used to model and analyze the pressure rise, and fluid migration following brine injection. Brine phase densities and viscosities are calculated as a function of pressure, temperature, and salinity. The Rowe and Chou correlation was used for densities, and the Kestin correlation was used for viscosities. The relevant theories and concepts of simulation are described as follows.

2.2.2. Theories and concepts of GEM simulation

GEM Simulation Model was created by Computer Modelling Group (CMG) program, which is the simulation software to build the 3D model. GEM is an advanced general Equation-of-State (EoS) compositional simulator that can be applied to the three-phase multi-component fluids flow model. Peng – Robinson is the Equation-of-State used to predict the phase equilibrium of composition and density of phase. At the

beginning, Cartesian grid is set to create grid which represents a geological formation. In this case, the permit of CMG program for academic purpose is only set at maximum 10,000 grids in I, J, K directions. Afterwards, component properties including components of fluid in formation, rock fluid type and initial conditions are specified. In the well and recurrent step, the important input parameters are injection rate and fracture pressure that can affect the storage capacity of brine. Finally, validation of dataset and normal run are performed [17]. The results of program show in 3D model plots. The flowchart of GEM Simulation is presented in Figure 2.3.

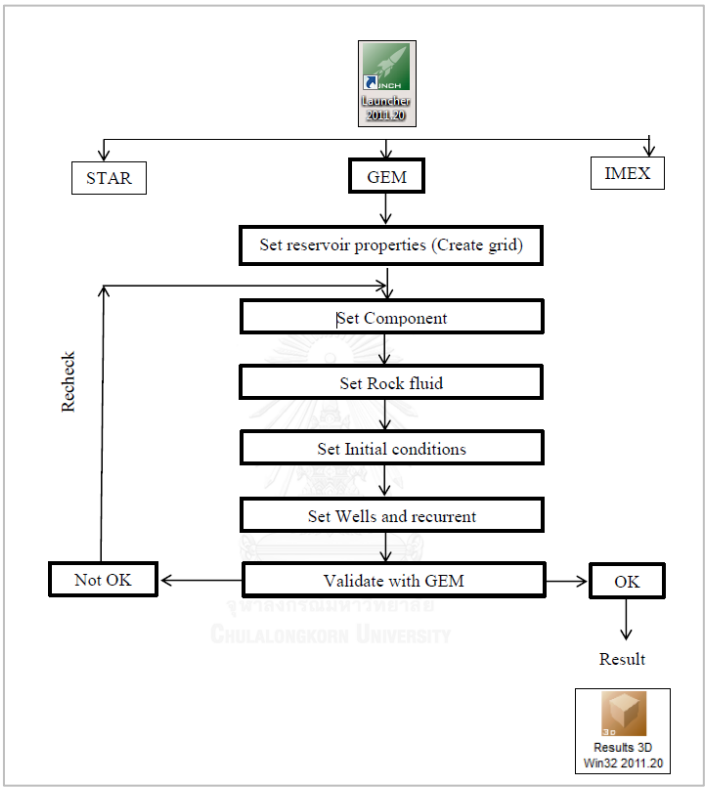

Figure 2.3: Flowchart of GEM simulation in CMG program [18].

To apply GEM Simulation as deep well injection method for liquid brine waste, the basic knowledge and theory of brine geological storage are presented.

❖ **Geological conditions (Properties of rock)**

Porosity

Pore space or porosity in rock gives ability to absorb and hold fluid. Porosity is measured as a percent of total rock volume. It is a proportion of pore space in rock

volume. Porosity of rock can be calculated by Equation 2.1. The average porosity of sandstone is approximately 10 - 25%.

$$\emptyset = \frac{Volume\ of\ void}{Volume\ of\ total\ rock} = \frac{V_{void}}{V_{rock}} \quad (2.1)$$

Water saturation

Water saturation is the fraction of water in a given pore space. It is expressed in volume/volume, percent or saturation units. The effective water saturation can be calculated by Equation 2.2. Values of S_w can range from 0 (dry) to 1 (saturated).

$$S_w = \frac{V_{water}}{V_{void}} = \frac{V_w}{V_{total} - V_{rock}} \quad (2.2)$$

Permeability

In 1856, Henry Darcy established an equation that describes the flow of a fluid through a porous medium known as Darcy's Law [19]. *Discharge rate* can be calculated by Equation 2.3:

$$Q = -\frac{k\rho g A(h_b - h_a)}{\mu . L} \quad (2.3)$$

where, Q = Volumetric flow rate, m^3/s

μ = Fluid viscosity, Pa.s

L = distance between two points, m

A = Cross sectional area of the aquifer, m^2

ρ = Fluid density, kg/m^3

g = Gravitational acceleration, m/s^2

h_a = Hydraulic head at point a, m

h_b = Hydraulic head at point b, m

If there is a *pressure gradient*, flow will occur from higher pressure towards lower pressure. The greater the pressure gradient, the greater the discharge rate. The hydraulic gradient between any two points and the *pressure loss* (Pa) are represented by the following equation:

$$i = \frac{(h_b - h_a)}{L}$$

$$\Delta P = \rho g(h_b - h_a)$$

The proportionality constant specifically for the flow of water through a porous media is called the *hydraulic conductivity*. Given the value of hydraulic conductivity for a subsurface system, the permeability can be calculated as follows:

$$k = K\frac{\mu}{\rho g} = \frac{Q\mu}{A\frac{\Delta P}{L}} \quad (2.4)$$

where

k = permeability, m^2, k = 1 Darcy = 9.87×10^{-9} cm^2 = 9.87×10^{-13} m^2

K = hydraulic conductivity, m/s

μ = Fluid viscosity, Pa.s or kg/m.s

ρ = Fluid density, kg/m^3

g = Gravitational acceleration, m/s^2

Rock Compressibility

Compressibility describes the amount a rock formation will compact and expand under stress. The compressibility of rock (or formation) is given by the following equation:

$$c_f = \frac{1}{V_p}\left(\frac{\Delta V_p}{\Delta P}\right) = \frac{1}{V_p}\left(\frac{\Delta V_p}{P_2 - P_1}\right) \quad (2.5)$$

Or $$\Delta V_p = c_f V_p \Delta P$$

where, V_p = pore volume, m^3

ΔV_p = change in volume, m^3

ΔP = change in pressure, psi

c_f = rock compressibility, 1/psi

Under static conditions, downward overburden force must be balanced by upward forces of the matrix and fluid in pores. Therefore, $F_{ob} = F_{matrix} + F_{fluid}$

$$P_{ob} = P_{matrix} + P_{fluid} \quad (2.6)$$

As fluid are produced from reservoir, the fluid pressure is reduced in a reservoir while overburden is constant, and the reservoir matrix will compress as the overlying stress is transferred from the water in the pore space to the reservoir matrix (bulk

volume and pore space volume decreases). Conversely, the reservoir matrix will expand as liquid pressure in the reservoir is increased due to fluid injection. When fluid is injected, the water in the interstitial pore space assumes the overlying pressure, allowing the rock formation to decompress and pore space increases. In this way, a reservoir can store more fluid than pore space would indicate. In addition, water itself is compressible, which has a compressibility of 3.3E-6 psi^{-1} [20].

Typical value for the formation compressibility ranges from $3x10^{-6}$ to $25x10^{-6}$ psi^{-1}. The compressibility of consolidated rock formations is typically low compared to unconsolidated materials. Pore compressibility ranges from $3–10x10^{-6}$ psi^{-1} for consolidated rocks to $30–100x10^{-6}$ psi^{-1} for unconsolidated sands. Rocks with a higher compressibility will be able to accommodate more fluid through storage. Although compressibility of rock formations is small, the compressibility of rocks becomes more important in evaluating storage capacities over large areas and thicknesses.

The actual measurement of rock compressibility is expensive, and it is required to have a formation sample. In practical, utilizing Hall correlation to determine rock compressibility is acceptable. The most well-known and used correlation for formation compressibility was developed by Hall, and is a function only of porosity. The Hall correlation is based on laboratory data and is considered reasonable for normally pressured sandstones as shown in Figure 2.4. The rock compressibility can be calculated by Equation 2.7 [21].

$$c_f = 1.87 * 10^{-6} * \emptyset^{-0.415} \quad (2.7)$$

where, c_f = rock compressibility, psi^{-1}

Φ = porosity, %

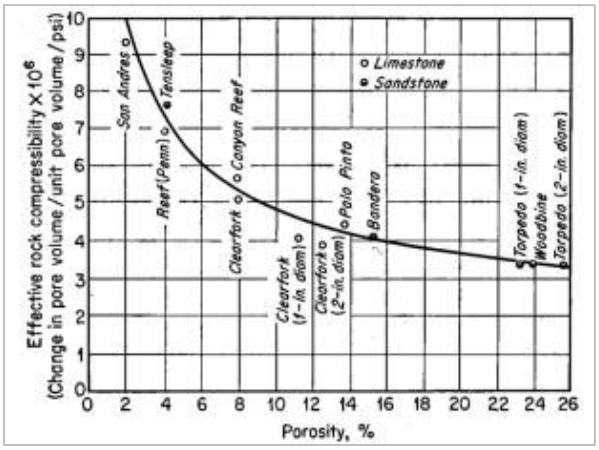

Figure 2.4: Graph based on laboratory tests used for estimation of rock compressibility for fluid flow analysis in reservoirs [21].

Newman also obtained the following correlation when measuring the isothermal compressibility and porosity values in 79 samples of consolidated sandstones. The rock compressibility can be calculated by Equation 2.8 [22].

$$c_f = \frac{97.32\times10^{-6}}{(1+55.8721\emptyset)^{1.42859}} \quad (2.8)$$

This correlation was developed for consolidated sandstones, which have a range of porosity values from $0.02 < \Phi < 0.23$.

❖ **Hydrological conditions**

Salinity

Salinity is the measure of all the salts dissolved in water. Salinity is usually measured in parts per million (ppm) or parts per thousand (1 ppt = 1,000 ppm). The U.S. Geological Survey classified the salinity of water as shown in Table 2.2.

Table 2.2: Water salinity based on dissolved salts [23]

Type of water	Salinity (mg/L)
Fresh	0 – 1,000
Slightly saline	1,000 – 3,000
Moderately saline	3,000 – 10,000
Very saline	10,000 – 35,000
Brine	35,000 and above

The concentration of dissolved solids in deep groundwater varies from much less than sea water to ten times higher than that of sea water. In general, the Total Dissolved Solids (TDS) concentrations increase with depth. Seawater has a salinity of roughly 35,000 ppm, equivalent to 35 grams of salt per one liter (or kilogram) of water [24]. The typical composition of seawater is shown in Table 2.3.

Table 2.3: Composition of seawater of 35,000 ppm (3.5%) [24]

Salt	**Mass (gram)**
$MgCl_2$	5.145
$CaCl_2$	1.155
KCl	0.735
NaCl	23.765
Na_2SO_4	3.990
$NaHCO_3$	0.210
Total	35.0

Since most anions in seawater are chloride ions, salinity can be determined from chloride concentration (Cl^-) as the following equation [24]:

$$\text{Salinity (ppt)} = 0.0018066 \times (Cl^-)\ \text{(mg/L)} \qquad (2.8)$$

Formation Fluid Density

There are two main factors: temperature and salinity of the water that make water more or less dense than fresh water (1,000 kg/m^3). Brine density varied on temperature and salinity at surface pressure is shown in Figure 2.5. When temperature increases, fluid density decreases. The density of seawater of 35,000 mg/L or 35 ppt is 1,025 kg/m^3 at surface pressure, making it heavier than freshwater (1,000 kg/m^3).

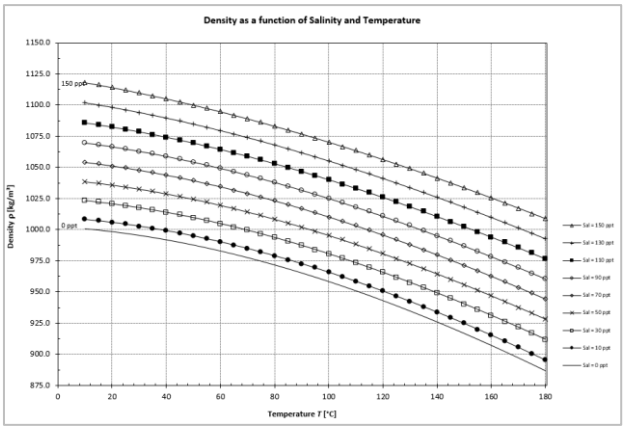

Figure 2.5: Variation in density of sea water as a function of temperature and salinity [25].

The density of water also depends on the pressure. The higher pressure, the denser fluid density [26]. Figure 2.7 shows the density data for brine water of 100,000 ppm and 200,000 ppm (at 122°F and 5,830 psi) are 66 lb/ft^3 and 70 lb/ft^3, respectively [27].

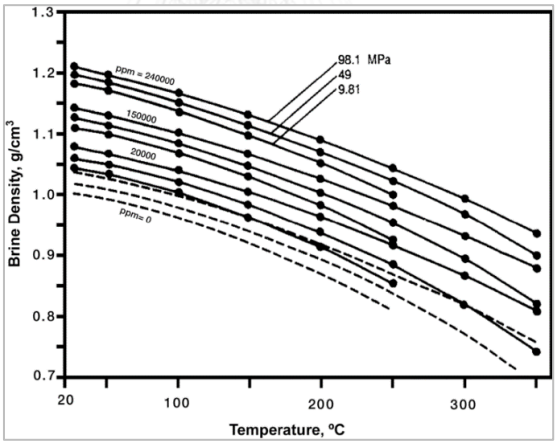

Figure 2.6: The calculated brine densities [26].

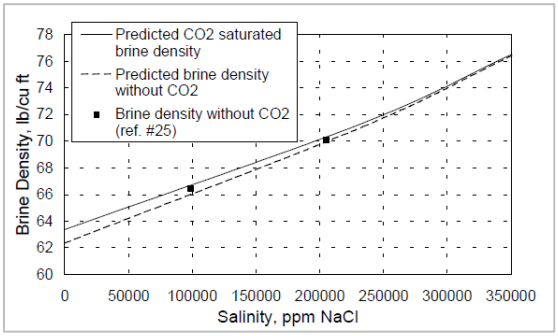

Figure 2.7: Brine density at 122°F and 5,830 psi [27].

Fluid pressure

Hydrostatic pressure is presented as:

$$HP_w = \left(\frac{dP}{dh}\right)_w \times h = \rho_w . g . h \quad (2.9)$$

where, ρw is fluid density, kg/m^3

h is the depth, m

g = Gravitational acceleration, m/s^2

$\left(\frac{dP}{dh}\right)_w$ is hydrostatic pressure gradient, KPa/m or psi/ft

Fluid pressure increases with depth that below water table h.

Formation Pressure

Formation pressure is the pressure of fluid contained in pore space of rock. The initial formation pressure is the average formation pressure measured in a discovery well before any fluid is produced or injected. Units are typically psi (field units) or kilopascals (SI units). Formation pressure is presented in Equation 2.10.

Formation Pressure, P_f = Surface Pressure (SP) + Hydrostatic Pressure (HP)

$$P_f = SP + HP = P_{atm} + \left(\frac{dP}{dh}\right)_w \times h = 14.7 + \rho_w . g . h \ (psia) \quad (2.10)$$

The hydrostatic pressure gradient (psi/ft) is the rate of change in formation fluid pressure with depth (ft). ρ_w is the average formation water density in aquifer. Fluid density is the controlling factor in the normal hydrostatic gradient. Table 2.4 shows typical density ranges and gradients for gas, oil, and water.

Table 2.4: Typical density ranges and gradients for different states [28]

Stages	Normal density range (g/cm^3)	Gradient range (psi/ft)
Gas (gaseous)	0.007-0.30	0.003-1.130
Gas (liquid)	0.2-0.40	0.090-0.174
Oil	0.4-1.12	0.174-0.486
Water	1.0-1.15	0.433-0.500

The concentration of salt in water affects the fluid pressure. The higher salt concentration in water, the higher specific gravity of water will be. The normal hydrostatic pressure gradient for freshwater is 0.433 psi/ft, or 9.792 kPa/m, and 0.465 psi/ft for water with 100,000 ppm TDS. Therefore, to calculate water pressure gradient (P_{grad}), the following equation is used:

$$P_{\text{gradient}} = \text{ave.}\,\rho_w \times 0.433 \frac{\text{psi}}{\text{ft}} \tag{2.11}$$

where, ρ_w = average water density (fresh water density = 1,0 g/cm^3)

In the Northern Thailand area, the pressure gradient is within the range of 0.436-0.452 psi/ft [29].

Fracture pressure

Fracture pressure is the stress sufficient to fracture a rock formation. It is related to pore fluid overpressure. The fracture pressure can be determined from leak-off tests. There are many equations to determine the fracture pressure, one of them is the *Hubbert and Willis* equation. The fundamental principal of the fracture pressure is "the minimum wellbore pressure required to extend an existing fracture, it is given as the pressure needed to overcome the minimum principle stress" [30].

$$P_{ff} = \sigma_{min} + P_f \tag{2.12}$$

The minimum principle stress in the shallow sediments is approximately one-third the matrix stress resulting from weight of the overburden. The fracturing pressure can be calculated by Equation 2.13.

$$P_{ff} = \frac{\sigma_{ob} + 2P_f}{3} \tag{2.13}$$

where, P_{ff} = Formation fracture pressure, KPa

P_f = Formation pressure or pore pressure, KPa

σ_{min} = Minimum matrix stress, KPa

σ_{ob} = Vertical overburden stress, KPa. It can be calculated by Equation 2.14

$$\sigma_{ob} = g\rho_g D_S - \frac{g(\rho_g - \rho_l)\phi_o}{K}\left(1 - e^{-KD_S}\right) \quad (2.14)$$

where, ρ_g = Average grain density, g/cm^3

ρ_l = Average pore fluid density, g/cm^3

g = Gravitational acceleration, m/s^2

D_s = Top formation, m

Φ_0 = Surface porosity, %

K = Porosity decline constant

The fracture pressure can also be calculated by the *fracture gradient*. The fracture gradient is expressed by:

$$F_{min} = \frac{1}{3}\left(1 + \frac{2P}{D}\right) \quad (2.15)$$

where, F_{min} = Fracture gradient, psi/ft or KPa/m

P/D = Pore pressure gradient, psi/ft or KPa/m. It is normally 0.45 psi/ft or 10.5 KPa/m

Bottom Hole Pressure, BHP

Bottom Hole Pressure is the pressure of a well at the bottom of the hole or wellbore. Basically, maximum BHP is about 90% of fracture pressure. Exercising minimum safety requirement of 10 per cent, BHP is expressed by:

$$BHP = P_{fracture} \times 0.9 \quad (2.16)$$

where, BHP = Bottom Hole Pressure, KPa

$P_{fracture}$ = Formation fracture pressure, KPa

Formation Fluid Temperature

Temperatures increase with depth as expressed by the geothermal gradient as shown in Equation 2.17. Some variations in the geothermal gradient occur due to groundwater flow regime, tectonic action, measurement method, and other factors. It is about 25°C per km of depth (1°F per 70 feet of depth) [31].

Aquifer temperature (^{o}F) = Surface temperature (^{o}F) + 0.017 x Depth (ft) (2.17)

where the geothermal gradient = 0.017 ^{o}F/ft.

2.3. Literature Reviews

The literature reviews separate into three parts. The first part deals with the general aspects of waste management in potash mine. The second and third specifically deal with the waste management of solid tailing and liquid brine waste by solidification and deep well injection method, respectively.

2.3.1. General introduction of waste management methods

The mineral processing of potash production leads to over 78% of solid or liquid tailings as shown in Figure 2.8. Brines may be disposed of by the reinjection into deep aquifers below the orebodies, discharging into the surface water (ocean or river), collection in evaporation ponds, and releasing into local rivers. The solid tailing may be backed with brine as the slurry backfill material into the underground mine-out room or is stacked into large piles near the mine site.

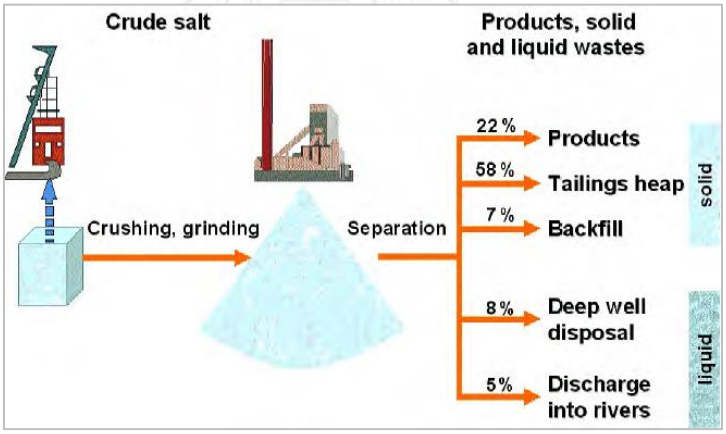

Figure 2.8: Solid and liquid tailings management after mineral processing [32].

The selection of potash waste disposal techniques depends on many factors. Mickley et al. (2001) identified the factors that influence the selection of a waste disposal method. These include (1) the quantity and quality of the waste (including tailings and brine), (2) composition of the concentrate, (3) geographical location of the mine site, and (4) availability of receiving site, permissibility of the option, public acceptance, capital and operating costs [33]. The cost of disposal depends on the

characteristics of the tailings and rejected brine, mass of tailings and volume of brine to be disposed of, and the nature of the disposal environment [34].

The mass and volume balance between extracted ore, products and wastes for two types of potash ore are shown in Figure 2.9. A low-grade Carnallitite ore and a high-grade Sylvinite ore show that the amount of product is relative small compared with the amount of waste material [3]. These relations are strongly controlled by the quality of the ore. The amount of disposal brine is higher for hot leaching of carnallitic ore as in Figure 2.9a, while the amount of solid tailings is higher for the sylvinite processing by flotation as in Figure 2.9b.

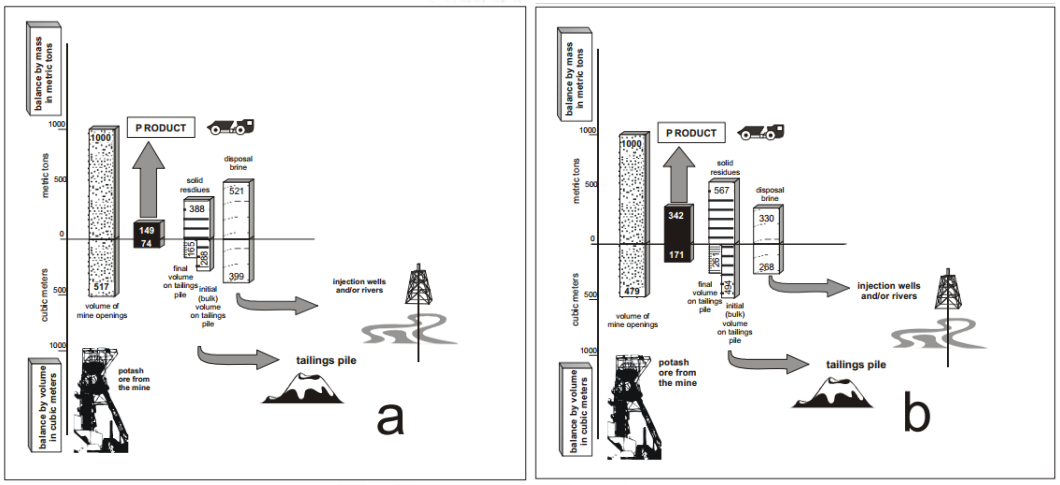

Figure 2.9: Mass and volume balance between extracted ore, final potash product, solid, and liquid waste material [3].

(a) Hot leaching of low-grade Carnallitite ore (in Germany)

(b) Flotation of high-grade Sylvinite ore (in Russia, Western Canada, North-Central Thailand)

2.3.2. Solidification method

In the research of Masniyom (2009), the minimum Uniaxial Compressive Strength (UCS) of 5 MPa is the requirement of backfilling materials at 28 days in Thailand potash mine [35]. Same as in the cemented backfill, the strength properties of concrete block are affected by such factors as cement content, curing conditions, water cement ratio, cement type, aggregate, and curing time.

❖ *Particle size distribution*

In 1981, Herget found that a backfill which contains well graded particles should offers more resistance to displacement and settlement than one with uniformly graded particles as shown in Figure 2.10. The research also found that permeability decreases with a decrease in the effective size of the material, which is the 10% passing size according to the grain size distribution. Therefore, backfill materials with a high percentage of minus 75 μm material yield a low permeability [35].

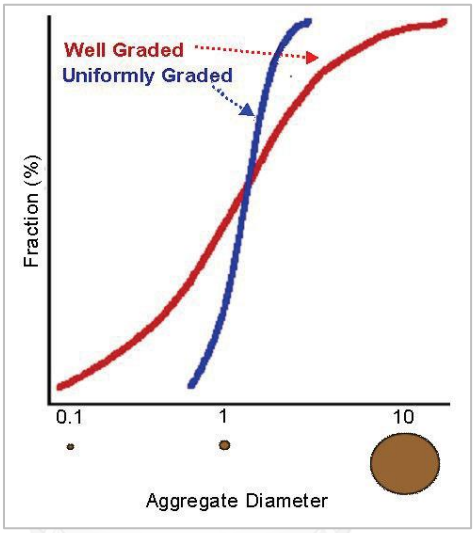

Figure 2.10: Typical Particle Size Distribution (PSD) curves for uniformly graded (A) and well graded (B) aggregate materials [35].

❖ *Cement content and Water to Cement (W/C) ratio*

For normal concrete, the compressive strength depends on the binder factor as well as the water to binder ratio. Increasing the binder factor or decreasing water to binder ratio will increase the compressive strength [35]. Figure 2.11 shows that the strength increases proportionally with the increasing cement content [36]. In 1983, Arioglu investigated how Cemented Rockfill (CRF) strength properties altered when the cement content varied and concluded that the compressive and tensile strengths, and the cohesion increase with increased cement content [37].

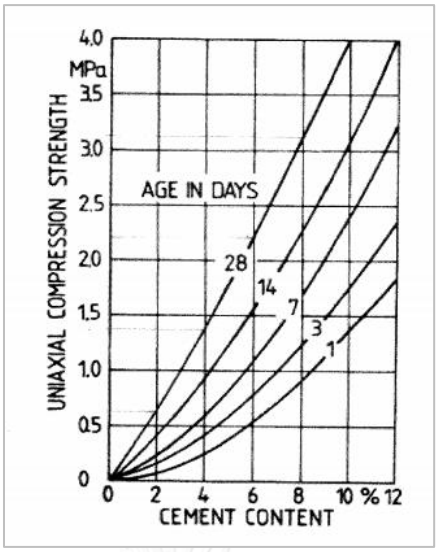

Figure 2.11: UCS strength with optimum Water to Cement ratio versus cement content for Cemented Rockfill [36].

Koo, D.S et al. recorded that the compressive strength of the cement solidification of metal hydroxide waste with waste/cement of 2.0 is 132 kg.f/cm^2, which is lower than the compressive strength of the cement solidification with waste/cement of 1.5 which is about 166 kg.f/cm^2 [38]. Figure 2.12 shows the reduction in water/cement (W/C) ratio leads to an increase in strength of concrete.

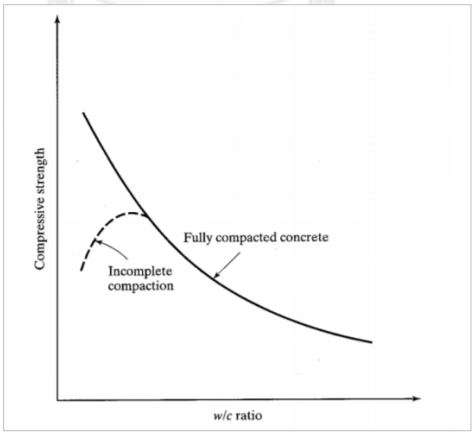

Figure 2.12: Relationship between compressive strength and W/C ratio [39].

Marar, K. (2011) investigated the effect of cement content and Water/Cement ratio on fresh concrete properties without admixtures. The experiments were prepared on eight different concrete mixtures using ordinary Portland cement (cement contents of 300, 350, 400, 450, 500, 550, 600 and 650 kg/m^3). The W/C ratio varied from 0.43 to

0.79. The results showed that increasing amount of cement in the mix and decreasing W/C ratio increased the strength, from 23.4 MPa at W/C = 0.79 to 57.1 MPa at W/C = 0.43 [40]. It is well known that the strength of concrete increases with increasing in cement content, because the Water/Cement ratio can be decreased without loss in workability. A logarithmic relationship between Water/Cement ratio and cement content gives a correlation coefficient of 0.9893 as shown in Figure 2.13.

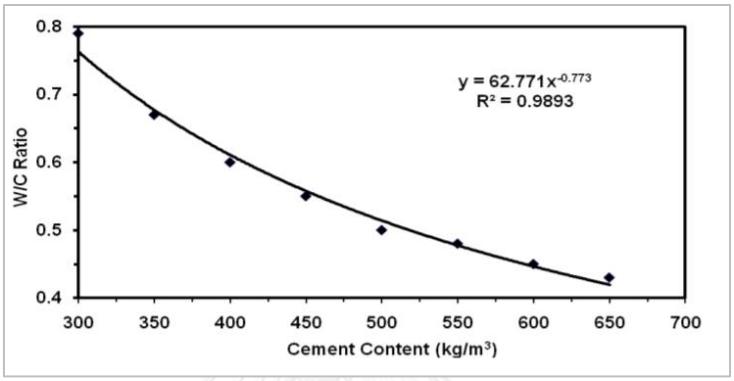

Figure 2.13: Relation between W/C ratio and cement content [40].

For a given cement content, the workability of the concrete is reduced if the Water/Cement ratio is reduced. A lower Water/Cement ratio means less water, or more cement and lower workability. Therefore, to achieve the strength requirement, the Water/Cement ratio should be reasonably adjusted to ensure the workability of the mixtures.

❖ *Aggregate*

Ruiz (1966) investigated the effects of aggregate content on the behavior of concrete, it was found that the compressive strength of concrete increases along with an increase in coarse aggregate content, up to a critical volume of aggregate, and then decreases. The initial increase is due to a reduction in the volume of voids with the addition of aggregate.

Rozalija Kozul and David Darwin (1997) also mentioned that the high-strength concrete containing basalt and normal-strength concrete containing basalt or limestone yield higher compressive strengths with higher coarse aggregate contents than with lower coarse aggregate contents [41].

❖ *Curing time*

The compressive strength of concrete is affected by curing time. It is generally accepted that the majority of the concrete strength has been achieved within 28 days curing time. Figure 2.14 - Figure 2.15 show that the compressive strength of concrete increase over time.

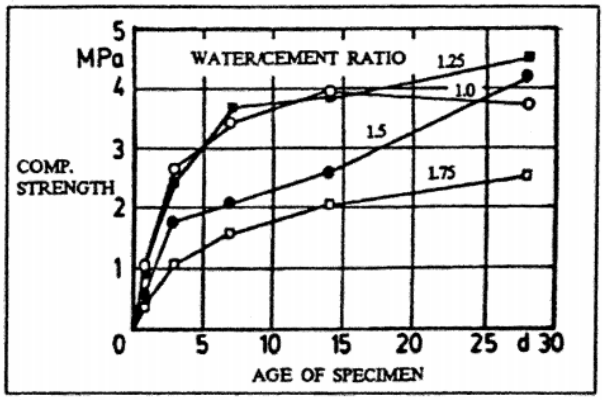

Figure 2.14: UCS strength of mixtures with different W/C ratios versus age of concrete (curing time) [36].

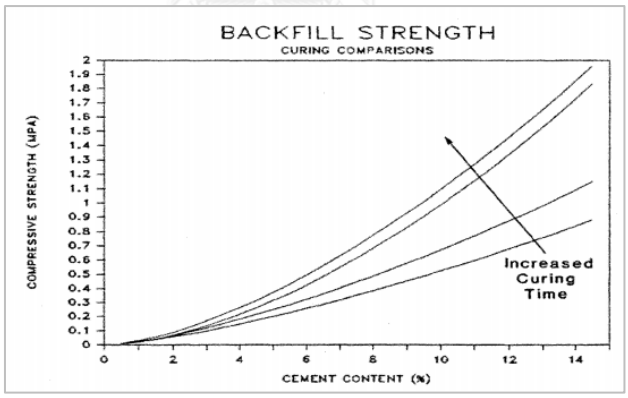

Figure 2.15: UCS strength versus cement content for a 7, 14, 28 and 90 day curing period [42].

2.3.3. Deep well injection method

Deep well injection can offer a feasible and reliable solution for disposing the rejected brine. This method is widely used for brine disposal from inland desalination plants and considered as a viable option [43]. In this method, a system of disposal wells is used to inject brine from desalination plants into an acceptable, confined, deep

underground aquifers that are not used for drinking water. The saline aquifers are geological formations that are saturated with brine water. The operating life of an injection well may be related to the volume of injected waste, because the distance injected waste can be allowed to spread laterally may be restricted by law or by other considerations. Therefore, the suitable locations for brine disposal wells can be potentially in areas with aquifers that can accept larger amounts of brine over the entire potash mine life.

Brine has been continuously injected since 1997 at several carefully evaluated sites to depths ranging between 1,300 and 2,000 meters. The construction of brine disposal well is intended to protect groundwater and require multiple layers of cement and steel to ensure that usable quality water is protected.

❖ *Criteria for well injection*

Performance of injection wells during the deep well injection of liquid brine wastes is critically dependent upon:

(1) the physical and chemical properties of the brine.

Saripalli et al. [15] identified that the high dissolved solids content of the liquid waste indicates that brine movement is probably very slow under natural condition. The injectivity is impacted by chemical and physical quality of the injected fluid, injection rate and pressure, as well as the nature and physical properties of subterranean strata. The high total suspended solid (TSS) in fluids, low injection rate, low injection pressure, and low porosity and permeability of the well strata will lead the rapid well plugging and diminished injectivity, hence poor injection performance.

(2) the hydrogeologic and geochemical character of the aquifer. The formation should be relatively thick with an adequate confining layer. Porosity and permeability are principal factors used to determine the suitability of a potential disposal formation. Adequate porosity and permeability to accept fluids is necessary for an aquifer to be considered for use as a disposal

reservoir [44]. The formation should be essentially homogeneous and isotropic.

The native ground water in the formation should be saline. The physical or chemical interactions between the fluid waste and the aquifer minerals or fluids can cause plugging of the aquifer pores and consequent loss of intake capacity. In 1959, Selm and Hulse listed the reactions between injected and interstitial fluids that can cause the formation of plugging precipitates: (1) precipitation of alkaline earth metals such as calcium, barium, strontium, and magnesium as relatively insoluble carbonates, sulfates, orthophosphates, fluorides, and hydroxides; and (2) precipitation of metals such as iron, aluminum, cadmium, zinc, manganese, and chromium as insoluble carbonates, bicarbonates, hydroxides, orthophosphates, and sulfides [45].

(3) the operational parameters such as injection rates and pressure

The intake rate of an injection well is limited, and its operating life may depend on the total quantity of fluid injected and the pore volume of formation as well. The variable limiting the injection rate or well life can be the injection pressure required to dispose of the waste.

Injection pressure is a limiting factor because excessive pressure causes hydraulic fracturing and possible consequent damage to confining strata [46], the pressure capacity of injection well pumps, tubing, and casing is limited.

Besides, the feasibility of subsurface storage as a solution to waste disposal also depends on economics and legal considerations [45].

According to Mark Moody [47], the key geologic issues for large-scale brine disposal are:

- Extent, thickness ⟶ Location
- Porosity ⟶ Capacity

- Permeability ⟶ Injectivity, pressure buildup
- Fracture pressure ⟶ Injection rate limits, safety

According to Mickley [33], the deep well injection is a practical method for brine disposal provided that long-term operation can be maintained, in order to dispose of large volumes of process fluid. It has been applied successfully for brine disposal from several membrane plants in Florida, USA [43]. If the potash industry in Saskatchewan, Canada were to continue to use present waste disposal techniques, the necessary storage volume of liquid waste over a 50-years period would be in the order of 160,000 acre ft (approx. 195 million m^3) [48]. Therefore, the major advantage of using brine disposal well is that it requires minimal land area and can utilize abandoned well sites, which would reduce costs for infrastructure. High reservoir quality and acceptable thickness that make them excellent sites for brine disposal [49]. In Saskatchewan, Canada, the excess brine is disposed of through deep well injection, which is the standard method of brine disposal for all the existing potash mines. The total volume of brine generated annually by ten potash mines in Saskatchewan is 3.0-3.8 million m^3 [48].

However, the deep well injection is feasible only in specific geological and site conditions, it is not feasible in areas subject to earthquakes or where faults are present that can provide a direct hydraulic connection between the receiving aquifer and an overlying potable aquifer [33]. Therefore, prior to drilling any injection well, a careful assessment of geological conditions of well site must be conducted in order to determine the depth and location of suitable porous aquifer reservoirs [43]. Besides, the extra costs involved in conditioning the rejected brine, corrosion and subsequent leakage in the well casing, and seismic activity which could cause damage to the well and subsequently contamination of groundwater [43].

The previous studies applied deep well injection to dispose of mine waste are listed below.

❖ *Belle Plaine Potash mine, Saskatchewan, Canada*

The Belle Plaine mine annually produces 1.1 million tons of potash products via evaporation and crystallization process and production pond. Deep well injection technology was employed to dispose of large quantities excess brine. In 2008, 2.63 million tonnes of salt and 42,000 m^3 of brine mound were produced and injected [50]. According to the Environmental Impact Statement (EIS) for the proposed Belle Plaine Expansion, two deep injection disposal wells have been drilled into the Winnipeg and Deadwood Formation at depths between 2,040 and 2,210 m below the surface. The average brine injection volume is between 3.3 and 4.6 million m^3/year based on data for 2000 to 2005 [51].

❖ *Mosaic Potash Esterhazy K2 Potash mine, Southeast Saskatchewan, Canada*

The Mosaic Potash Esterhazy K2 potash mine is located in Southeast Saskatchewan, approximately 14 km. East of Esterhazy, Saskatchewan. Mosaic Potash Esterhazy K2 uses deep well injection as a disposal strategy for excess brine at the sites. The principal disposal aquifers in the deep subsurface are the Silurian Interlake carbonates and the Cambro-Ordovician Deadwood-Winnipeg Clastics.

They dispose of surplus brine through eight deep injection wells into the Interlake Formation (fractured dolomite). These wells were installed to a depth of about 1,200 m. to 1,400 m. below ground. The formation is about 100 m. thick and 213 m. below the mining level, located at a depth of approximately 1,280 m. [52]. The waters of the Interlake Formation are generally a sodium chloride type, with TDS values typically ranging from 150,000 mg/L to over 300,000 mg/L [50]. The total brine injection required per year between all eight wells varies with mine inflow, precipitation, evaporation, and potash production. The total current brine injection annual capacity is approximately 12,087,000 m^3 (33,115 m^3/day). The brine injection volume in 2007 was 6.3 million m^3. The maximum injection rate of eight wells range from 3,130 m^3/day (well #4) to 5,390 m^3/day (well #7). The average salt concentration of the injected brine is about 25.4%.

While the Deadwood Formations are approximately 2,200 m. beneath the surface. It is 201 m. thick and about 396 m. below the mining levels [52]. The exact number of wells required will be determined based on observed performance during operations. Figure 2.16 shows the brine injection into Deadwood Formations, with the injection rates are 700 - 900 gpm at a pressure of 350 - 850 psi. Injection wells will be spaced at a minimum distance of 500 meters to prevent excessive interference between wells. The injection wells will be cased with steel like the operating wells and are regulated by the Saskatchewan Ministry of Energy and Resources.

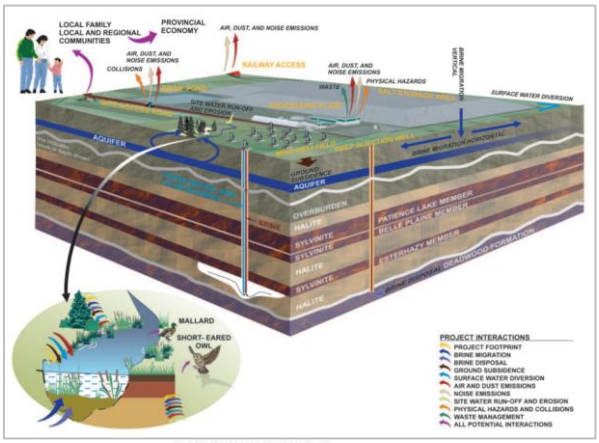

Figure 2.16: Brine injection into Deadwood Formations, Saskatchewan [52].

❖ *Brine disposal injection into Lockport-Newburg Formation, Northeast Ohio, USA*

The Lockport Dolomite ranges from less than 1,500 feet (450 meters) above sea level in Western Ohio and Eastern Kentucky to more than 8,500 feet (2,600 meters) below sea level in Western Pennsylvania. Thickness of the Lockport Dolomite ranges from zero feet in Eastern Kentucky to more than 500 feet (150 meters) in central Pennsylvania. The Lockport-Newburg is a common formation for injection in Northeast Ohio. The formation is a Silurian carbonate rock type [53]. The 3D fluid flow GEM Simulator was used to model and analyze the pressure rise, fluid migration following brine injection into Lockport Dolomite Formation.

The model consisted of 36,750 grids that spanned about 4,500 ft in either direction from the injection well. The depth of well is 2,070 ft (630 m.). The 344 ft-thick model was split into an upper zone and a lower zone, the 10-layer upper zone

is less porous and more confining than the 20-layer lower zone. The upper zone has an average of 2% porosity and 0.009 mD permeability, while the lower zone has an average of 7% porosity and 43 mD permeability. A 3D-Cartesian grid, used for more resolution closer to the injection well, can also be seen in Figure 2.17.

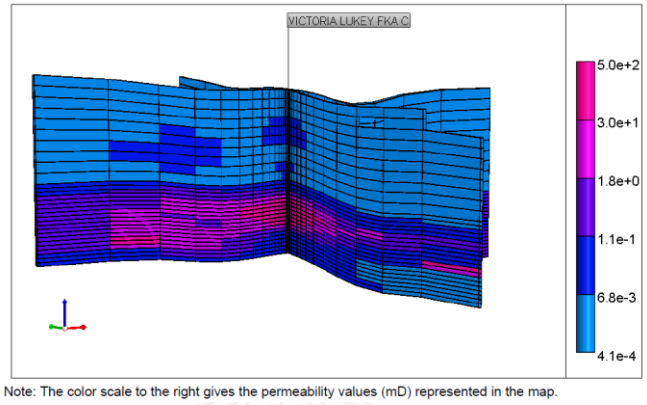

Figure 2.17: Lockport permeability model [53].

This study initialized the model to be at hydrostatic pressure (assuming a pressure gradient of 0.45 psi/ft) and to be filled with native brine with salinity of 278,000 ppm. The injected brine was of lower salinity than the native brine, about 250,000 ppm. The well was operated at a constant injection rate of 300 bbl/day (48 m^3/day) for a 10-year injection period followed by 40 years of post-injection monitoring with minimum BHP constraint of 2,000 psi. Figure 2.18 shows the simulation result at a constant injection rate over time.

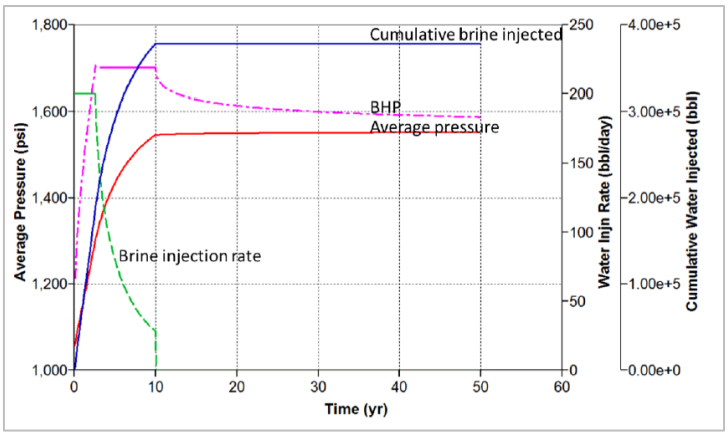

Figure 2.18: Brine injection simulation results at a constant injection rate over time [53].

In this model, pressure migrated to the boundaries and overlying formations, leading to a higher average pressure compared to the initial conditions (residual pressure of 500 psi (3,447 KPa) was present at the end of 10-years injection period. Figure 2.19 shows the salinity profile for a chosen model slice. The study observed that the injected brine filled the reservoir, with minimal brine migration after injection stopped.

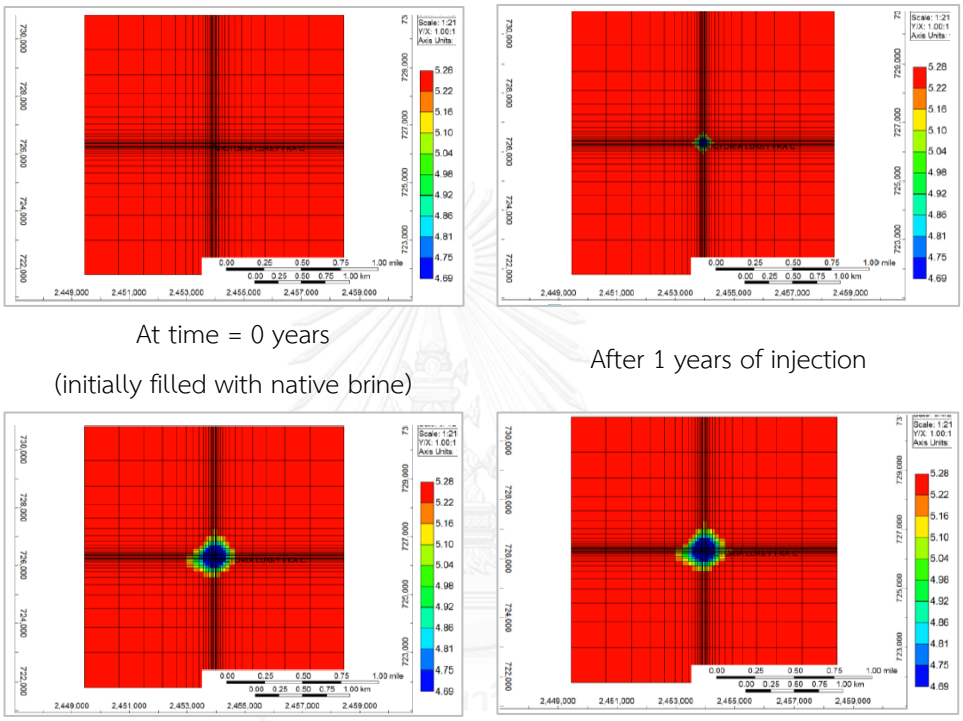

At time = 0 years
(initially filled with native brine)

After 1 years of injection

End of injection

End of post-injection monitoring period

Figure 2.19: Salinity profile for the constant injection Lockport-Newburg GEM Model (top view) [53].

CHAPTER 3

METHODOLOGY

To assess the technical aspect of the two proposed alternative approaches waste disposal programs, the study is divided into two sections: the experimental design for the solidification process of solid tailings and GEM simulation conceptual study for the deep well injection process of liquid brine waste. The methodological framework is summarized in Figure 3.1.

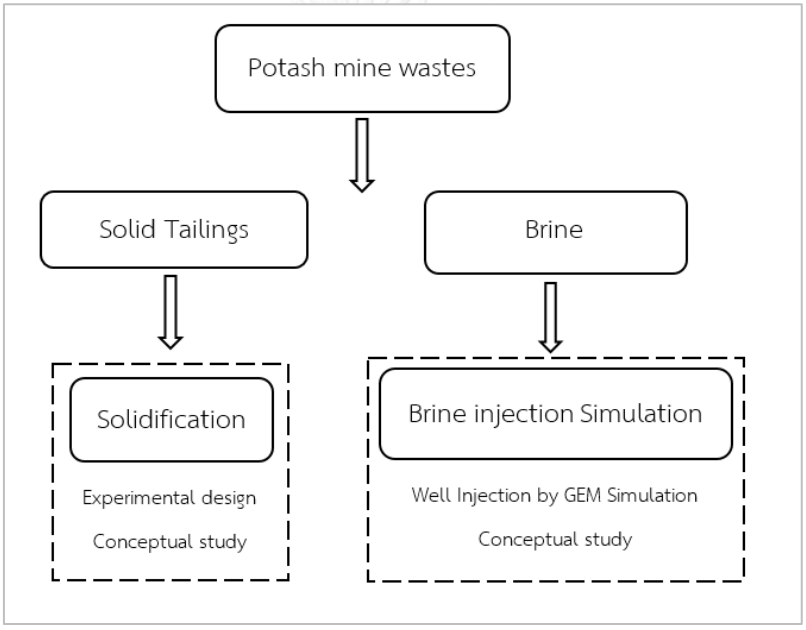

Figure 3.1: Methodological framework of the study.

The outputs are the conceptual design for the solidification and brine injection process that maximizing the amount of disposed solid and brine wastes of the potash mine.

3.1. Experimental design of Solidification method

The solidification process was proposed for the disposal of solid tailing salt from the underground potash mine. It involves two main aspects: (1) physical and chemical characterization of salt sample, (2) the optimizing mixing ratio for concrete block

mixture materials in relation to the Uniaxial Compressive Strength (UCS). The expected result is the optimal mixture that maximize the tailing concentration and archives the minimum UCS strength of 5 MPa, which is requirement of backfilling materials at 28 days in Thailand potash mine [35].

In the first step, as the salt sample is taken from the industrial salt produced from evaporated farm. The physical and chemical characteristic comparison between the salt sample and the solid tailing has to be made in order to justify the sample representation. The following tests were used to characterize the salt sample from the evaporated farm: particle size measurement by Sieve Analysis and chemical composition analysis by X-Ray Fluorescence. The properties of solid tailing were adopted from the previous studies of Asia Pacific Potash Corporation Potash Mine [10]. Secondly, this tailing materials were mixed with cement, water, fine and coarse aggregates to setup the concrete blocks, and tested on the UCS test.

3.1.1. Solid waste from Udon South Potash mine (APPC Project)

The solid tailing from flotation process in Udon South Potash mine have the following relevant characteristics. The moisture is approximately 13%, the grain size is less than 1.5 mm., and the raw density of the rock salt (NaCl) is 2.14 t/m³ [12]. The composition of tailing is depicted in Table 3.1.

Table 3.1: Tailing compositions in Udon South Potash Deposit [12]

Tail component	Percentage
Magnesium chloride, $MgCl_2$	0.1
Calcium chloride, $CaCl_2$	0.9
Potassium chloride, KCl	2.6
Sodium chloride, NaCl	92.4
Insoluble	4.0
Total	100.00

3.1.2. Solidification procedure

3.1.2.1. Materials preparation

The materials used in this test work were salt sample as tailing material, fine aggregate (sand), coarse aggregate (limestone), water and cement as a binding material.

a) Tailing material

In this study, the salt sample taken from the evaporated salt farm was used as the representation of solid tailing of potash mine waste. Its physical and chemical characteristics were performed in order to compare with solid tailing waste of Asia Pacific Potash Corporation (APPC) mine.

b) Binding agent

The binder used is Sulfate Resistant Portland Cement (SRC), it was added to the mixture to increase the support potential.

c) Aggregate

Limestone aggregate with a maximum nominal size of 19mm. was used as coarse aggregate, while sand with a maximum size of 0.85mm. was used as fine aggregate.

d) Mixing water

The water used for the mixture is potable municipal water.

3.1.2.2. Mixing properties

In this study, saturated brine was prepared by mixing part of salt sample mass with water. The salt concentration is about 3.5% by weight. This step was implemented to avoid the dissolve of tailing salt sample in mixture during the mixing procedure. The total dry solid concentration was fixed at 86.5% by weight of concrete block. The other mixing materials (cement, aggregates, tailing) were mixed according to their weight ratio.

Cement was used at content of 20% and 25% by mass of dry solids to solidified tailing material. The tailing concentration of 50%, 60% and 70% by mass of dry solids

were chosen for the mixtures. The tailing material and cement were mixed, the cement to tailing ratios are varied from 1:2 to 1:3.5. In this experiment, the Water/Cement ratio of 0.6 (at cement content of 20%) and 0.8 (at cement content of 25%) were used. Other aggregates content (sand and limestone) was adjusted to add to the mixture. Standard concrete cube mold of 150mm. x 150mm. x 150mm. as shown in Figure 3.2 was used to setup the solidified concrete block. Figure 3.3 shows the material mixture of 1:2 cement to solid tailing ratio, with 25% cement and 50% tailing material. The mixture scenarios are summarized in Table 3.2.

Figure 3.2: Standard concrete mold of specimen.

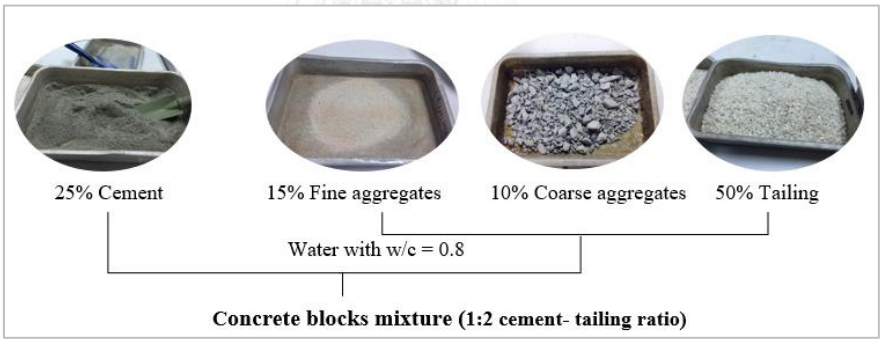

Figure 3.3: The material mixture for concrete block of 1:2 Cement to Tailing (C/T) ratio (Mixture ID 25/15/10/50T).

Table 3.2: Material mixture scenarios of concrete blocks

Water/ Cement ratio	Mixture ID (C/FA/CA/T)	Tailing salt (% by mass)	Cement	Fine Aggregate	Coarse Aggregate	Tailing Salt
			C	FA	CA	T
			(kg/m^3)	(kg/m^3)	(kg/m^3)	(kg/m^3)
0.6	25/25/0/50T	50	473	473	0	947
	25/15/0/60T	60	473	284	0	1,136
	25/5/0/70T	70	473	95	0	1,325
	25/20/5/50T	50	473	379	95	947
	25/10/5/60T	60	473	189	95	1,136
	25/0/5/70T	70	473	0	95	1,325
	25/15/10/50T	50	473	284	189	947
	25/5/10/60T	60	473	95	189	1,136
	25/10/15/50T	50	473	189	284	947
	25/0/15/60T	60	473	0	284	1,136
0.8	20/30/0/50T	50	379	568	0	947
	20/20/0/60T	60	379	379	0	1,136
	20/10/0/70T	70	379	189	0	1,325
	20/25/5/50T	50	379	473	95	947
	20/15/5/60T	60	379	284	95	1,136
	20/5/5/70T	70	379	95	95	1,325
	20/20/10/50T	50	379	379	189	947
	20/10/10/60T	60	379	189	189	1,136
	20/15/15/50T	50	379	284	284	947
	20/5/15/60T	60	379	95	284	1,136
	20/10/20/50T	50	379	189	379	947
	20/0/20/60T	60	379	0	379	1,136

** % = Percentage of total dry solid by weight*

*** C = Cement, FA = Fine Aggregate (Sand), CA = Coarse Aggregate (Limestone), T = Tailing Salt*

The resulted solidified concrete block was then tested by UCS test to determine their compressive strength as shown in Figure 3.4.

Figure 3.4: The sample of solidified concrete block.

3.1.3. Uniaxial Compressive Strength (UCS) test

The physical strength of the solidified concrete block is important, because it determines the suitability of the solidified concrete blocks as backfill materials into the mine-out room of the underground potash mine. In this study, the sample concrete blocks were cured at the room temperature (98% humidity at 25℃) for 7 days. Then, all the specimens were subjected to UCS test using a Compression machine - TMC 3000 MM - Serie No 5310, with the maximum capacity of 3,000 kN, as seen in Figure 3.5.

Figure 3.5: Compressive machine for UCS test.

The compressive strength was calculated using equation 3.1.

$$\sigma_c = \frac{F}{A} \qquad (3.1)$$

In which, σ_c is the compressive strength (kN/m^2); F is the failure load (kN); and A is the cross-section area of specimen (m^2).

The experimental flowchart of solidification process is summarized in Figure 3.6.

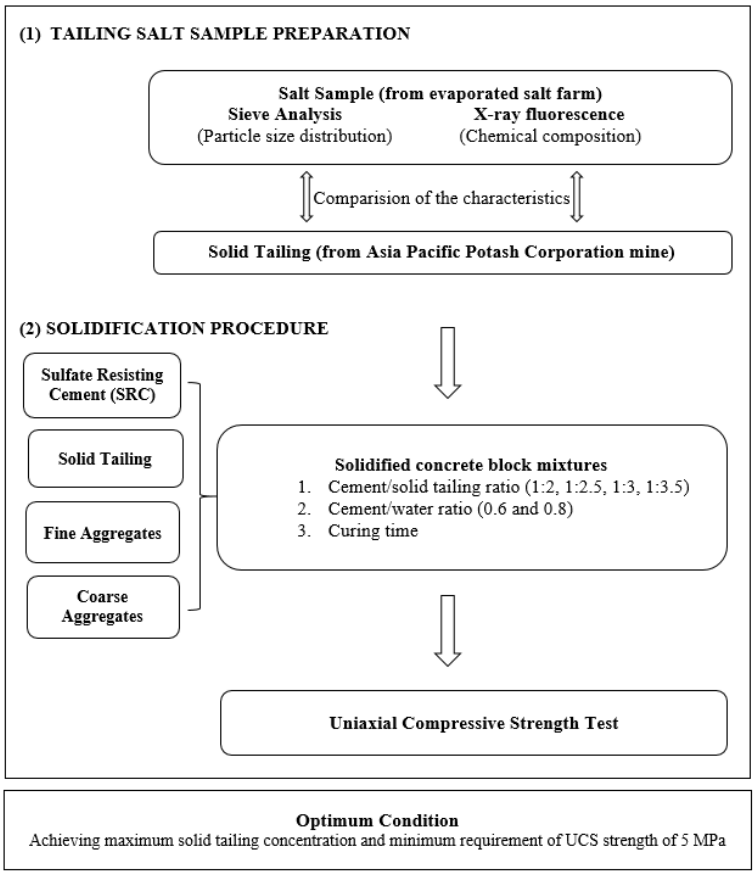

Figure 3.6: Experimental flowchart of solidification process.

3.2. Simulation of brine injection into Khok Kruat Formation

3.2.1. Liquid brine waste from Udon South Potash mine (APPC Project)

The water used in the ore dressing plant comes from rain water ponds collected within the project area. Water is blended with the ore and become the saturated brine. This concentrated brine is recycled in the flotation process with some loss from evaporation. Each year, a large amount of concentrate brine has to be eliminated from the system because it contains too high concentration of Mg dissolved to be accepted in the brine stream circuit. The high Mg brine concentration discharged annually from the processing plant is shown in Table 3.3. The highest volume brine eliminated was in Year 9, at 481,094 m^3.

Table 3.3: High magnesium brine eliminated from ore dressing process [10]

Year	Brine amount from production	
	m^3/year	m^3/day
1	5,207	14.3
2	12,845	35.2
3	24,549	67.3
4	74,391	203.8
5	89,269	244.6
6	105,345	288.6
7	158,557	434.4
8	308,663	845.7
9	481,094	1318.1
10	153,467	420.5
11	112,358	307.8
12	76,026	208.3
13	67,542	185.0
14	63,271	173.3
15	171,434	469.7
16	164,838	451.6
17	302,026	827.5
18	207,424	568.3
19	86,293	236.4
20	79,102	216.7
21	60,260	165.1

The amount of brine output in the different years depends strongly on the chemical composition of the Run Of Mine (ROM) from underground mine operation. With increasing content of Mg, the brine amount increases dramatically. Therefore, the amount of disposal brine depends on the Mg content and the amount of ROM per year. Disposal brine has a $MgCl_2$ concentration of approx. 320 g/l. Table 3.4 shows the composition of eliminated brine from ore dressing plant. The total salt concentration

of brine is 415,800 mg/l, which is primarily magnesium chloride, potassium chloride, and sodium chloride.

Table 3.4: Composition of brine from ore dressing plant [12]

Composition	Concentration		Percentage
	g/L	mg/L	%
$MgCl_2$	319.5	319,500	25.0
KCl	61.3	61,300	4.80
NaCl	31.6	31,600	2.47
$CaSO_4$	3.4	3,400	0.27
H_2O	862.1	-	67.46
Total TDS	415.8 g/L brine	415,800	100.0

3.2.2. Khok Kruat Formation

This study will investigate the possibility of injecting the high concentrated brine into the deep geological formation. The logical site selection is the area in the vicinity of the mine site. Since, the mine site is located within the influence of the Sakhon Nakhon basin, and the underground mine exploits the potash layer within the Maha Sarakham (Ms) Formation. Underlying the potash layer is the very thick sedimentary of Khok Kruat (Kk) Formation. The Khok Kruat Formation offers a strong potential for brine waste deep well injection program considering its favorable hydrological properties and overlying impervious layer. The overview geology of the basin and Khok Kruat Formation will be discussed in details.

❖ **Geology**

Figure 3.7 shows the potash deposit in Northeast Thailand, dividing in 2 basins, Khorat basin and Sakhon Nakhon basin. Both are separated by the Phu Phan Range along Northwest to Southeast direction.

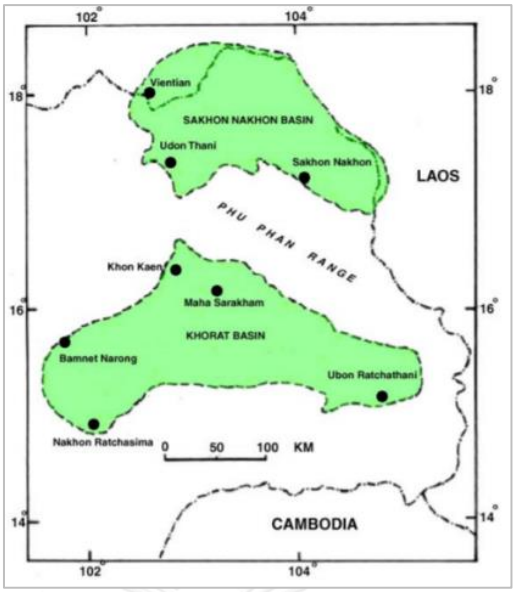

Figure 3.7: The Khorat Basin and Sakhon Nakhon Basin (green area) on the Khorat Plateau (white area) in Northeastern Thailand [54].

Figure 3.8 indicates that the depth to the rock salt (yellow layer) increases from the west rim of the Khorat basin and toward the center of the basin. Data from two and three dimensional geophysical surveys also indicate that rock salt has undulated surface all over the resource area, with slope down and deeper to the east of the Sakhon Nakhon basin (0-5 degrees dip angle) [10].

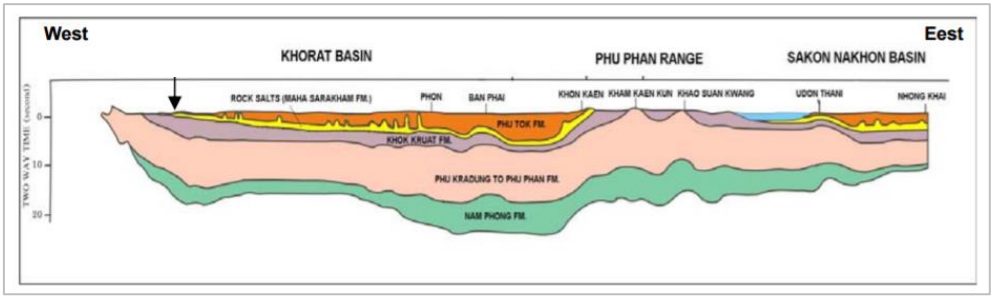

Figure 3.8: Geologic cross-section from Ban Phai, Khon Kaen Province to Udon Thani Province [55].

The Khok Kruat was deposited in early Cretaceous and immediately underlies the Maha Sarakham Formation. This formation is found in the shape of an arch between the Phu Phan and the Maha Sarakham formations. Khok Kruat Formation is

more than 400m depth in area of Udon South Deposit as shown in Figure 3.9 and Table 3.5. The deposit basin is deeper toward the East direction.

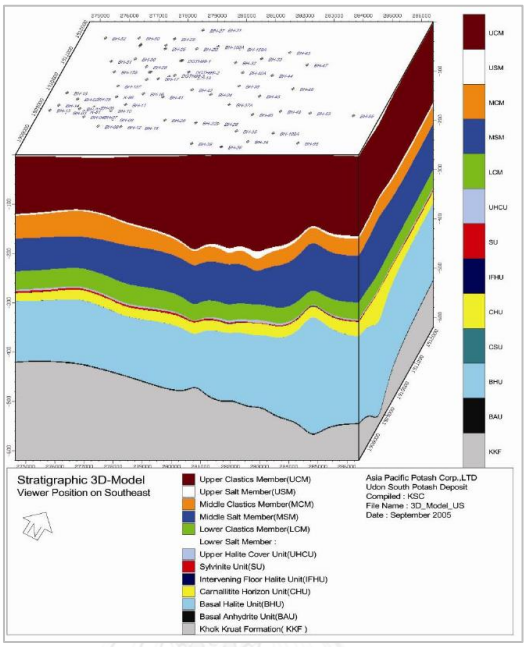

Figure 3.9: 3D-Stratigraphic model of Udon South Deposit (SW-NE) [10].

Table 3.5: Stratigraphic of Udon South Deposit [12]

Formation	Layer	Depth (m)
Maha Sarakham, MS	Upper Clastics Member, UCM	142.5
	Upper Salts Member, USM	146.9
	Middle Clastics Member, MCM	183.9
	Middle Salts Member, MSM	268.9
	Lower Clastics Member, LCM	309
	Upper Halite Cover Unit, UHCU	315.82
	Sylvinite Unit, SU	
	Intervening Floor Halite Unit, IFHU	
	Carnalite Horizon Unit, CHU	
	Basal Halite Unit, BHU	404.02
	Basal Anhydrite Unit, BAU	406.02
Khok Kruat, KK	Conglomerate, Sandstone	420

According to the Department of Mineral Resources (DMR), the total thickness of formation ranges from 430 m to 700 m. Khok Kruat Formation is composed of

sandstone, siltstone, claystone, and conglomerate, with reddish brown in color. The grain size is ranging from medium to coarse grain. According to Meesook, 2011, the detailed stratigraphy of the Khok Kruat Formation is shown in Figure 3.10. The sandstones are pale red to grayish-red and reddish brown in color, mostly fine to medium grained as shown in Table 3.6.

Table 3.6: Properties of Khok Kruat sandstone [56]

Density (g/cm^3)	2.45
Grain size (mm)	0.1-1.5 mm (100-1,500 μm)
Grain shape	angular
Color	reddish brown to brownish white

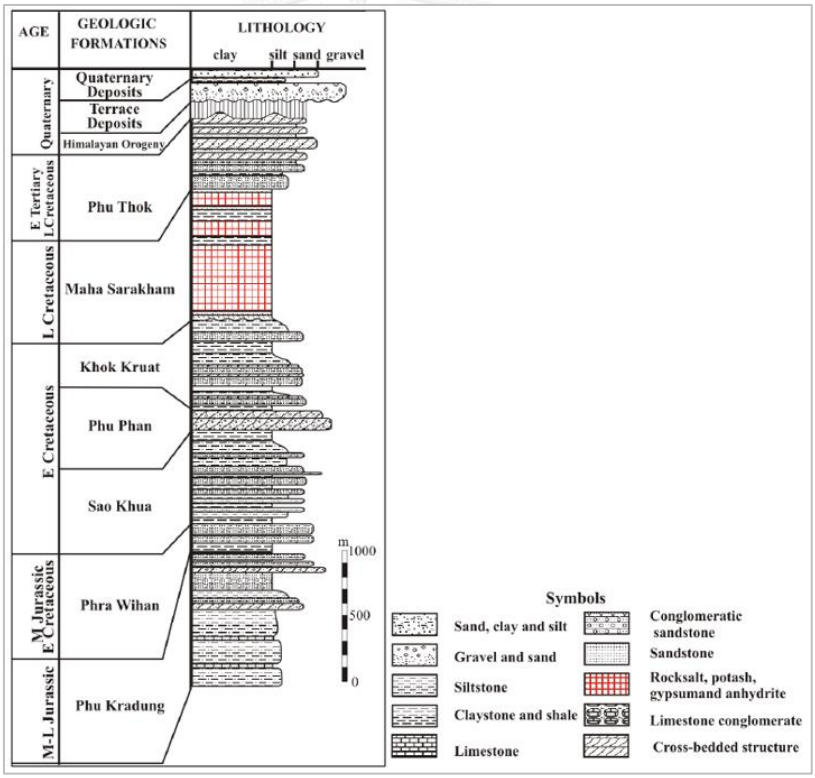

Figure 3.10: Stratigraphy of the Khok Kruat Formation [57].

❖ **Hydrogeology**

Consolidated aquifer units are recognized in the Phu Tok, the Maha Sarakham and the Khok Kruat Formation. Hydraulic properties of the hydrogeological units were determined using direct measurement in the aquifer by pumping test of Department

of Groundwater Resources (DGR). The transmissivity values range from $1.08x10^{-5}$ to $9.51x10^{-5}$ m^2/s as shown in Figure 3.11, while the hydraulic conductivity (K) values are ranging from $7.89x10^{-8}$-$6.86x10^{-6}$ m/s of Khok Kruat unit as shown in Figure 3.11.

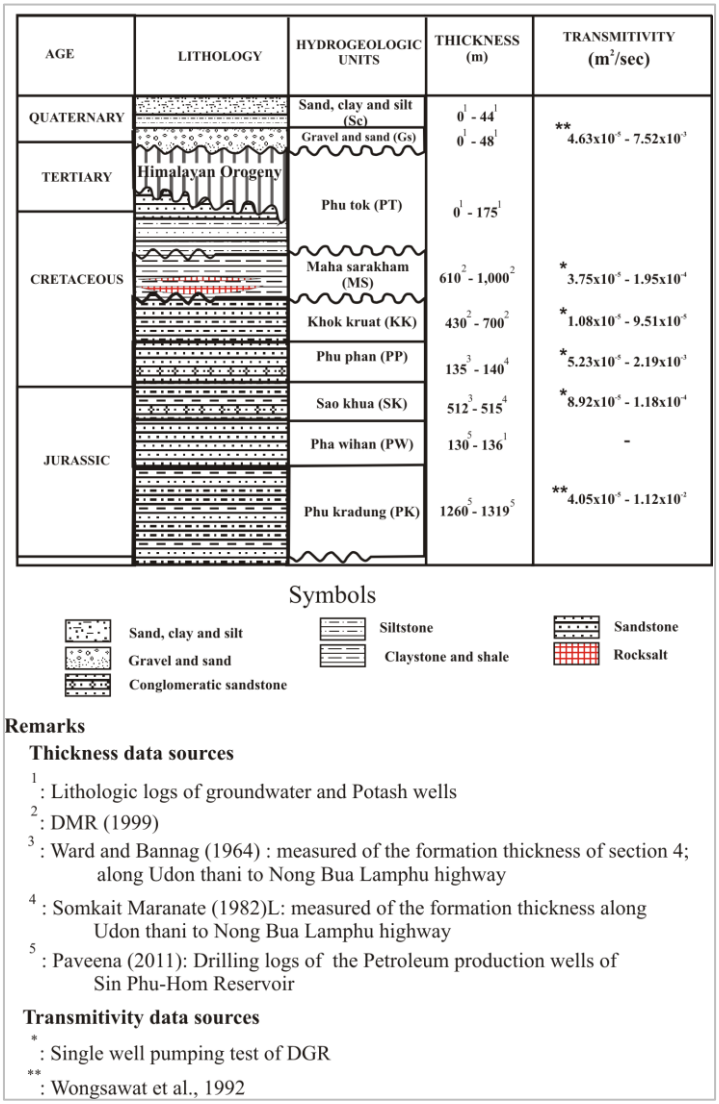

Remarks

Thickness data sources

[1] : Lithologic logs of groundwater and Potash wells

[2] : DMR (1999)

[3] : Ward and Bannag (1964) : measured of the formation thickness of section 4; along Udon thani to Nong Bua Lamphu highway

[4] : Somkait Maranate (1982)L: measured of the formation thickness along Udon thani to Nong Bua Lamphu highway

[5] : Paveena (2011): Drilling logs of the Petroleum production wells of Sin Phu-Hom Reservoir

Transmitivity data sources

[*] : Single well pumping test of DGR

[**] : Wongsawat et al., 1992

Figure 3.11: Hydrostratigraphic units of the Khorat group [58] .

Table 3.7: Properties of hydrostratigraphic units in Maha Sarakham (Ms) and Khok Kruat Formation (Kk) [58]

Hydrogeologic units	Component	Groundwater quality	Hydraulic conductivity, K	TDS
			m/s	mg/L
Maha Sarakham (Ms)	- Claystone interbedded with salt, gypsum, anhydrite, and potash. - Late Cretaceous	Brine water	$9.95x10^{-8}$-$7.82x10^{-5}$	1,500-3,000
Khok Kruat (Kk)	- Sandstone, siltstone, claystone, and conglomerate, with reddish brown in color. - Late Cretaceous - The grain size is ranging from medium to coarse	Fresh water	$7.89x10^{-8}$-$6.86x10^{-6}$	500-1,500

Table 3.7 also shows that the salinity (TDS) of Khok Kruat Formation ranges from 500 to 1,500 mg/L. That means this formation water is fresh water (1,000 mg/L). However, salty water can be found in the upper contact with Maha Sarakham Formation. Sodium Chloride (NaCl) is recognized predominately in the Northern part influenced by rock salt, or it can say that this type of groundwater mainly occurs in Maha Sarakham Formation. The groundwater flow direction in Udon South Potash mine is Southwest to Northeast direction [58], the dip angle ranges from 0 to 5 degrees, which is horizontally flat. According to Srisuk et al., (1994) a hydrogeologic profile in South – North direction of Northeast Thailand area shows that the deep groundwater convection (regional flow) flows downward [59].

3.2.3. Base case conceptual model

This section presents the development of the base case conceptual model using CMG-GEM simulation to study the ability and storage capacity of Khok Kruat Formation for waste brine deep well injection program during 21 years period. The program modeled and analyzed the pressure rise and fluid migration (molality of Cl^-) following brine injection. It is important to state here that the geological data of this study area are obtained from the APPC's report and referred to previous studies in Northeastern

Thailand area. The model is shown in 3D model and used SI units. The descriptions of base case simulation are presented here.

3.2.3.1. Formation description and data proceeding

According to the section 3.2.2, the descriptions of the target formation used in GEM Simulation are presented here. Khok Kruat Formation lies at depths greater than 400 m in Udon South Deposit. The aquifer is overlain by relatively impermeable deposits (anhydrite) of the lower Maha Sarakham Formation, which an average thickness of 1 m. and depth of around 400 - 560 m. The aquifer is underlain by a siltstone with 100 m. thickness belonging to the lower Khok Kruat Formation. The aquifer comprises approximately 210m (689ft) of conglomeratic sandstone. The formation dips Eastwards with 0 – 5 degrees dip angle. Within the aquifer formation, all layers have the constant vertical grid.

There is no direct measurement of aquifer properties such as flow test, or the indirect measurement such as data of well log interpretation is not available. The study is mainly referred to the secondary information collected from previous studies for proceeding input data in the model. The given value of hydraulic conductivity of Khok Kruat Formation is ranging from 7.89×10^{-8} to 6.86×10^{-6} m/sec. According to Morris and Johnson (1967), porosity of sedimentary rocks are shown in Table 3.8. and from Domenico and Schwartz (1990), hydraulic conductivity of sedimentary rocks are tabulated in Table 3.9. The permeability can be calculated by Equation (2.4) to define the porosity and permeability of each layer (anhydrite, siltstone and sandstone) in the modelled formation. The hydraulic properties of formation used in model are tabulated in Table 3.10.

Table 3.8: Porosity, Φ (%) of sedimentary rocks

Rock Type	Porosity (%)
Limestone	7 -56
Sandstone	14 - 49
Siltstone	21 - 41
Claystone	41 - 45
Dolomite	19 -33
Shale	1-10

Table 3.9: Hydraulic conductivity, K (m/sec) of sedimentary rocks

Rock Type	Hydraulic conductivity, K (m/sec)
Limestone, dolomite	1×10^{-9} to 6×10^{-6}
Sandstone	3×10^{-10} to 6×10^{-6}
Siltstone	1×10^{-11} to 1.4×10^{-8}
Salt	1×10^{-12} to 1×10^{-10}
Anhydrite	4×10^{-13} to 2×10^{-8}
Shale	1×10^{-13} to 2×10^{-9}

Table 3.10: Summarized of hydraulic properties of Formation used in model

Formation	Parameters	Hydraulic conductivity, K (m/s)	μ = Fluid viscosity (kg/m.s)	Permeability, k = K μ/ρ_g (mD)	Porosity, Φ (%)
Maha Sarakham (Ms) $K = 9.95\times10^{-8}$-7.82×10^{-5}	Anhydrite	(1×10^{-8})	0.00078	8.1	10
Khok Kruat (Kk) $K = 7.89\times10^{-8}$ to 6.86×10^{-6}	Siltstone	(7×10^{-9})	0.00078	6.4	30
	Conglomeratic Sandstone	(3×10^{-6})	0.00078	244	25

(Fluid density, ρ (kg/m^3) = 994 kg/m^3 at 42.4 ^oC, salinity=1,000 mg/L and 5,802 KPa)

The study initializes the model at hydrostatic pressure, assuming a pressure gradient of 0.45 psi/ft. The hydrostatic pressure of 0.436 to 0.452 psi/ft is assigned, and were correlated from the Northern Thailand basin [29]. The native brine salinity of 1,000 mg/L was assigned based on data from consolidated Khok Kruat aquifer ($TDS_{Khok\ Kruat}$ = 500 – 1,500 mg/L).

The *Hubbert and Willis* Equation is used to calculate the fracture pressure. The minimum principle stress in the shallow sediments is approximately one-third the matrix stress resulting from weight of the overlying overburden. The matrix stress of weight of the overburden in Khok Kruat Formation is calculated based on the average grain density of rocks in Maha Sarakham Formation as shown in Table 3.11.

$$\text{Average grain density} = \frac{\sum_{i=1}^{5} \text{thickness}_i \times \sum_{i=1}^{5} \text{density}_i}{\sum_{i=1}^{5} \text{thickness}_i} = 2.3\ \text{g/cm}^3$$

Table 3.11: Various rock layers in Udon South Deposit [10]

Member		Type of Rock	Thickness min-max (avg.) (m)	Density (t/m^3)
Overburden		Gravel, clay, siltstone	0-21 (5)	1.75
Upper Clastics Member, UCM		Siltstone, Claystone	21-205 (144)	2.49
Upper Salts Member, USM		Anhydrite, Claystone, Halite	1-25 (5)	2.89
Middle Clastics Member, MCM		Claystone, Mudstone	17-175 (40)	2.15
Middle Salts Member, MSM		Halite, Anhydrite	1-129 (82)	2.14
Lower Clastics Member, LCM		Claystone, Mudstone	7-107 (42)	2.18
Lower Salts Member, LSM				2.1
Potash Zone	Upper Halite Cover Unit, UHCU	Halite	3.8	2.12
	Sylvinite Unit, SU	Sylvinite	3.8	1.87
	Intervening Floor Halite Unit, IFHU	Halite	3.7	2.12
	Carnalite Horizon Unit, CHU	Carnalite	22.6	2.12

3.2.3.2. Well locations

Owning to its favorable geological conditions around the mining area, the Khok Kruat Formation is lied directly underneath the exploited potash layer. Therefore, it is logical to consider locating the injection wells closes to the plant. The injection wells will be

located at Udon South Plant, Udon Thani Province, with the coordinate 260,000E – 300,000E and 1,900,00N – 1,940,00N as shown in Figure 3.12.

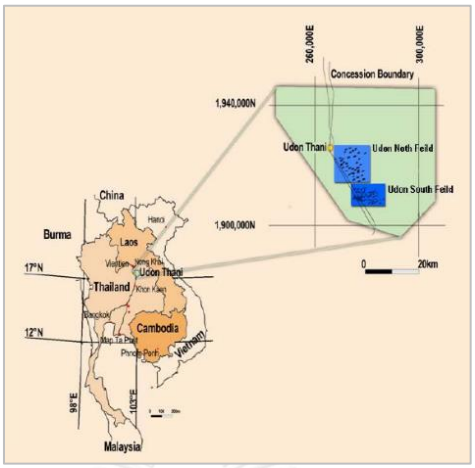

Figure 3.12: Location of injection wells at Udon South plant, Udon Thani Province.

3.2.3.3. Model descriptions

❖ *Formation properties (homogenous domain)*

A three-dimensional (I, J, K-coordinates) Cartesian grid was used to model the area. SI units were adopted in the model. With the permit of CMG for academic purpose, the maximum member of grids is allowed only 10,000 grids in total. Therefore, the model consists of 33 grids in the I-direction (Easting), 27 grids in the J-direction (Northing), and 10 grids in the K-direction (Vertical). The injection model consists of 8,910 grids that spanned about 3,225 m. (33 grids x grid spacing) in I-direction, 3,100 m. (27 grids x grid spacing) in J-direction. Figure 3.13 displays the variable grid spacing in the I, J-directions with increased grid resolution near injection well.

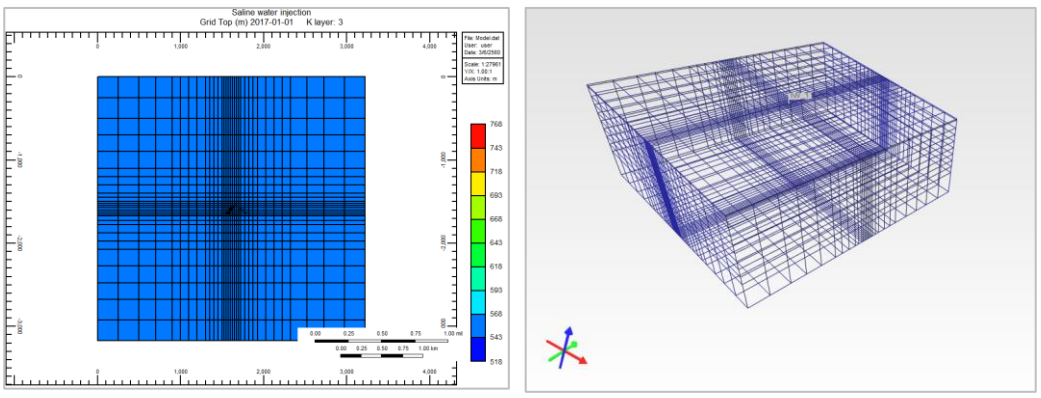

Figure 3.13: Simulation grid in top view and three-dimensional viewing well location.

The formation is modeled with ten layers in the K-direction. The 345-m. thick model was split into an upper zone, middle zone and lower zone. The two layers upper zone represents the overlying basal anhydrite of lower Maha Sarakham Formation, and siltstone of upper Khok Kruat Formation. The bottom layer represents the siltstone of lower Khok Kruat Formation. These layers are less porous and more confining than the 7-layers in the middle zone, which represents the conglomeratic sandstone of Khok Kruat Formation as shown in Figure 3.14.

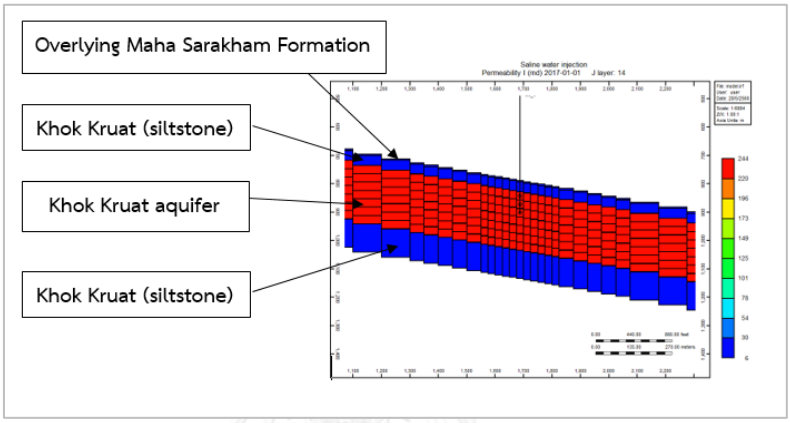

Figure 3.14: The aquifer model showing the description of the vertical gridded layers.

Normally, isopachs generated from the well log analysis were used to assign thickness for each layer in the K-direction. The thickness for each injection zone layer is assumed to be 30 m. Due to a lack of log analysis, the model is assumed homogeneous domains. The porosity and permeability are referred from the data of Khok Kruat formation (presented in section 3.2.2) for each layer due to a lack of the direct measurements of the rock strata.

- The upper zone has an average of 1% porosity and 8.1mD permeability of anhydrite, and an average of 30% porosity and 6.4mD permeability of siltstone.
- The center of main injection zone has an average of 25% porosity and 244 mD permeability of conglomeratic sandstone.
- The lower zone has an average of 30% porosity and 6.4mD permeability of siltstone.
- A anisotropic kv/kh value of 0.1 was used.

The properties of each layer are summarized in Table 3.12.

Structurally, the Udon South Deposit dips Eastwards, but the dip angle is very gentle ranging from 0 to 5 degrees. According to GEM and other petroleum reservoir models, the 0-5 formation dip angle doesn't any impact on the modelling results. Therefore, it is assumed horizontal flat (Dip = 0) in this simulation model. Figure 3.15 - Figure 3.16 show the permeability and porosity in injection aquifer zone. The initial pressure map is shown in Figure 3.17.

Table 3.12: Properties of Khok Kruat Formation

Zone	Layer	Depth (m)	Grid thickness(m)		Thickness (m)	Porosity	Permeability
Upper	1	520.0	5.0	Anhydrite	5.0	0.1	8.1
	2	525.0	35.0	Siltstone	35.0	0.3	6.4
Injection	3	560.0	30.0	Conglomeratic Sandstone	210.0	0.25	244
	4	590.0	30.0			0.25	244
	5	620.0	30.0			0.25	244
	6	650.0	30.0			0.25	244
	7	680.0	30.0			0.25	244
	8	710.0	30.0			0.25	244
	9	740.0	30.0			0.25	244
Lower	10	770.0	100.0	Siltstone	100.0	0.3	6.4

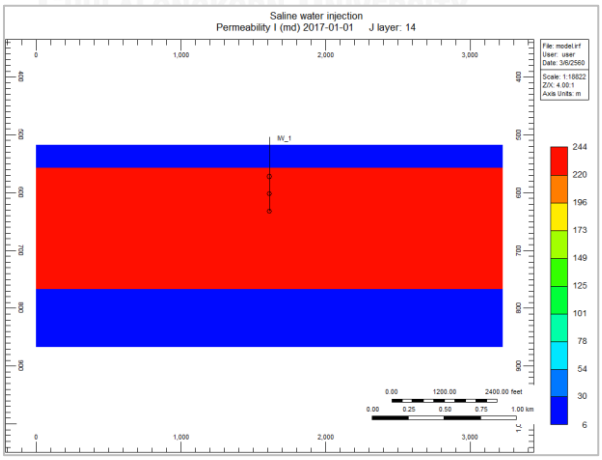

Figure 3.15: Khok Kruat permeability model map (cross section SW-NE) (mD).

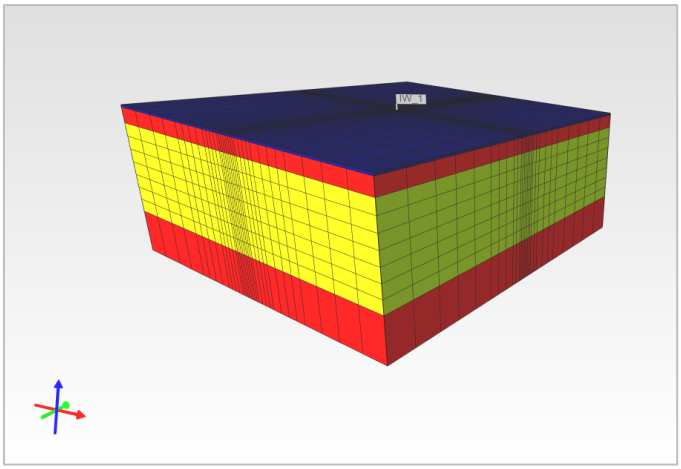

Figure 3.16: 3D-Porosity map and injection well.

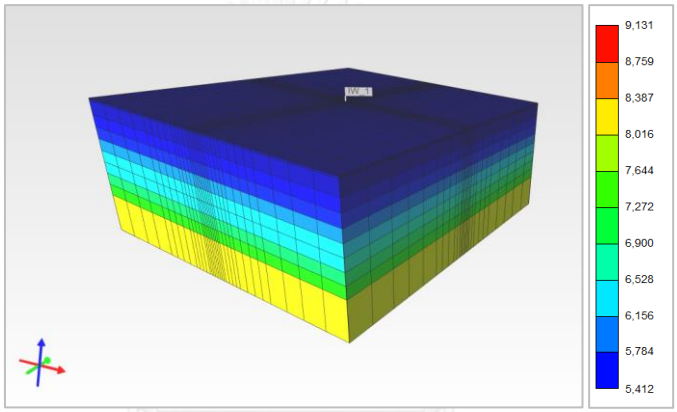

Figure 3.17: 3D-Initial pressure map (KPa).

The input parameters for the base case simulation are summarized in Table 3.13.

Table 3.13: Simulation input parameters for base case simulation model

Parameters	Value	
Domain	3,225m x 3,100m x 210m	
Length (m)		3,225
Width (m)		3,100
Cartesian grid blocks		33 x 27 x 10 = 8,910 grids
Grid spacing (m)	Max = 250 x 250 m Min = 25 x 25 m	Variable grid spacing with grid increased grid resolution increased near injection well
Layer	10 layers -520 m to -870 m	Upper zone = 2 layers Injection zone = 7 layers Lower zone = 1 layer

Parameters	Value	
Aquifer thickness (m)	210 m	Layer 1 = Anhydrite (5m) Layer 2 = Siltstone (35m) Layer 3 – 9 = Conglomeratic Sandstone (210m) Layer 10 = Siltstone (100m)
Depth of top of aquifer (m)		560 m = 1837 ft
Porosity (fraction)		0.25
Horizontal permeability (mD), k_h	Homogeneous	Layer 1 = 8.1 mD Layer 2 = 6.4 mD Layer 3 – 9 = 244 mD Layer 10 = 6.4 mD
Vertical permeability (mD), k_v		0.1 x k_h
Rock Compressibility (kPa^{-1})	Constant rock compressibility	4.82E-07
Pressure gradient, (psi/ft)	Higher than freshwater (0.433 psi/ft) because the brine is denser	0.45 psi/ft
Initial Aquifer Pressure (KPa)	(14.7 psi + 0.45 psi/ft × 1837 ft)	5802
Initial Aquifer Temperature (°C)	(77°F +0.017 x 1837 ft)	42.4
Salinity of formation water (mg/L)	$TDS_{Khok\ Kruat}$ = 500 – 1500 mg/L	1,000
Density of aquifer water (kg/m^3)	at 42.4 °C, 1000 ppm and 5802 KPa	994
Compressibility of water (kPa^{-1})		4.45E-07
Viscosity of formation water (cp)		0.78
Dip angle (degree)	0 to 5 degrees	0 degrees

**Layer 1 is the top layer*

**viscosity, μ = 0.78 cp or 0.00078 kg/m.s at 42.4 °C, salinity=1000 mg/L)*

**Dip angle = 0 to 5 degrees [12]*

**SI Metric Conversion Factors*

ft x 3.048E-1 = m, psi x 6.894757 = KPa, lb/ft^3 x 1.601846E1 = kg/m^3

(1°F - 32) × 5/9 = °C, cp x 1E-3 = kg/m.s

❖ Component properties

In GEM options, there is no oil and gas in this zone, so it was basically brine injection into a brine saturated aquifer layer. Therefore, the model becomes basically single-phase flow simulation.

The Peng-Robinson EOS was used to model phase behavior. Because of the simulator cannot function without any hydrocarbon components, thus a 'dummy'

component such as "CH_4" is put in the model. Therefore, the model consists of C1 as pure components. It should be noted that the Peng-Robinson EOS is only used to calculate the gas phase behavior. C1 is used as a trace component to add compressibility to the near incompressible system. This helps in the convergence of the equations in the reservoir simulator.

Typically, water (aqueous phase) is included in the components so the model need not explicitly define it in the components list. This H_2O included will act as both aquifer and injection fluid depending on the salinity specifications. The aqueous phase density is calculated from the Rowe and Chou correlation, while aqueous viscosity is calculated using the Kestin correlation. These correlations are built into GEM and are functions of pressure, temperature and salinity.

NaCl is the main dissolved solid in both formation fluid and injection fluid. The model didn't assign any other dissolved components. In GEM, simulations were run in compositional mode with rock fluid properties main component as NaCl in WINPROP. The density data for brine water of 1,000 ppm at 42.4°C and 5,830 psi is 994 kg/m^3.

❖ ***Rock-Fluid***

Relative permeability data is presented in Table 3.14. Figure 3.18 shows the Water-Gas relative permeability curves obtained by using the data of Kumar et al., 2005 [27].

Table 3.14: Relative permeability data [27]

Initial water saturation	0.936
Residual water saturation	0.25
Water end point relative permeability, krw	0.334
Initial gas saturation	0.005
Residual gas saturation	0.75
Gas end point relative permeability, krg	1.0
Water relative permeability exponent	2
Gas relative permeability exponent	2.5

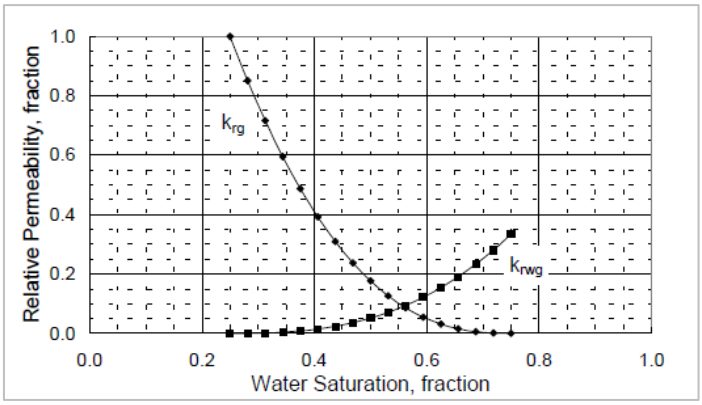

Figure 3.18: Water-Gas relative permeability curves [27].

❖ *Initial conditions*

The initial overall mole fraction of C1 in the aquifer is 1.0, where the global mole fraction of water is one. The initial aquifer pressure at 560 m (1,837 ft) is 5,802 KPa, which is calculated using a hydrostatic gradient of 0.45 psi/ft.

❖ *Injection design and well constraints*

High concentration $MgCl_2$ brine from ore dressing plant was injected into the disposal well, through perforation made in the top layer of the aquifer. In this case, the injected brine concentration of 415,800 mg/L is much higher salinity than the native brine concentration of 1,000 mg/L. The model specifies INJ-SALIN of 415,800 ppm for the INJECTOR well parameters.

The injection rate and fracture pressure will affect the storage capacity of Khok Kruat Formation. The constant rate injection simulation will be run for a 21-year injection period. The maximum pressure is calculated and used as criteria to terminate the simulation process. Bottom hole pressure is calculated by Equation (2.16). The injection wells are designed to accommodate different volume of brine made available from the processing plant. As can be seen, the brine amount from production of APPC project each year is different, with the lowest volume of 14.3 m^3/day in Year 1, and the highest volume of 1,318 m^3/day in Year 9 as shown in Table 3.3. Intentionally, the base case modeled is designed for the highest volume brine of 1,318 m^3/day (481,094 m^3 in Year 9).

It is assumed that there are total eight injection wells for the maximum brine discharged year, the brine injection rate is calculated as follows:

$$\text{Brine injected by each well} = \frac{\text{Brine Volume}\left(\frac{\text{m}^3}{\text{day}}\right)}{\text{Number of well}} = \frac{1{,}318\left(\frac{\text{m}^3}{\text{day}}\right)}{8 \text{ wells}} = 165\left(\frac{\text{m}^3}{\text{day}}\right)$$

Therefore, in base case model, the formation modeled of one injection well at constant rate of 165 m^3/day is prepared. The fundamental data of an injection well is shown in Table 3.15.

Table 3.15: Parameters of injection well at constant rate for base case simulation model

Parameters	IW-1
Depth (m)	560 - 770
Grids well completion (I, J, K)	17, 14, 3-4-5
Injection duration	21 years
Well radius (m)	0.0762 m
Injected salinity (ppm)	415,800
Maximum Bottom-hole Pressure (KPa)	6,825 kPa
Maximum injection rate (m^3/day)	165

CHAPTER 4

RESULTS AND DISCUSSIONS

Since, this study carries two pronged objectives; the solidification process of solid tailing and deep well injection of liquid brine waste. The results and discussions of experimental works and simulation model will be dealt with accordingly.

4.1. Experimental results of Solidification method

4.1.1. Characteristics of tailing salt

In this step, the physical and chemical characteristics between the salt sample (taken from the evaporated salt farm) and solid tailing are compared by the Sieve Analysis and XRF results. Figure 4.1 shows the solid tailing and salt sample taken from evaporated salt farm.

(a) (b)

Figure 4.1: (a) Solid tailing from APPC Potash mine [35], and (b) Salt sample from evaporated salt farm.

The main chemical components of salt sample are NaCl (89%), KCl (3.6%) and $MgCl_2$ (1.5%). The chemical comparison between salt sample and solid tailing states that both primarily contain sodium chloride, and the overall chemical characteristic is comparable as shown in Table 4.1.

The Particle Size Distribution (PSD) of salt sample is varied from 1mm. to 10mm., corresponding to medium size particle (60.4% by wt. of 75μm. - 4.75mm. particles) and coarse size particle (39.6% by wt. of > 4.75mm. particles). The salt sample can be

classified as a coarse sand size particle with a relatively low potential for water retention to form a homogeneous mixture. The D10, D30, and D60 are 2.3, 3.25, and 4.8mm., respectively. The coefficient of uniformity C_u of the particle size composition is 2.09. From the previous study of Masniyom (2009), the solid tailing from APPC Potash mine has the particle size less than 1.0mm., with 36% by wt. of <75μm. fine particles and 64% by wt. of 75μm. - 4.75mm. medium particles [35]. The D10, D30, and D60 are 0.036, 0.065, and 0.16mm., respectively. The coefficient of uniformity (C_u) of the particle size composition is 4.44. The physical comparison between salt sample and solid tailing are summarized in Table 4.2.

Table 4.1: Chemical composition of salt sample and solid tailing from APPC Potash mine [35]

Component	**Content (%)**	
	Salt sample	**Solid tailing**
Sodium chloride, NaCl	89.0	92.4
Potassium chloride, KCl	3.6	2.6
Magnesium chloride, $MgCl_2$	1.5	0.1
Magnesium sulfate, $MgSO_4$	1.1	-
Calcium chloride, $CaCl_2$	0.3	0.9
Other	4.5	4.0
Total	100.0	100.0

Table 4.2: Physical properties and particle size distribution of salt sample and solid tailing from APPC Potash mine [35]

Physical properties			**Particle Size Distribution**		
	Salt sample	**Solid tailing**	(mm)	**Salt sample**	**Solid tailing**
Color	white & clear solid	red & white	D_{10}	2.3	0.036
Specific gravity	2.165	2.62	D_{30}	3.25	0.065
Bulk density, t/m^3	1.41	1.33	D_{60}	4.8	0.16
Grain size, mm	< 10	< 1	C_u	2.09	4.44
			C_c	0.96	0.73

The density of salt sample is close to solid tailing of APPC Potash mine, but larger grain size. The significant portion of salt sample corresponds to coarse sand size particles, while the solid tailing of APPC Potash mine contains more fine grain materials as 36% by wt. of < 75 μm. particles as shown in Figure 4.2.

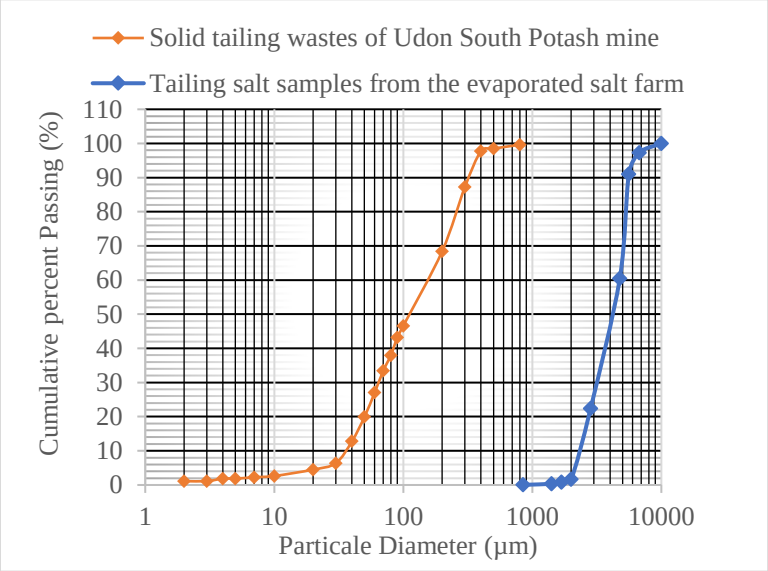

Figure 4.2: The particle size distribution of salt sample and solid tailing of APPC Potash mine [35].

From this comparison, it is clear that the salt sample has less fine content (< 75μm.), so it is necessary to add sand as additional fine material into the prepared salt sample, and bring it close to the size distribution of solid tailing of APPC Potash mine. Sand tends to decrease the void spaces between the tailing particle, and consequently lower porosity or void space within backfill mass. The decreasing porosity or void space causes an increase in paste backfill strength. With this regard, by adding aggregates of sand and limestone will increase strength property of concrete block.

The specific gravities of the fine, coarse aggregates and tailing are 2.65, 2.63 and 2.165, respectively. The Particle Size Distribution (PSD) obtained for materials used in this work is presented in Table 4.3 and Figure 4.3.

Table 4.3: Particle Size Distribution (PSD) of materials in mixture

	Tailing Salt	Fine Aggregate (Sand)	Coarse Aggregate (Limestone)
Specific gravity	2.165	2.65	2.63
D_{10} (mm)	2.3	0.1	3.0
D_{30} (mm)	3.25	0.28	14.0
D_{60} (mm)	4.8	0.51	17.5
C_u (mm)	2.09	5.1	5.83
C_c (mm)	0.96	1.54	3.73

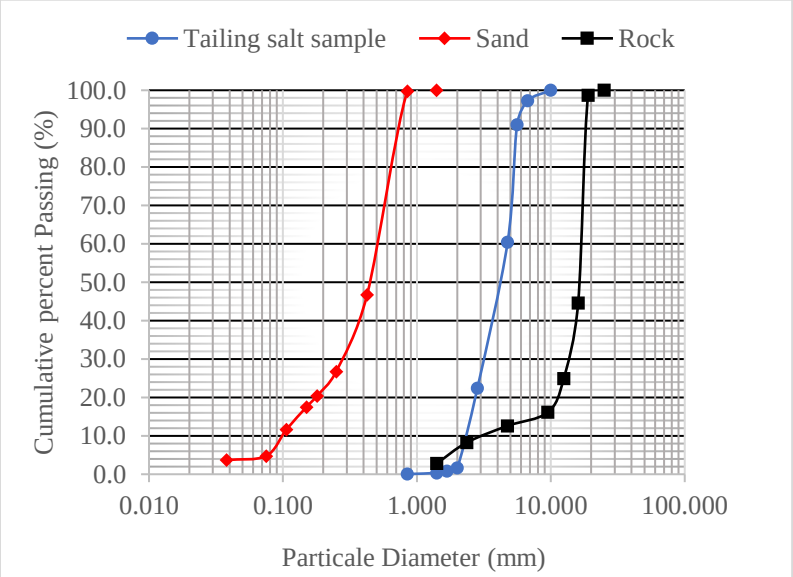

Figure 4.3: Materials Particle Size Distribution (PSD) curves.

4.1.2. Uniaxial Compressive Strength (UCS) test

The results show that the UCS values of all blocks are greater than the minimum requirement of 5 MPa [35]. The UCS value varies from 4.65 MPa (ID 20/10/0/70T) to 11.59 MPa (ID 25/15/10/50T). The concrete blocks before and after the UCS test are shown in Figure 4.4. The typical fracture at failure exhibits longitudinal and oblique line fracture pattern. It is a common fracture patterns which occur as a result of compressive loading mode.

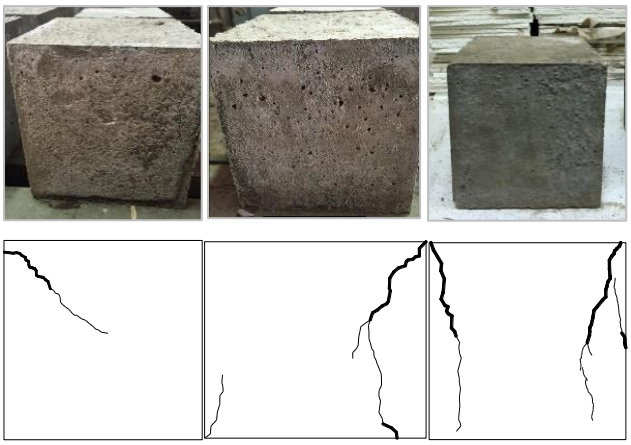

Figure 4.4: Solidified concrete blocks before and after UCS test and the developed fracture patterns.

The results show that the UCS values of the concrete blocks are affected by the following factors; cement content, water to cement ratio, and curing time. These factors will be discussed as following.

- ***Uniaxial Compressive Strength (UCS) with Cement to Tailing Salt (C/T) ratio from 1:2 to 1:3.5***

Figure 4.5 shows the UCS of the solidified concrete blocks related to the C/T ratio. The more tailing content solidified by the constant cement content, the less value of strength value. It points out that the optimum C/T ratio has to be properly defined to serve the purpose of maximizing the amount of tailing and achieve the minimum strength requirement. The decreasing trend of UCS strength values in Figure 4.5 shows that C/T ratio of 1: 3.5 is at the maximum tailing content limit, while it generates the lowest strength close to the minimum requirement of 5 MPa [35]. In this experiment, the optimum C/T ratio of 1:3.5 is adopted, as it maximizes the tailing concentration and meets the minimum UCS requirement.

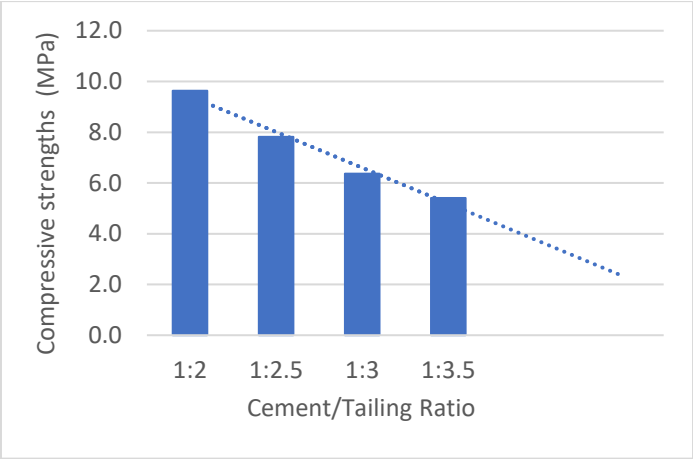

Figure 4.5: UCS strength of solidified concrete blocks with different Cement/Tailing ratio.

- ***Uniaxial Compressive Strength (UCS) with Water/Cement (W/C) ratio of 0.6 and 0.8***

The UCS is presented in Figure 4.6 according to the W/C ratio of 0.6 (at cement content of 20%) and 0.8 (at cement content of 25%). At 50%, 60% and 70% tailing concentration, the average UCS strength generated at W/C ratio of 0.6 is higher than at W/C ratio of 0.8. The results have shown that the W/C ratio is obviously sensitive to the UCS strength.

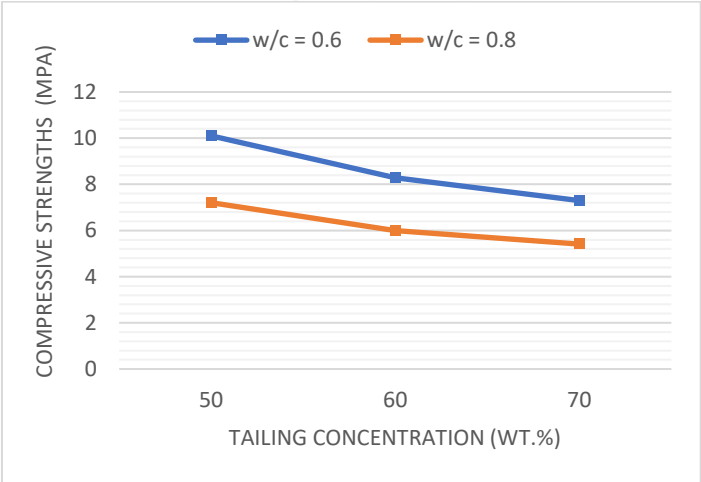

Figure 4.6: Average UCS strength of solidified concrete blocks with W/C = 0.6 and W/C = 0.8 categories in different wt.% of tailing concentration.

The W/C ratio of 0.6 is at the minimum limit of water needed for the solidified blocks. The mixtures could not mix with the W/C ratio lower than 0.6. Because it will significantly reduce the mixture workability, thus can not form the durable concrete block. And the maximum limit of water is W/C = 0.8, because too much water in the mixture generates the lowest strength close to the minimum requirement of 5 MPa [35]. Therefore, the optimum condition for W/C ratio in this experiment is 0.6, considering the UCS strength generated.

In this experiment, the optimum condition of percentage of coarse and fine aggregate materials are determined in response to W/C ratio. The results have shown that the optimum percentage of aggregate materials is founded at the mixture of 15% fine aggregate and 10% coarse aggregate, at the constant W/C ratio of 0.6. It yields the maximum UCS strength of 10.8 MPa as shown in Figure 4.7.

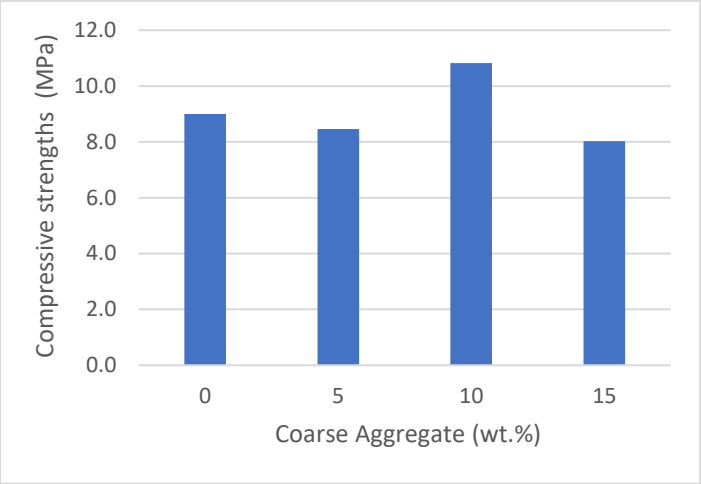

Figure 4.7: UCS strength with varying coarse aggregate wt.%.

- ***Uniaxial Compressive Strength (UCS) with curing time***

From the results, the maximum UCS strength of the concrete blocks after 7 days curing time is founded at mixture ID 25/15/10/50T and ID 25/5/10/60T with the UCS of 11.59 MPa and 10.05 MPa, respectively. These two mixture IDs were then used to observed the UCS strength for longer period of curing time of 14 days and 28 days. The results as displayed in Figure 4.8 clearly show that the UCS of both mixtures gradually increase with longer curing periods. It is observed that the concrete blocks have reached 99% strength capacity within 28 days. Even though, it continues to gain strength after that

period, but the rate is very less compared to that in 28 days. Table 4.4 shows the solidified concrete blocks gains 75% and 85% of developed strength within 7 and 14 days, respectively. It can be recommended that the curing time of concrete blocks should be adequated for this solidification process of this tailing materials.

Table 4.4: UCS strength with different curing time

Mixture ID	UCS (MPa)		
	7 days	14 days	28 days
25/15/10/50T	11.59	12.39	15.25
25/5/10/60T	10.05	11.43	13.30
Strength development percentage, %	75%	85%	99%

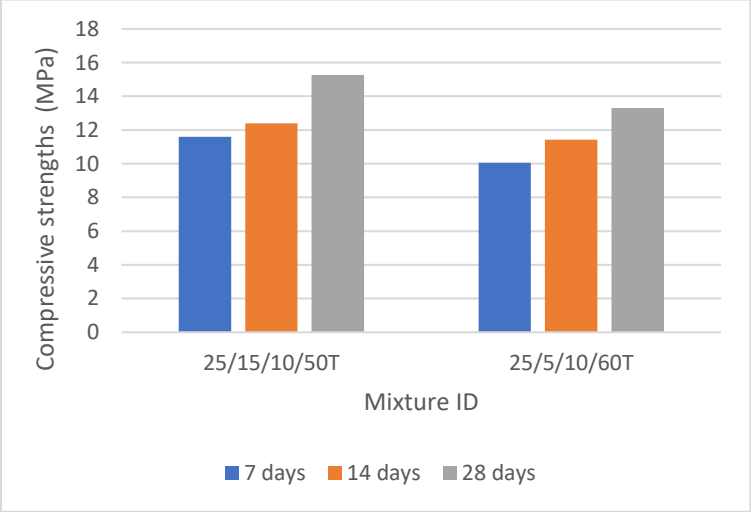

Figure 4.8: UCS strength of solidified concrete blocks after 7, 14, 28 days curing time.

4.1.3. Conceptual design for backfilling process

To apply the solidified tailing concrete blocks as backfill material in APPC Potash Mine, the conceptual design for backfilling process need to be considered. The panel design of APPC Potash mine project is introduced. The annual material balance between total tailings volume and the mine-out room generated by mining operation of APPC Potash Mine during 21 years is calculated. Tributary area method is used to determine the gained pillar strength after the backfill process.

4.1.3.1. Backfill in Udon South Potash mine

The APPC Potash mine is a conventional underground mine using the room and pillar method of mining to recover sylvinite ore from the variable depths of 300 to 380 m. The total mining area covers about 22.4 km^2, and it is divided into panels. The developed panel design of APPC Potash mine project in Udon Thani as shown in Figure 4.9.

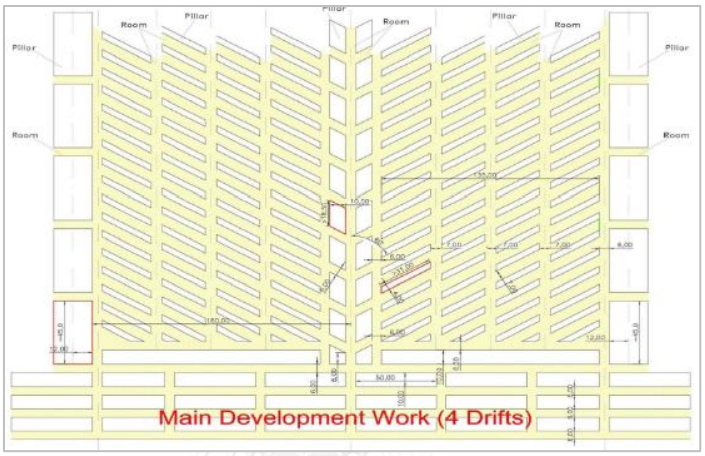

Figure 4.9: Developed panel design of APPC Potash mine project [10].

Applying the solidification backfill method, the solidified concrete blocks backfill will be designed in the second year of operation, when 261,500 m^3 of room opening is available as shown in Appendix I.

4.1.3.2. Material balance calculation for backfill process

In 21-years mine life, the total tailings generated is about 60.35 million tons, including primary salt tailings and small amount of solid residue from the construction. For the entire mine life, by applying solidification method of concrete block with maximum 70% of solid tailings concentration, the total mass of tailings disposed as backfill material into the mine-out room is about 90% of total mass of tailings generated in APPC project as seen in Table 4.5.

Table 4.5: Material balance calculation for backfill process in APPC Potash mine

Solidified tailing concrete block				Mass of Tailing		% of tailing can be disposed
Volume	Mass	% of tailings	Mass of tailings	Disposed	Remaining	
m^3	ton	%	tons	tons	tons	%
0.00338	0.0064	70	0.0045	54,403,129	5,946,103	90

In operation, about 80 concrete blocks are packed into a big bag as shown in Figure 4.10. The big bags are transported into the underground via the shaft, and to the backfilling rooms by LHD loaders. Forklift-trucks install the big bags into the backfilling room in layers. Sand or salt are applied to overfill the gap in the big bag and also to cover the alternative storage to reduce the pores among the big bags.

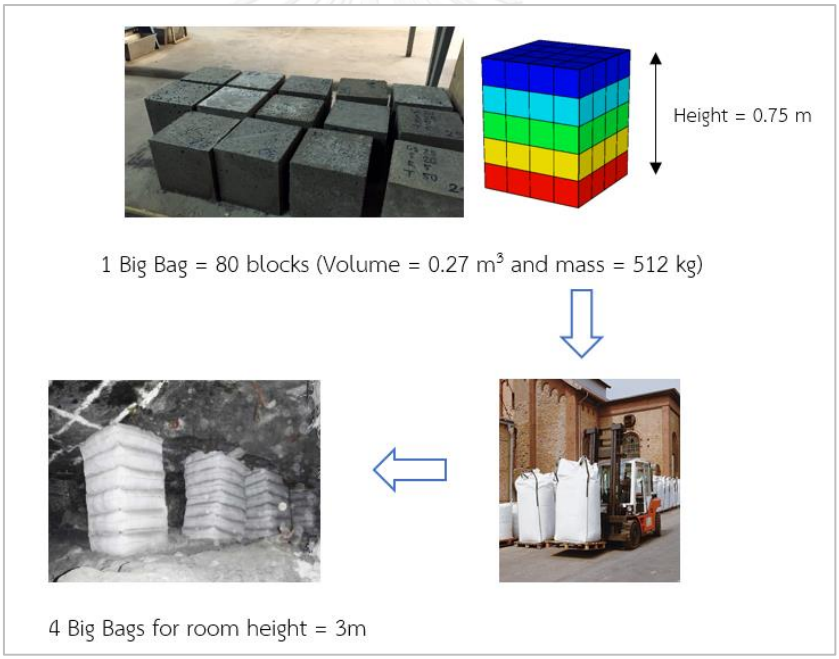

Figure 4.10: Backfill operation.

4.1.3.3. Pillar stress distribution

To investigate the ability of applying solidified concrete block as backfill material in supporting the pillars, the in-situ stress in pillar and tributary area method for determining the pillar strength are examined. The vertical in situ stress is generally taken as the unit weight of the overlying rock (γ) times the depth (z) [60]:

$$\sigma_v = \gamma . z = \rho . g . z \quad (4.1)$$

where, σ_v is the vertical stress, MPa.

γ is the unit weight of the overlying rock

z is the depth below surface.

ρ is rock density, kg/m^3

g is gravitational acceleration, m/s^2

Tributary area method is the simplest method of determining the pillar load. This method is based on a force balance between the load carried by the pillar and the tributary area conveying load on to the pillar. This method only uses average loading of the pillar not the actual stress distribution. Brady and Brown (1992) give a simple diagram to explain the calculation of e (a = b for square pillars and a ≠ b for rectangular or rib pillars) as shown in Figure 4.11.

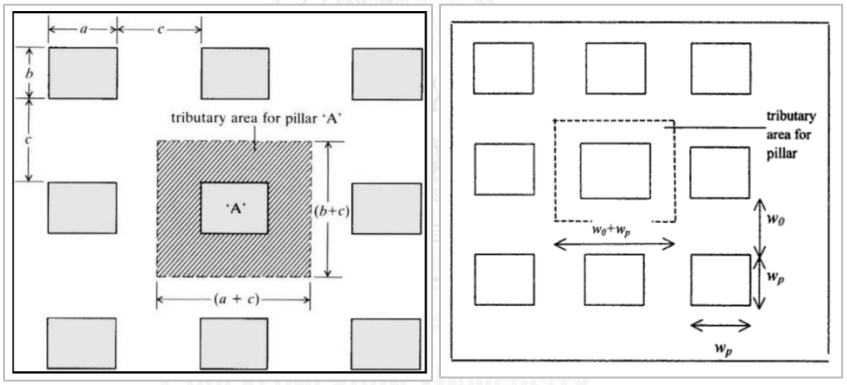

Figure 4.11: The geometry for tributary area analysis of pillars in uniaxial loading [61].

For the rib pillars a ≠ b (rectangular pillars), the pillar strength can be calculated by equation 4.2

$$\sigma_P = \gamma z \left(\frac{w_o + w_p}{w_p}\right) = \gamma z \left(1 + \frac{w_o}{w_p}\right) \quad (4.2)$$

Applying the tributary area method for determining the pillar strength in the panel No.209 of APPC Potash mine project. Table 4.6 shows the details of panel which has rib pillars, with the width of room, w_o= 3.75 m, and width of pillar, w_p= 3 m.

Table 4.6: Pillar design in panel No.209 of APPC Potash mine project [12]

Panel No.	Roof thickness*/Room width			Depth	α	Room height	Pillar width	Pillar length
	1.5m*	2m*	3m*					
	3.75m	5m	7m	m		m	m	m
209	3.75	5	7	300	1.0	3.0	3.0	30

Using the equation 4.2, the ultimate pillar strength, MPa before backfill is:

$$\sigma_p = \gamma z\left(1 + \frac{w_o}{w_p}\right) = \gamma_{salt} z\left(1 + \frac{3.75}{3}\right) = 2.25\ \gamma_{salt} z$$

The ultimate pillar strength, MPa after backfill is:

$$2.25\ \gamma_{salt} z + 2.25\ \gamma_{concrete} z - \gamma_{concrete} z = z\,(2.25\ \gamma_{salt} + 1.25\ \gamma_{concrete})$$

$$\frac{After}{Before} = \frac{z\,(2.25\ \gamma_{salt} + 1.25\ \gamma_{concrete})}{2.25\ \gamma_{salt} z} = \frac{(2.25\ \rho_{salt} + 1.25\ \rho_{concrete})}{2.25\ \rho_{salt}}$$
$$= \frac{(2.25 \times 2140 + 1.25 \times 1890)}{2.25 \times 2140} = 1.49$$

where

$$\rho_{salt} = 2.14 \frac{t}{m^3} = 2140 \frac{kg}{m^3}$$

$$\rho_{concrete} = 1.89 \frac{t}{m^3} = 1890 \frac{kg}{m^3}$$

According to Table 4.7, the maximum pillar strength is about 52.3 MPa

$$\alpha = \frac{\text{pillar width}}{\text{pillar height}} = \frac{3}{3} = 1 \qquad \mu = \frac{\text{pillar width}}{\text{pillar length}} = \frac{3}{30} = \frac{1}{10}$$

Table 4.7: Maximum pillar strength [12]

α	μ	σ_{Pmax} [MPa]
1	1/6	52.3
1.5	1/6	63.5
2	1/6	74.8

So, the ultimate pillar strength after applying the backfilling concrete blocks into the room will be increase 1.49 times, $1.49 \times 52.3\ MPa = 78\ MPa$. It can significantly support the stability of the pillar.

4.1.4. Discussions

The experimental design of solidification method gives an optimum mixture that can solidify the solid tailings at the expense of strength requirement. From the experimental results, the following conclusions can be drawn:

- The 1:3.5 Cement/Tailing (C/T) ratio mixture represents the optimum C/T ratio, which is deemed suitable ratio to solidify the tailing material.
- The UCS strength generated at Water/Cement (W/C) ratio of 0.6 is selected as the optimum condition.
- The UCS strength increases with longer curing periods, the solidified concrete blocks gain 75% of developed strength within 7 days.
- Mixture ID 20/5/5/70T which made from 20% cement, 5% fine aggregate, 5% coarse aggregate and 70% solid tailing, is the optimum mixture that satisfy the maximum solid waste concentration of 70%. It generates the compressive strength of 6.17 MPa, which is greater than the minimum requirement of 5 MPa. The mixture was cured at the room temperature (98% humidity at 25°C) within 7 days.
- Approximately 54.5 million tons of solid tailing can be disposed into the mine-out panels for the entire mine life by the solidification method. The backfill will be designed in the second year of operation that can minimize the environmental impact from surface tailing pile of potash mine waste. In general, the backfill can support the stability of the pillar and minimize the subsidence of the underground mine. Finally, the solidification method provides the potash mine waste disposal program taking care of solid potash mine waste.

4.2. Deep well injection simulation results

Deep well injection simulation involves two steps. First, the base case conceptual model is developed to test on the storage capacity, pressure buildup, and brine volume migration. Second, the base case model is being applied for the operational

conceptual model where the geological storage, injection well, and the brine volume are optimized.

4.2.1. Base case conceptual model

Figure 4.12 shows brine injection simulation results at a constant injection rate of 165 m^3/day over time. Pressure and salinity are tracked through time in the model domain to examine the effects of subsurface injection. The well Bottom-Hole Pressure and cumulative brine injected increases significantly in 19 years. To prevent the breaking caprock, the injection rate is reduced from 165 to 117 m^3/day in year 19, thus the well Bottom-Hole Pressure remains constant. The cumulative brine injected increases slowly in the following last 2 years.

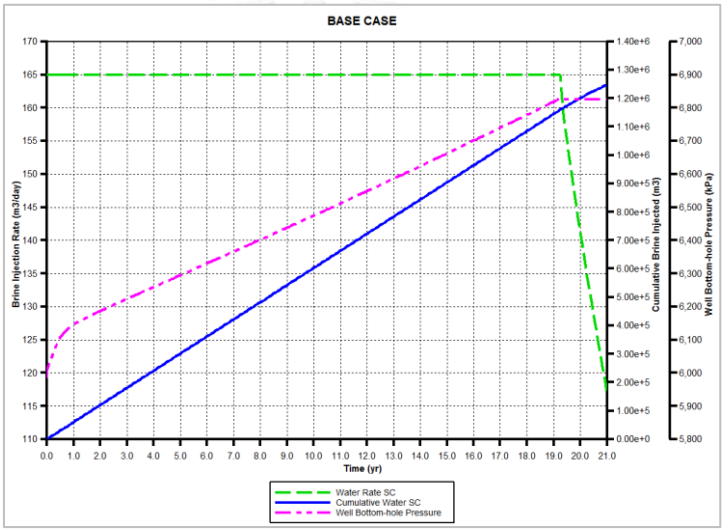

Figure 4.12: Brine injection simulation results at a constant injection rate over time.

❖ **Storage capacity**

Figure 4.13 shows the cumulative brine injected with time. Brine is continuously injected into the aquifer at 165 m^3/day for 21 years. After 19 years, the injection rate is reduced from 165 to 117 m^3/day, against the backdrop of BHP monitoring constraint at 6,825 KPa. At the end of 21 years period, approximately 1.25 million cubic meters of brine has been injected into the Khok Kruat aquifer unit.

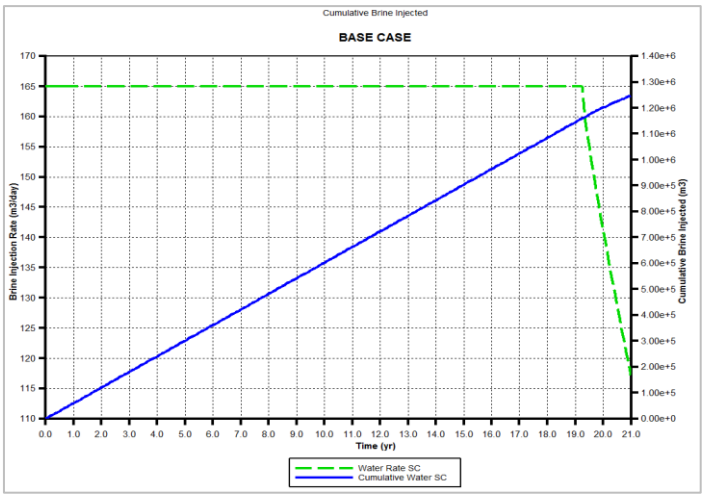

Figure 4.13: Cumulative brine injected with time for the base case simulation model.

❖ **Pressure buildup**

After injecting at a constant rate of 165 m^3/day for a period of 21 years, the average aquifer pressure has increased to 785.5 KPa. The well Bottom-Hole Pressure profiles in Figure 4.14 show that the Bottom-Hole Pressure is increased to 842 KPa during the injection period. Figure 4.15 gives the plot of pressure buildup in an injection well for the entire 21-years injection period. At constant injection rate, the Bottom-Hole Pressure increases gradually over the time, but maintains well below the formation fracture pressure.

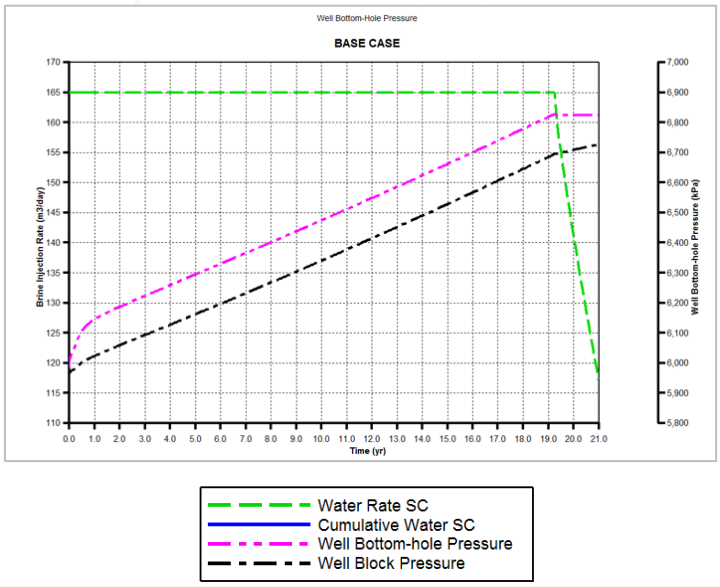

Figure 4.14: Bottom-Hole Pressure (BHP) profiles for the base case simulation model.

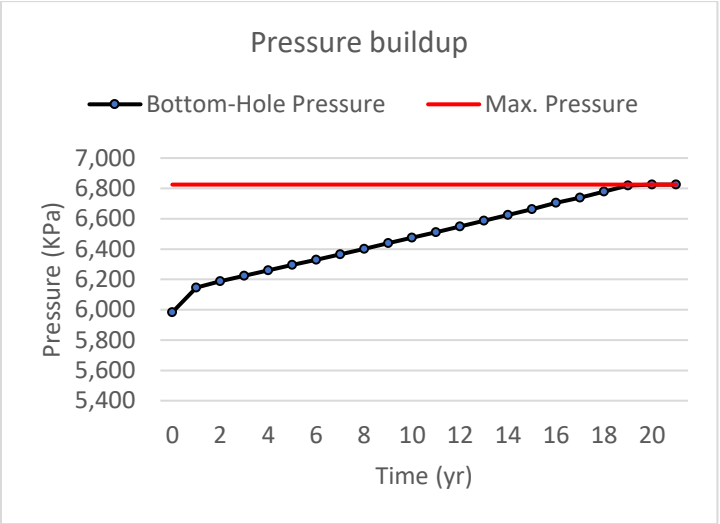

Figure 4.15: Plot of pressure buildup in injection well.

❖ **Plume migration**

The salinity is tracked through time in the model domain to examine the effects of subsurface injection. Figure 4.16 shows the plume migration in response to the injection well. The area of brine plume is 141,862.5433 m^2 = 0.142 km^2 (radius of plume migration = 212.5 m) at the bottom of target aquifer (Layer 9) after 21-years period.

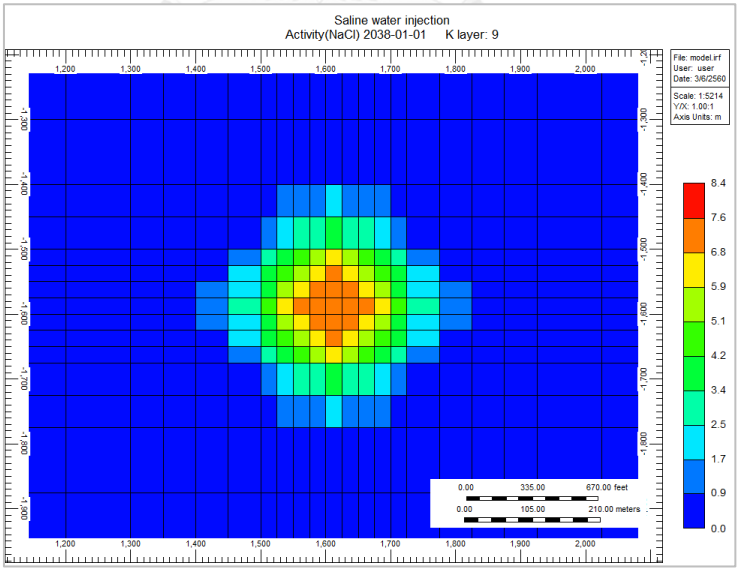

Figure 4.16: Area of plume migration of well = 141,862.5433 m^2 = 0.142 km^2 (radius = 212.5 m) at the bottom of target aquifer (Layer 9) after 21 years.

Figure 4.17- Figure 4.20 show the salinity profile of a model over time in top view, 3D view and cross-section, respectively. It can be seen that brine moves downward from the injection point toward the bottom layer.

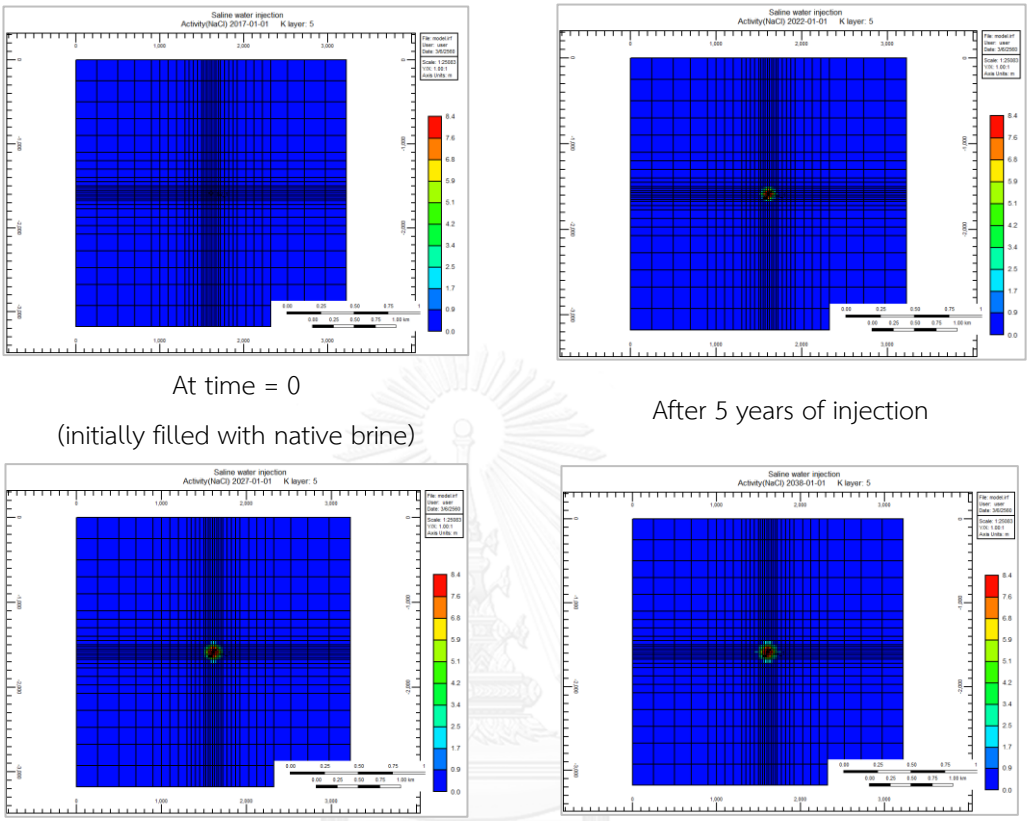

At time = 0

(initially filled with native brine)

After 5 years of injection

After 10 years of injection

End of injection

Figure 4.17: Brine salinity profile snapshots for the brine injection of base case simulation model (top view).

In this study, the composition of salinity components in aqueous phase is presented in molality (mol/kg H_2O). As can be seen that, the salinity is higher near the well during the injection, because the injected brine is higher salinity than that of the native brine. Before the injection, the native brine is 1,000 mg/L which equal molality (NaCl) = 0.017 (blue color). The molality of a solution is defined as Equation 4.3, in which the amount of substance (in moles) of solute (n_{solute}), is divided by the mass (in kg) of the solvent ($m_{solvent}$).

$$\text{Salinity (Molality), moles/kg } H_2O = n_{solute} / m_{solvent} = n_{salt} / m_{H2O} \qquad (4.3)$$

An example of salinity concentration calculation is demonstrated in Table 4.8.

Table 4.8: Salinity concentration calculation

If molality of NaCl is 8.4 (red color), the salinity in mg/L can be calculated as:

Salinity (Molality), moles/kg H_2O = X mole/ Y kg H2O =8.4 moles NaCl/kg H_2O

Mass of solute NaCl = X mole x 58.5 g/mole = 58.5X (g)

The density of brine is 1.28 g/mL [12].

Assuming one litter of brine, mass of brine (solution) equals to 1,280 g (1,000 mg/L x 1.28 g/mL).

Mass of brine (solution) = Mass of solute NaCl + Mass of solvent H_2O = 58.5X + 1,000Y = 1,280

With X = 8.4Y therefore, 58.5 x 8.4Y + 1,000Y = 1,280

Therefore, Y = 0.86 kg H_2O, and X = 7.224 mole and the mass of solute NaCl is 58.5X = 422.604 g.

$$\text{The Salinity in}\frac{\text{mg}}{\text{L}} = \frac{\text{mass of solute}}{\text{liter of solution}} = \frac{422.604\ \text{g}}{1\ \text{L}_{\text{brine}}} = 422{,}604\ \text{mg/L}$$

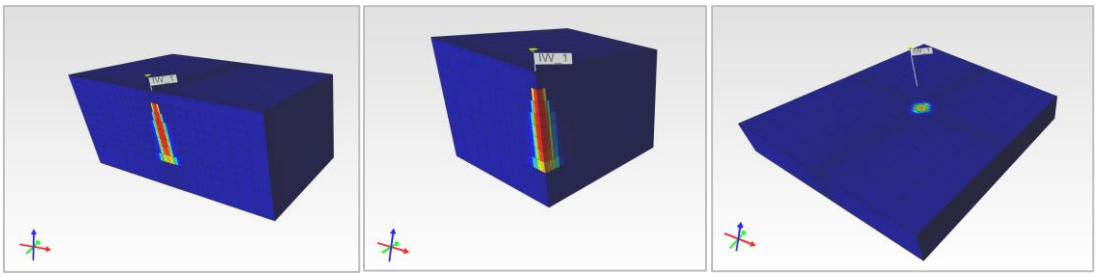

Figure 4.18: Brine salinity at the end of 21-years injection period at the bottom layer of base case simulation model (3D view).

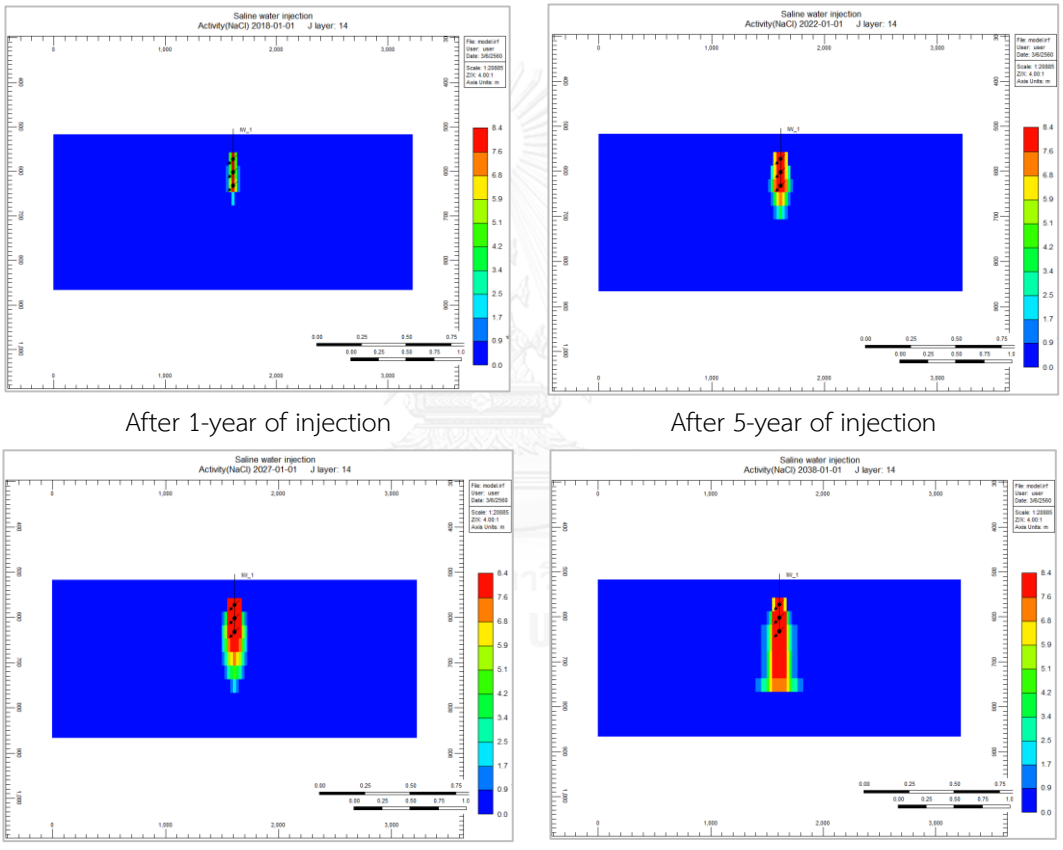

After 1-year of injection

After 5-year of injection

After 10-year of injection

21 years End of injection

Figure 4.19: Brine salinity over time for the brine injection of base case simulation model (J-cross section).

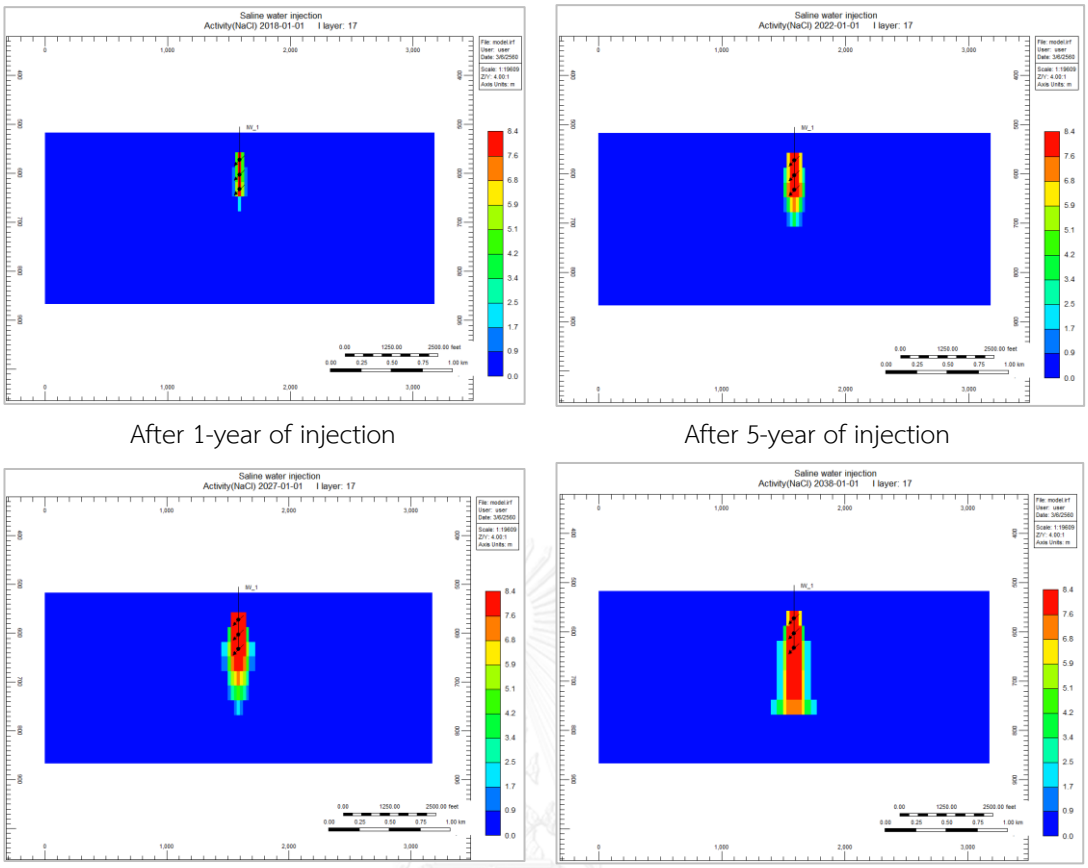

After 1-year of injection

After 5-year of injection

After 10-year of injection

21 years end of injection

Figure 4.20: Brine salinity over time for the brine injection of base case simulation model (I-cross section).

Base on the base case model simulation results, the operational conceptual model is designed for eight injection wells with an injection rate of 165 m^3/day. The eight injection wells scheme is developed to discharge the brine rate of 1,318 m^3/day, the highest volume brine production in APPC project.

At the highest injection rate, the simulation result shows that the area of plume migration is 0.142 km^2 over 21 years. In considering, the capacity of formation (pore volume) is 525 million cubic meters (0.25 x (3,225m x 3,100m x 210m)).

In fact, the brine amount from production of APPC project varies every year as shown in Table 3.3. Therefore, to operate this amount of brine year by year, and ensure that there is as less brine as possible stored on the surface brine pond each year, the operational optimum condition need to be considered.

4.2.2. Operational optimum condition

In the operational optimum condition, the studied area is subdivided equally into 4 areas (Area I-IV). Each area is accompanied by two injection wells. A total of eight injection wells (IW-1 - IW-8) is distributed within the domain, as can be seen in Figure 4.21.

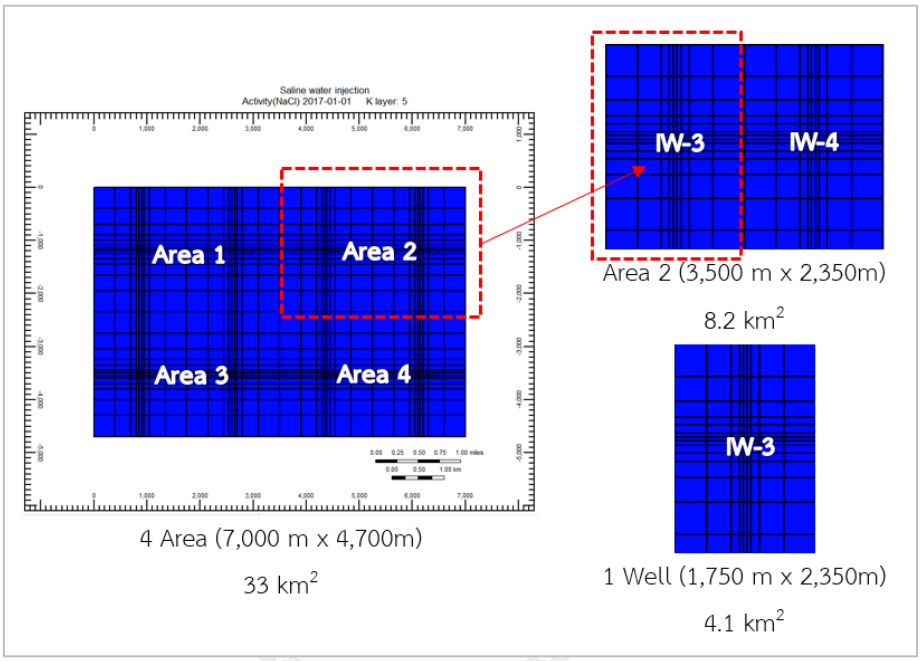

Figure 4.21: Simulation grid in top view for operational optimum conceptual model.

From Figure 4.21, all the injection wells are presented at depths exceeding 560 m. Figure 4.22 gives the 3D view of the constructed grid.

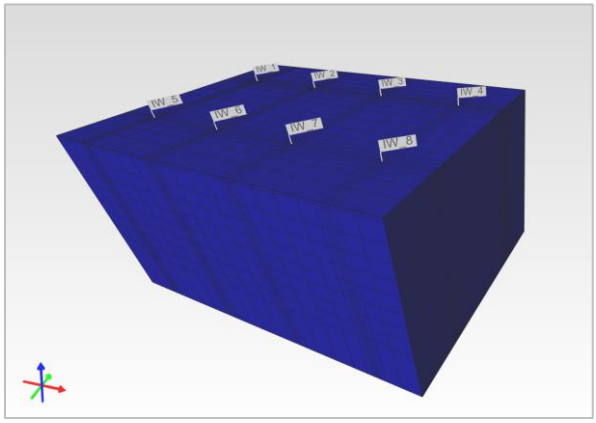

Figure 4.22: 3D view of the constructed grid.

Based on the annual brine production of APPC project, the injection rate for each well is designed differently as shown in Table 4.9.

In the model, the screen opening depth is the same at 560-770 m. for all wells, however at the different grid well completion (I, J, K). The maximum BHP is set constant at 6,825 KPa throughout. The *Area 1* and *Area 3* are designed with lower injection rate of 50 m^3/day, while the *Area 2* and *Area 4* are designed with the higher injection rate of 100 and 200 m^3/day, respectively. This is totally in consideration of the thickness and storage capacity of the subdivided area.

Table 4.9*:* Parameters of injection wells in operational optimum conceptual model

Parameters	**Area 1 (3,500 m x 2,350m)**		**Area 2 (3,500 m x 2,350m)**	
	IW-1	**IW-2**	**IW-3**	**IW-4**
Depth, m	560 - 770	560 - 770	560 - 770	560 - 770
Grids well completion (I, J, K)	5, 7, 3-4-5	14, 7, 3-4-5	23, 7, 3-4-5	32, 7, 3-4-5
Maximum Bottom-hole Pressure, kPa	6,825	6,825	6,825	6,825
Maximum injection rate, m^3/day	50	50	100	100
Parameters	**Area 3 (3,500 m x 2,350m)**		**Area 4 (3,500 m x 2,350m)**	
	IW-5	**IW-6**	**IW-7**	**IW-8**
Depth (m)	560 - 770	560 - 770	560 - 770	560 - 770
Grids well completion (I, J, K)	5, 20, 3-4-5	14, 20, 3-4-5	23, 20, 3-4-5	32, 20, 3-4-5
Maximum Bottom-hole Pressure, kPa	6,825	6,825	6,825	6,825
Maximum injection rate, m^3/day	50	50	200	200

Similar to the base case model, the operational condition mainly concerns the brine migration of both horizontal and vertical directions throughout the injection periods. Figure 4.23 – 4.24 show the plume migration of salinity over time in top view and cross-section, respectively.

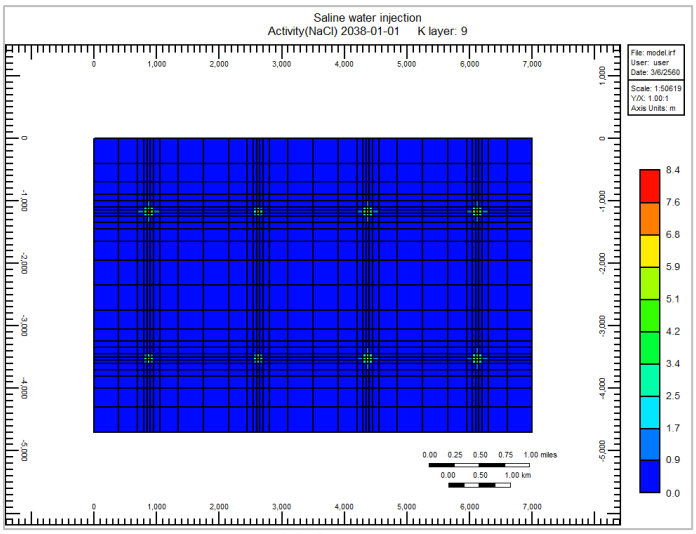

Figure 4.23: Plume migration of eight wells at the bottom layer at the end of 21-years period (top view).

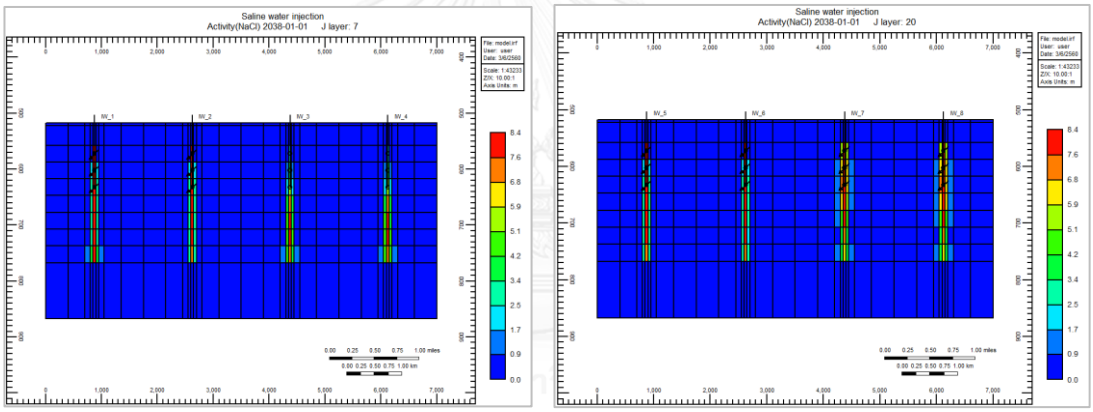

(a) (b)

Figure 4.24: Plume migration of wells IW_1, IW_2, IW_3, IW_4 (a) and wells IW_5, IW_6, IW_7, IW_8 (b) at the end of 21-years period (cross-section).

The simulation results of operational optimum conceptual model are shown in Table 4.10. In this conceptual model, the highest remaining brine still left on the surface is 218,314 m^3 in Year 8, which need to store in the storage pond facilities. As previously stated the objective of this deep well injection program is to investigate maximum discharge potential of the highly saturated brine waste into the target Khok Kruat geological storage. With this plan, the accumulated injected brine after 21 years stands at 2.8 million cubic meters, all of brine can be disposed into the Khok Kruat aquifer via deep well injection.

Table 4.10: Simulation model results for eight injection wells of operational optimum conceptual model

Year	Area 1		Area 2		Area 3		Area 4		Total brine volume per day	Remaining Brine Volume
	IW_1	IW_2	IW_3	IW_4	IW_5	IW_6	IW_7	IW_8		
	m^3		m^3		m^3		m^3		m^3	m^3
0	50								50	0
1	50								50	0
2	50	50			50	50			200	6,299
3	50	50			50	50			200	7,690
4	50	50	100	100	50	50			400	23,959
5	50	50	100	100	50	50			400	0
6	50	50	100	100	50	50	200	200	800	12,557
7	50	50	100	100	50	50	200	200	800	29,220
8	50	50	100	100	50	50	200	200	800	218,314
9	50	50	100	100	50	50	200	200	800	79,781
10	50	50	100	100	50	50			400	0
11	50	50	100	100	50	50			400	0
12	50	50	100	100	50	50			400	0
13	50	50	100	100	50	50			400	0
14	50	50	100	100	50	50			400	25,434
15	50	50	100	100	50	50	200	200	800	44,272
16	50	50	100	100	50	50	200	200	800	54,298
17	50	50			50	50			200	0
18	50	50			50	50			200	13,293
19	50	50			50	50			200	19,395
20	50	50							100	6,655
21										0

4.2.3. Discussions

From the simulation model results, the following discussions can be made.

- The results of waste brine injection from the base case simulation model at maximum injection rate (165 m^3/day) increase the Bottom-Hole Pressure to 842 KPa, and not exceeding the formation fracture pressure during the 21-years injection period. The salinity of brine moves downward from the injection point to the bottom of the conglomeratic sandstone layer, and the plume migration of salinity covers the area of 0.142 km^2 (radius of plume migration = 212.5 m) at the bottom layer.
- The operational conceptual model of eight wells was designed to discharge the maximum amount of brine as much as possible. The cumulative injected brine volume is 2.8 million cubic meters through 21-years injection program. Although there is still small volume of brine left, that can be stored on the surface brine storage pond. From this investigation, deep well injection can be applied to treat the liquid potash mine wastes.

CHAPTER 5

CONCLUSIONS AND RECOMMENDATIONS

In this chapter, conclusions and recommendations drawn from experiment and simulation results are presented.

5.1. Conclusions

This thesis presents a conceptual study of two alternative approaches for potash mine waste disposal: solidification of solid tailing and deep well injection for liquid brine waste.

Solidification of solid tailing

Through the study, experimental work yields an optimum mixture that can solidify the solid tailings into a stable concrete block. Most of the influential factors in compressive strength of concrete block are investigated. From results of the experimental study of solidification method, the following conclusions can be made:

1) The 1:3.5 Cement/Tailing (C/T) ratio mixture represents the optimum C/T ratio, which is deemed suitable ratio to solidify tailings in consideration to the strength requirement.
2) The UCS strength generated at water/cement (W/C) ratio of 0.6 is selected as the optimum condition.
3) The UCS increases with longer curing periods, the solidified concrete blocks gains 75% of developed strength within 7 days.
4) Mixture ID 20/5/5/70T is the optimum mixture condition. It contains the maximum solid waste concentration of 70% that can be solidified in the concrete blocks. It registers the compressive strength of 6.17 MPa, which is greater than the minimum requirement of 5 MPa. The mixture was cured at the room temperature (98% humidity at 25°C) within 7 days.

5) Approximately 54.5 million tons of solid tailing can be disposed into the mine-out panels for the entire mine life by the solidification method. The backfill will be designed in the second year of operation that can minimize the environmental impact from surface tailing pile of potash mine waste. Moreover, the pillar strength increases about 1.49 times and can support the stability of the pillar and minimize the subsidence of the underground mine.

Finally, the solidification method provides the potash mine waste disposal program taking care of solid tailing from potash mine.

Deep well injection simulation

1) The target Khok Kruat aquifer contains 525 million cubic meters of pore volume. The top Khok Kruat conglomeratic sandstone aquifer with 30 meters thickness is modelled for the deep well injection for 1.25 million cubic meters of brine in 21 years at the constant rate of 165 m^3/day.

2) Based on the results from base case model, the fracture pressure is important in brine injection that can control the pressure buildup to prevent the caprock breaking. In this study, the fracture pressure is 7.6 MPa.

3) The results of waste brine injection from the base case simulation at maximum injection rate of 165 m^3/day increase the Bottom-Hole Pressure, BHP to 842 KPa, and not exceeding the formation fracture pressure during the 21-years injection period. The brine moves downward from the injection point toward the bottom of the conglomeratic sandstone layer, and the brine plume migration of salinity covers the area of 0.142 km^2 (radius of plume migration = 212.5 m) at the bottom layer.

4) The operational conceptual model of eight wells was designed to discharge the maximum amount of brine as much as possible. The cumulative injected brine volume is 2.8 million cubic meters through 21-years injection program. Although there is still small volume of brine left that can be stored on the surface brine storage pond. From this investigation, deep well injection can be applied to treat the liquid potash mine waste.

These two conjunctive potash mine waste disposal approaches will achieve the close to zero waste potash mining operation, and consequentially provide the benefits of technical aspects and reduce the environmental impacts in Potash industry of Thailand. Table 5.1 highlights important criterias of each method.

Table 5.1: Criterias of two alternative approaches

Criteria	Deep well injection	Solidification
Waste Materials	Liquid Brine Waste	Solid Tailing
Surface Storage Area	Smaller	Smaller
Environmental Impact	Less	Less
Current Practice	Well-developed technique and can be adopted in Thailand Potash mine	Well-developed technique and can be adopted in Thailand Potash mine
Type of Measure	Permanent storage and long-term monitoring	Permanent storage and long-term monitoring
Requirements	Well injection development	Solidification plant and Backfilling operation

5.2. Recommendations

The following ideas are recommendations for future study;

- The backfill operation is closely related to mine design (decline, room and pillar) and mining operation (transportation equipment). Therefore, to applying the concrete block as backfill materials, the backfill operation has to be adjusted according to mining operation.
- The primary data is assumed to set up the boundary conditions for the injection model. The in-situ test for log data, core data (porosity, permeability**,** formation depth and thickness) is needed to define the realistic geological description of Khok Kruat Formation in the model.

- The more advance geological modeling software is needed for the better portraying of the studied geological medium.
- The flow test should be accomplished to measure the groundwater system and its chemical composition.
- The study only assesses the alternative approaches in term of technical aspect, it is not included the financial and economic assessment.

REFERENCES

1. Yearbook, M., *US Dept. of Interior, Bureau of Mines.* 1937.

2. Sakamornsnguan, K. and J. Kretschmann, *Substance flow analysis and mineral policy: The case of potash in Thailand.* The Extractive Industries and Society, 2016. 3(2): p. 383-394.

3. Rauche, H.A., D. Fulda, and V. Schwalm. *Tailings and Disposal Brine Reduction–Design Criteria for Potash Production in the 21 st Century*. in *Tailings and mine waste*. 2001.

4. Cocker, M.D. and G.J. Orris. *World potash developments*. in *Proceedings of the 48th Annual Forum on the Geology of Industrial Minerals, Phoenix, Arizona*. 2012.

5. Assessment, G.M.R., *Potash—A Global Overview of Evaporite-Related Potash Resources, Including Spatial Databases of Deposits, Occurrences, and Permissive Tracts.*

6. Fall, M., M. Benzaazoua, and S. Ouellet. *Effect of tailings properties on paste backfill performance*. in *Proceedings of the 8th International Symposia on Mining with Backfill, Beijing, China*. 2004.

7. GmbH, K.S.K., *Global potash deposits*.

8. Warren, J.K., *Evaporites: sediments, resources and hydrocarbons*. 2006: Springer Science & Business Media.

9. Marx, H., *Possibilities for a Discharge Reduced Salt and Potash Production*, in *Exchange Conference on Potash*. 2013.

10. APPC, A.P.P.C.C.L., *Overview of Geology, Resources and Reserves of the APPC Udon South Potash (Sylvinite) Deposit, UdonThani Province, Thailand* 2013.

11. Wannakomol, A., *Soil and Groundwater Salinization Problems in the Khorat Plateau, NE Thailand*. 2005, Freie Universität Berlin.

12. Corporation, A.P.P., *Environmental Impact Assessment, APPC, Udon Thani Potash Project*. 2014: Bangkok, Thailand.

13. Spence, R.D. and C. Shi, *Stabilization and solidification of hazardous, radioactive, and mixed wastes*. 2004: CRC press.

14. Ranjan, A., *Industrial Waste Management*. 2017.

15. Saripalli, K., M. Sharma, and S. Bryant, *Modeling injection well performance during deep-well injection of liquid wastes.* Journal of Hydrology, 2000. 227(1): p. 41-55.

16. McCurdy, R. *Underground injection wells for produced water disposal*. in *Proceedings of the Technical Workshops for the Hydraulic Fracturing Study: Water Resources Management. EPA*. 2011.

17. CMG, *GEM User Guide_Compositional & Unconventional Reservoir Simulator Version 2016.* 2016.

18. Guide–Version, G.U.s., *Computer Modelling Group Ltd.* Calgary, AB, Canada, 2009.

19. Darcy, H., *Les fontaines publiques de la ville de Dijon: exposition et application*. 1856: Victor Dalmont.

20. Domenico, P. and M. Mifflin, *Water from low-permeability sediments and land subsidence.* Water Resources Research, 1965. 1(4): p. 563-576.

21. Hall, H.N., *Compressibility of reservoir rocks.* Journal of Petroleum Technology, 1953. 5(01): p. 17-19.

22. Newman, G., *Pore-volume compressibility of consolidated, friable, and unconsolidated reservoir rocks under hydrostatic loading.* Journal of Petroleum Technology, 1973. 25(02): p. 129-134.

23. Survey, U.S.G., *Saline Water*. 2016.

24. Johnson, R.L., K. Redding, and D.D. Holmquist, *Water Quality with Vernier.* Vernier Software and Technology, Beaverton, 2007.

25. El-Dessouky, H.T. and H.M. Ettouney, *Fundamentals of salt water desalination*. 2002: Elsevier.

26. Zarembo, V. and M. Fedorov, *DENSITY OF SODIUM-CHLORIDE SOLUTIONS IN TEMPERATURE-RANGE 25-350 DEGREES C AT PRESSURES UP TO 1000 KG-CM2.* JOURNAL OF APPLIED CHEMISTRY OF THE USSR, 1975. 48(9): p. 2021-2024.

27. Kumar, A., et al., *Reservoir simulation of CO 2 storage in aquifers.* Spe Journal, 2005. 10(03): p. 336-348.

28. Beaumont, E.A. and F. Fiedler, *Treatise of Petroleum Geology/Handbook of Petroleum Geology: Exploring for Oil and Gas Traps. Chapter 5: Formation Fluid Pressure and Its Application.* 1999.

29. Sridej, A. and A. Wannakomol, *Pressure Gradient Estimation Using Seismic Data In San Sai Oilfield, Fang Basin.*

30. Bourgoyne, A.T., et al., *Applied drilling engineering*. Vol. 2. 1991: Society of Petroleum Engineers Richardson, TX.

31. Fridleifsson, I.B., et al. *The possible role and contribution of geothermal energy to the mitigation of climate change*. in *IPCC scoping meeting on renewable energy sources, proceedings, Luebeck, Germany*. 2008. Citeseer.

32. Commission, B.R.D.B.-E., *Management of Tailings and Waste-Rock in Mining Activities*. 2009.

33. Mickley, M.C., *Membrane Concentrate Disposal: Practices and Regulation, Final Report*. 2001: US Department of the Interior, Bureau of Reclamation, Technical Service Center, Water Treatment Engineering and Research Group.

34. Ahmed, M., et al., *Use of evaporation ponds for brine disposal in desalination plants.* Desalination, 2000. 130(2): p. 155-168.

35. Masniyom, M., *Systematic Selection and Application of Backfill in Underground Mines*. 2009.

36. Knissel, W. and W. Helms. *Strength of Cemented Rockfill from Washery Refuse Results from Laboratory Investigations*. in *Proceedings of International Symposium on Mining with Backfill, AA Balkema, Rotterdam*. 1983.

37. Arioglu, E., *Design of supports in mines*. 1983, Wiley and Sons, New York.

38. Koo, D.-S., et al., *Characteristics of cement solidification of metal hydroxide waste.* Nuclear Engineering and Technology, 2017. 49(1): p. 165-171.

39. Mindess, S., J.F. Young, and D. Darwin, *Concrete*. 2003: Prentice Hall.

40. Marar, K., *Effect of cement content and water/cement ratio on fresh concrete properties without admixtures.* International Journal of Physical Sciences, 2011. 6(24): p. 5752-5765.

41. Kozul, R. and D. Darwin, *Effects of aggregate type, size, and content on concrete strength and fracture energy*. 1997, University of Kansas Center for Research, Inc.

42. Scoble, M., L. Piciacchia, and J.-M. Robert, *In situ testing in underground backfilled stopes.* CIM Bulletin, 1987. 80(903): p. 33-38.

43. Glater, J. and Y. Cohen, *Brine disposal from land based membrane desalination plants: A critical assessment.* Prepared for the Metropolitan Water District of Southern California, 2003.

44. Greene, C.J., *Underground injection-control technical assistance manual: subsurface disposal and solution mining*. 1983, Texas Dept. of Water Resources, Austin (USA).

45. Warner, D.L., *Subsurface disposal of liquid industrial wastes by deep-well injection.* 1968.

46. Hubbert, M.K. and D. Willis, *Measurement of Hydraulic Fracturing.* Petroleum Transaction, Shell Development Co, 1957.

47. Moody, M., *Geologic Characterization of Stratigraphic Sequences in the Upper Ohio River Valley for Determination of Brine Storage Capacity*.

48. Vonhof, J., *Waste disposal problems near potash mines in Saskatchewan, Canada.* Inland Waters Directorate, Environment Canada, Scientific Series, 1975.

49. Kolkas, M.M. and G.M. Friedman, *Diagenetic history and geochemistry of the Beekmantown-Group dolomites (Sauk Sequence) of New York, USA.* Carbonates and Evaporites, 1998. 13(1): p. 69-85.

50. Corp., M.E.S., *Mosaic Potash Esterhazy K2 Phase IV TMA Expansion_Environmental Impact Statement Volume I – Main Document*. January 2009.

51. Chairawiwut, W., *Chloride Salts Removal by non Planted Constructed Wetlands Receiving Synthetic Brines from Belle Plaine Potash Mining*. 2015, Faculty of Graduate Studies and Research, University of Regina.

52. Donald, E., *Potash deposits, processing, properties and uses*. 1996, London: Chapman and Hall.

53. Joel R. Sminchak, N.G., *Development of Subsurface Brine Disposal Framework in the Northern Appalachian Basin*. 2015.

54. Suwanich, P. *Potash-evaporite deposits in Thailand*. in *Geothai'2007, Proceedings of the International Conference on Geology of Thailand*. 2007.

55. Sattayarak, N. and S. Polachan. *Rock salt beneath the Khorat Plateau*. in *Proceedings of the Conference on Geology and Mineral Resources of Thailand*. 1990.

56. Walsri, C., et al., *Simulation of sandstone degradation using large-scale slake durability index testing device.* Songklanakarin Journal of Science and Technology, 2012. 34(5): p. 587-596.

57. Meesook, A., *Cretaceous.* The Geology of Thailand. Geological Society, London, 2011: p. 169-184.

58. Kriengsak Srisuk, T.C., Laa Archwichai, *Groundwater Flow Regime Analysis Based on Physical and Chemical Characteristics of the Chi River Subbasin Part II...* November 2008.

59. Srisuk, K., *Genetic characteristics of the groundwater regime in the Khon Kaen drainage basin, Northwest Thailand.* 1994.

60. Hoek, E. and E.T. Brown, *Practical estimates of rock mass strength.* International Journal of Rock Mechanics and Mining Sciences, 1997. 34(8): p. 1165-1186.

61. Brady, B.H. and E.T. Brown, *Rock mechanics: for underground mining*. 2013: Springer Science & Business Media.

APPENDIX

APPENDIX I

UCS strength results are categories in W/C ratio

W/C Ratio	Mixture ID	UCS Strength (MPa)
0.6	25/25/0/50T	9.4
	25/15/0/60T	8.59
	25/5/0/70T	7.71
	25/20/5/50T	9.33
	25/10/5/60T	7.6
	25/0/5/70T	6.88
	25/15/10/50T	11.59
	25/5/10/60T	10.05
	25/10/15/50T	9.19
	25/0/15/60T	6.87
0.8	20/30/0/50T	6.8
	20/20/0/60T	5.78
	20/10/0/70T	4.65
	20/25/5/50T	6.92
	20/15/5/60T	6.65
	20/5/5/70T	6.17
	20/20/10/50T	6.06
	20/10/10/60T	5.26
	20/15/15/50T	9.61
	20/5/15/60T	6.69
	20/10/20/50T	6.63
	20/0/20/60T	5.58

Tailing and mine-out room generated by mining annually in APPC Potash mine

Year	Mass of tailing	Mine-out room
	tons	m^3
0	227,200	0
1	182,338	0
2	455,727	261,500
3	1,110,699	700,200
4	1,861,075	1,219,500
5	2,712,166	1,906,500
6	3,193,477	2,266,800
7	3,195,088	2,257,500
8	3,230,717	2,311,200
9	3,229,684	2,334,200
10	3,249,757	2,275,200
11	3,211,799	2,229,500
12	3,466,118	2,339,600
13	3,342,408	2,274,400
14	3,565,081	2,318,000
15	3,180,646	2,224,000
16	3,182,618	2,299,500
17	3,637,343	2,507,900
18	3,618,780	2,494,500
19	4,116,012	2,507,900
20	3,936,608	2,507,900
21	2,443,891	1,748,700
22	0	0
Total	60,349,232	40,984,500

APPENDIX II

Cumulative brine injected and pressure buildup at constant rate of 165 m^3/day in 21 years of base case simulation model

Year	Injection Rate	Cumulative Brine	Well Bottom-hole Pressure	Max. Pressure
	m^3/day	m^3	KPa	KPa
0	165	2	5,983	6,825
1	165	60,225	6,146	6,825
2	165	120,450	6,187	6,825
3	165	180,675	6,223	6,825
4	165	241,065	6,259	6,825
5	165	301,290	6,295	6,825
6	165	361,515	6,330	6,825
7	165	421,740	6,366	6,825
8	165	482,130	6,402	6,825
9	165	542,355	6,438	6,825
10	165	602,580	6,475	6,825
11	165	662,805	6,511	6,825
12	165	723,195	6,549	6,825
13	165	783,420	6,586	6,825
14	165	843,645	6,624	6,825
15	165	903,870	6,662	6,825
16	165	969,375	6,704	6,825
17	165	1,024,485	6,740	6,825
18	165	1,084,710	6,779	6,825
19	165	1,144,935	6,818	6,825
20	141	1,201,300	6,825	6,825
21	117	1,247,966	6,825	6,825

VITA

Thao Nguyen Anh Ngo was born on September 11th, 1991 in Kien Giang, Vietnam. She received her Bachelor of Engineering in Environment from the Faculty of Environment, Ho Chi Minh City University of Technology in 2014. After her graduation, she had got one semester scholarship in Water Resource Engineering, Chulalongkorn University. In August 2015, she continued her studies in Master of Mining Engineering program at the Department of Mining and Petroleum Engineering, Faculty of Engineering, Chulalongkorn University.